THE UNIVERSITY
of EDINBURGH

Identification of RISC-associated microRNAs and their targets during $CD8^+$ T cell activation

Matilda Toivakka

Thesis submitted for the degree of Doctor of Philosophy

The University of Edinburgh

2019

I. Declaration

I declare that this thesis has been composed solely by myself and that it has not been submitted, in whole or in part, in any previous application for a degree. Except where states otherwise by reference or acknowledgment, the work presented is entirely my own.

Matilda Toivakka

Date

II. Acknowledgements

I have countless people to thank for their help and support during the completion of this thesis. Firstly, I must thank my supervisors: Rose Zamoyska for guidance and inspiration throughout the four years, and Amy Buck for indispensable advice on the microRNA related aspects of the project. I would like to express my sincerest gratitude to everyone in the Zamoyska and Buck groups for their help during this project. While there are too many people to mention by name, I want to thank Kat for her work on optimising the CLASH protocol and her extensive help at the start of the project; Sujai for his assistance with the bioinformatic data analysis and David for help with GW182 related experiments. I would also like to thank my fellow PhD students for scientific and non-scientific discussions over much-needed coffee breaks. Finally, I want to thank my parents and my sister Maliina for support and encouragement in pursuing a PhD.

III. Lay Summary

The mammalian immune system contains various types of white blood cells that protect the body from invading microbes. A key cell type required for effective immune responses is the T cell. T cells can be further classified into 'helper' T cells and 'cytotoxic' T cells. While helper T cells coordinate the immune response by secreting immunomodulatory molecules, cytotoxic T cells have the capacity to kill virus-infected or cancerous cells. Strict regulation of T cell responses is crucial to protect the body from infectious diseases and cancer, while simultaneously avoiding autoimmunity and allergy, which are caused by inappropriate immune cell activation. In order to understand how T cells function, we must study the molecular mechanisms that regulate T cell activation and differentiation into effector cells.

In this study we focused on the role of cytotoxic T cells. Cytotoxic T cells are activated by binding small fragments of microbes called 'antigens' that are present on the surface of infected cells. Binding of the T cell receptor (TCR) to its specific antigen in appropriate conditions activates the cell through intracellular signalling pathways. Small signalling molecules in the cell propagate in signalling cascades that result in altered gene expression. Two key steps are required for gene expression. First, DNA is transcribed into messenger RNA (mRNA) which is a template from which proteins can be made. The second step is the translation of mRNA into protein by cellular machines called ribosomes. Gene expression can be regulated either at the level of gene transcription, or at the level of mRNA translation. A type of RNA called microRNA can regulate mRNA translation. microRNAs can bind their target mRNAs and promote their destruction, thus stopping their translation into proteins. Hundreds of different microRNAs exist, each specifically targeting a set of mRNAs.

We aimed to study the role of microRNAs in cytotoxic T cell activation. We first identified the most abundant microRNAs from non-activated and activated T cells and found that these were largely different. To further understand

microRNA function in activated T cells, we measured changes in the abundance of microRNA-associated proteins. microRNAs bind their target mRNAs in a protein complex called the RNA-induced silencing complex (RISC). T cell activation has been shown to cause changes in the protein composition of RISC. Specifically, T cell activation induces the formation of a large protein complex called high molecular weight (HMW) RISC which is not found in non-activated cells. microRNAs in this complex have been suggested to be particularly potent at inhibiting their target mRNAs. We isolated RNAs that were bound to the HMW RISC and from this identified a microRNA named miR-7, the role of which we further studied in cytotoxic T cells. Blocking the function of this microRNA in T cells caused changes in cell activation and expansion, suggesting it may be important for regulating T cell responses. To understand microRNA function, we must know which mRNAs they bind to. In order to find microRNA targets, we used a biochemical method called CLASH (cross-linking, ligation and sequencing of hybrids). This method can be used to determine which mRNAs a particular microRNA binds to and targets for degradation. From the CLASH datasets obtained from cytotoxic T cells, we identified some potential novel mRNA targets for several different microRNAs.

microRNAs are known to play an important role in immune cell function and regulate many aspects of T cell immunity. Furthermore, dysregulation of microRNAs can be seen in many human diseases, including autoimmune diseases and cancer. Therefore, potential novel therapeutic strategies could be based on promoting or inhibiting specific microRNAs. Expanding our knowledge on how microRNAs function in T cells will be crucial to developing such treatments.

IV. Scientific abstract

microRNAs (miRNAs) are short (~22 nucleotide long) single-stranded non-coding RNAs that regulate gene expression post-transcriptionally in the RNA-induced silencing complex (RISC). miRNAs play an important role in immune cell function and affect many aspects of T cell immunity. Activation of naive T cells induces dramatic changes in the expression of miRNAs and RISC-associated proteins. We studied these changes in expression of miRNAs in $CD8^+$ T cells using the OT-I transgenic T-cell receptor (TCR) mouse model, in which all T cells are $CD8^+$ and respond to ovalbumin peptides. Upon *in vitro* activation, we saw dynamic changes in the expression of individual miRNAs, which were influenced by whether the T cells responded to high or low affinity peptides and whether they were differentiating to effector or memory cells.

It was recently shown that in naive T cells, miRNAs are predominantly found in a low molecular weight (LMW) RISC composed of Argonaute (Ago)-proteins and miRNAs. Upon activation of T cells, biologically active miRNAs interacting with their target messenger RNAs (mRNAs) were shown to redistribute to a high molecular weight (HMW) RISC, which additionally contains RNA metabolism factors and Ago-interacting proteins such as GW182. We followed the development of HMW and LMW complexes in activated $CD8^+$ T cells in order to determine their role and to identify the miRNAs and their targets present in both.

We confirmed that GW182 protein was induced upon $CD8^+$ T cell activation and associated with Ago-2, forming HMW complexes. To study the distribution of miRNAs between HMW and LMW RISC, we undertook small RNA sequencing of the associated miRNAs. From these data we identified specific miRNAs that were enriched in HMW RISC in activated $CD8^+$ T cells. We also found that miRNA abundance did not always reflect its association with HMW RISC. Lastly, to discover miRNA targets, we used a novel method called cross-linking, ligation and sequencing of hybrids (CLASH), which directly identifies

miRNAs and their targets by immunoprecipitation of RISC and RNA sequencing. From these data we found potential novel targets for key miRNAs in $CD8^+$ T cells.

Expanding our knowledge of the role of miRNAs in T cell activation beyond observations of miRNA expression changes, by focusing on biologically active miRNAs and their targets in HMW RISC will deepen our understanding of the mechanism of action of miRNAs as well as the signalling pathways surrounding T cell activation.

V. List of Abbreviations

3'UTR – 3' untranslated region
5'UTR – 5' untranslated region
Ago – Argonaute
APC – Antigen presenting cell
CDS – Coding sequence
CLASH – Cross-linking, ligation and sequencing of hybrids
CLIP – Cross-linking immunoprecipitation
CPM – Counts per million
CTL – Cytotoxic lymphocyte
d – Day
DAG – Diacylglycerol
Eomes – Eomesodermin
FDR – False discovery rate
h – Hour
HMW RISC – High molecular weight RISC
IFNg – Interferon gamma
IL-15 – Interleukin 15
IL-2 – Interleukin 2
IP – Immunoprecipitation
IP3 - Inositol 1,4,5-trisphosphate
LAT – Linker of activation of T cells
LCMV – Lymphocytic choriomeningitis mammarenavirus
LMW RISC – Low molecular weight RISC
MHC – Major histocompatibility complex
min – Minute
miRNA – microRNA
mRNA – messenger RNA
mTOR – Mechanistic target of rapamycin
p:MHC – Peptide:MHC
PABP – Poly(A) binding protein
pc – Protein coding

PI3K – Phosphoinositide 3 kinase

PIP2 – Phosphatidylinositol 4,5-bisphosphate

PKC – Protein kinase C

PLCg1 – Phospholipase C-gamma

pri-miRNA – primary miRNA

qPCR – Quantitative real-time polymerase chain reaction

RBP – RNA binding protein

RISC – RNA induced silencing complex

rRNA – Ribosomal RNA

s – Second

Tcm – Central memory T cell

TCR – T cell receptor

Tem – Effector memory T cell

Tfh – T follicular helper

TGFb – Transforming growth factor beta

Th – T helper

TNFa – Tumour necrosis factor alpha

TNRC6 – Trinucleotide repeat containing protein 6

Treg – Regulatory T cell

Trm – Resident memory T cell

tRNA – Transfer RNA

WB – Western blot

ZAP-70 – Zeta-chain associated protein kinase 70

VI. Table of contents

CHAPTER 1: Introduction

1.1 Function of T cells in the immune system

1.1.1 The immune response

Immune responses in vertebrates are orchestrated by the innate and adaptive immune systems. The innate immune system forms a first line of defence consisting of physical immune barriers and secretions, inflammatory signals and innate immune cells. The innate response is immediate and provides rapid protection against infection. Innate immune cells include cells derived from the common myeloid progenitor, such as granulocytes, mast cells, macrophages and dendritic cells, and Natural Killer (NK) cells that are derived from the common lymphoid progenitor (Turvey and Broide, 2010, Janeway 2012). These cells have important roles in killing invading pathogens and alerting the body to the presence of invaders through secretion of inflammatory signals. Granulocytes, which include neutrophils, eosinophils and basophils, contain granules of cytotoxic molecules and enzymes, the contents of which can be released upon activation. Phagocytic cells, such as macrophages and neutrophils, can engulf and destroy pathogens. Dendritic cells are phagocytic as well: uptake of pathogens results in maturation into antigen-presenting cells (APCs) that can activate cells of the adaptive immune system. NK cells can recognise abnormal cells, such as virus-infected or tumorous cells and kill these with lytic granules.

The adaptive immune response takes longer to develop but is adapted to combat specific infections. The adaptive immune system is composed of T and B lymphocytes which have specific antigen-recognition receptors on their surface. The B cell receptor (BCR) and T cell receptor (TCR) are similar in their basic structure and consist of constant regions and variable regions at the antigen-binding site. The BCR recognises antigen directly whereas the TCR recognises antigen fragments that are presented on Major

Histocompatibility Complex (MHC) molecules on the surface of other cells (Rudolph, Stanfield and Wilson, 2006). MHC Class I molecules, that are expressed on all nucleated cells in the body, display peptides from all proteins produced in the cell. MHC Class II molecules are only expressed on specialised APCs which include dendritic cells, B cells and macrophages. T cells can be divided into $CD4^+$ 'helper' T (Th) cells and $CD8^+$ 'cytotoxic' T cells. $CD4^+$ T cells recognise antigen presented on MHC Class II molecules, whereas $CD8^+$ T cells require MHC Class I.

The adaptive immune response first begins with uptake of antigen by dendritic cells that travel to secondary lymphoid organs and present antigen to $CD4^+$ T cells. T cells require three signals for activation (Curtsinger *et al.*, 1999). Firstly, they must recognise their cognate antigen through their TCR, which binds peptides that are presented on MHC proteins. Secondly, T cell activation is regulated through co-stimulatory receptors such as CD27, CD28, 4-1BB, CD40 and OX40 (Jenkins and Johnson, 1993; Kaech and Cui, 2012). Activated dendritic cells are able to provide co-stimulatory signals to T cells. Finally, T cells require cytokines and inflammatory signals to fully differentiate into functional effector cells (Curtsinger *et al.*, 1999). Pro-inflammatory cytokines cause upregulation of cytokine and co-stimulatory receptors on T cells. The combined duration and strength of these signals will predict the fate of the cell. TCR stimulation alone is insufficient to promote cell activation and proliferation, and co-stimulation and cytokine signals are required for a full response. Presentation of antigen in the absence of co-stimulation can lead to cell tolerance instead of activation (Schwartz, 2003).

1.1.2 Adaptive immune cell subsets

Following activation by an activated dendritic cell, a naive $CD4^+$ T cell will differentiate into an effector Th cell. Th cells coordinate the adaptive immune response by interacting with multiple immune cell types, influencing their subsequent activation and differentiation. Naive $CD8^+$ T cells require additional

co-stimulation from APCs, which can be provided by $CD4^+$ T cells interacting with the same APC (Wodarz and Jansen, 2001). B cell activation relies on direct co-stimulation from an activated $CD4^+$ T cell, to which the B cell presents antigen (Parker DC, 1993). 'Signature' cytokine profiles and master transcription factors characterise subtypes of Th cells, which include Th1, Th2, Th17, Th9, Th22, follicular helper Tfh and regulatory Treg cells (Raphael *et al.*, 2015). Each of these subtypes is specialised in combatting different types of infection by secreting cytokines and recruiting and activating appropriate immune cells, whereas Tregs have an important role in preventing immune pathology. It has recently become apparent that this classification is an oversimplification, and the transcriptional landscape of Th cells is more complex and plasticity is common between the subtypes (Wang, Collins and Kuchroo, 2015; Hirahara and Nakayama, 2016). Tfh cells are of crucial importance in providing help to B cells, which following activation differentiate into antibody-secreting plasma cells. Some activated B cells migrate together with Tfh cells into lymphoid follicles where they form germinal centres in which they undergo affinity maturation and antibody class-switching before differentiating into plasma cells (Victora and Nussenzweig, 2012).

$CD8^+$ T cells have the capacity to differentiate into cytotoxic T lymphocytes (CTLs) upon activation. CTLs secrete cytokines such as Interferon gamma (IFNγ) and Tumour necrosis factor alpha (TNFα) and produce cytotoxic effector molecules such as perforin and granzymes that can lyse target cell membranes causing cell death (Kaech and Cui, 2012). CTLs recognise antigen presented on MHC Class I on the surface of abnormal cells, such as virus-infected or cancer cells.

1.2 T cell activation

1.2.1 Initiation of TCR signalling

T cells are activated by binding peptide:MHC complexes (pMHC) with their TCRs (Davis *et al.*, 2002). Several non-exclusive models exist to explain how TCR signalling is initiated (Courtney, Lo and Weiss, 2018). Mechanosensory models suggest that a conformational change in the TCR initiates signalling, by facilitating the phosphorylation of TCR-associated immunoreceptor tyrosine-base activation motifs (ITAMs) (Basu and Huse, 2015). The structural understanding of such conformational change is however unclear. The kinetic segregation model suggests that the spatial reorganisation of signalling molecules on the cell surface leads to the segregation of the TCR signalosome from negative regulators, allowing signalling to take place (Davis and van der Merwe, 2006). According to the serial engagement model, multiple TCRs are required to be sequentially engaged to accumulate sufficient signalling (Valitutti *et al.*, 1995; Valitutti and Lanzavecchia, 1997).

1.2.2 TCR signal propagation

The TCR signalosome is composed of numerous molecules that can have positive or negative effects on TCR signal propagation, with a complex network of intersecting signalling pathways (Acuto, Bartolo and Michel, 2008; Brownlie and Zamoyska, 2013). The TCR is associated with its co-receptors CD3, and CD4 or CD8, which aid with binding pMHC and signal propagation (Davis *et al.*, 2002). The CD3 co-receptor is composed of CD3γ, CD3δ and two CD3ε chains and forms a complex with the TCRαβ chains and the intracellular TRC-associated ζ chains. However, the TCR-CD3 complex does not have intrinsic enzymatic activity and instead relies on the SRC-family kinases Lck and Fyn to initiate the TCR signalling cascade (Salmond *et al.*, 2009). Lck is found associated with the CD4 and CD8 co-receptors, and when activated can phosphorylate ITAMs in CD3 chains and the associated ζ chains (Veillette *et al.*, 1988; Shaw *et al.*, 1990). Lck activity is controlled by the differential

phosphorylation of inhibitory and activating tyrosine residues (Couture *et al.*, 1996). The stand-by model suggests that Lck is found in a constitutively active form, and signalling is initiated not by changes in Lck enzymatic activity, but rather its distribution in the cell or availability of its target ITAMs (Nika *et al.*, 2010). Recent data however suggest that *de novo* phosphorylation of Lck may also be required (Philipsen *et al.*, 2017).

Phosphorylated CD3 chain ITAMs become docking sites to other signalling molecules such as the Zeta-chain associated protein kinase (ZAP)-70 which is also phosphorylated by Lck (Pelosi *et al.*, 1999). ZAP-70 subsequently phosphorylates Linker for activation of T cells (LAT), an important scaffold protein that recruits key enzymes and adapter proteins leading to downstream signal diversification and amplification. The LAT signalling complex is essential to T-cell signal propagation and contains various signalling molecules that influence one another and cooperate through multiple protein interactions (Balagopalan, Coussens and Sherman, 2010; Samelson *et al.*, 2015). The activation of phospholipase C-gamma (PLCγ1) requires interaction with LAT and phosphorylation by Itk. PLCγ1 catalyses the formation of IP_3 (inositol 1,4,5-trisphosphate) and DAG (diacylglycerol) from PIP_2 (phosphatidylinositol 4,5-bisphosphate). DAG activates the Ras signalling pathway and PKC (Protein kinase C), whereas IP_3 production leads to release of intracellular Ca^{2+} stores. These signalling pathways eventually lead to activation of key transcription factors such as NFAT, NF-κB and AP-1 (Balagopalan, Coussens and Sherman, 2010).

The GRB2 (Growth factor receptor bound protein 2) family members GRB2, GADS and GRAP also bind LAT. GRB2 plays a role in the activation of the Ras pathway through recruitment of SOS1. GADS links SLP-76 to the complex, which in turn recruits multiple effector proteins, including VAV, NCK, ITK, ADAP, and Phosphoinositide 3 kinase (PI3K) (Balagopalan, Coussens and Sherman, 2010). VAV activates Rho-family G-proteins and cooperates with NCK and WASp to induce cytoskeletal changes in activated cells. ITK

plays a crucial role in the phosphorylation and activation of PLCγ1. ADAP regulates cell adhesion and integrin function in activated T cells. PI3K catalyses the formation of PIP_3 from PIP_2 which contributes to activation of the mechanistic target of rapamycin (mTOR). Therefore, the effects of LAT associated signalling molecules on the cell are wide-spread and lead to activation of transcription factors and changes in the cytoskeleton and cell adhesion (Fig.1.1).

Further signalling through co-stimulatory receptors such as CD28 increases and supports these functions. CD28 binding to its ligands CD80 and CD86 induces cell proliferation, survival and IL-2 production in response to low concentrations of antigen that would not elicit a response in its absence (Boomer and Green, 2010). Signalling through co-stimulatory receptors is also important for promoting the sustained activation of mTOR through activation of the PI3K-AKT pathway. mTOR is a threonine/serine kinase, that plays an important role in regulating cell proliferation, metabolism, and T cell fate decisions. mTOR can form two different protein complexes, MTORC1 and MTORC2, both of which are activated following TCR signalling through multiple pathways that integrate input signals from co-stimulatory receptors, cytokines, growth factors and nutrients (Chi, 2012).

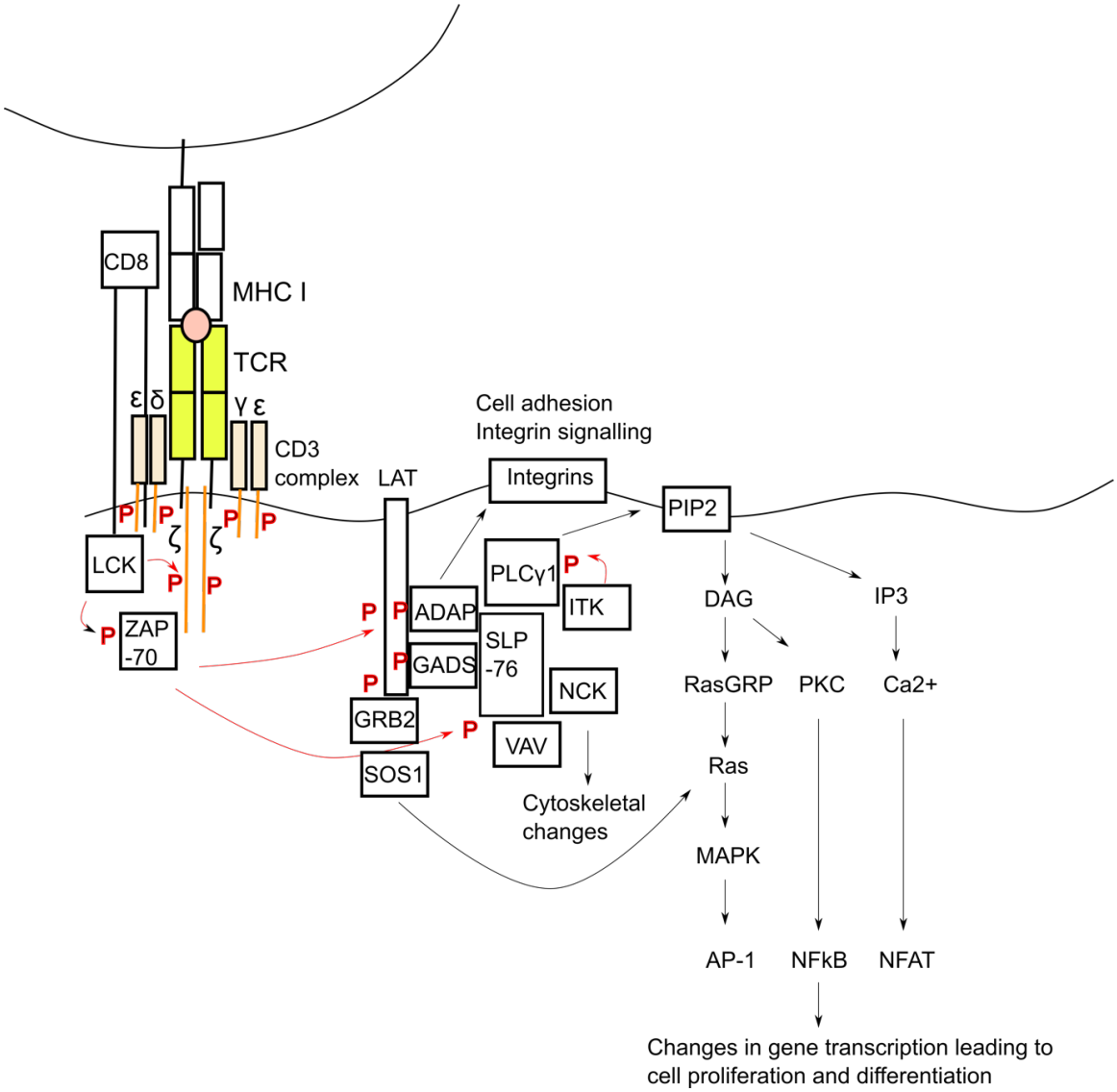

Figure 1.1 TCR signalling pathway
A simplified figure depicting the TCR signalling pathway in $CD8^+$ T cells. Antigen is presented on MHC Class I to the TCR. Lck, which interacts with the CD8 co-receptor, phosphorylates ITAMs in CD3 chains and the associated ζ chains. ZAP-70 binds to the ITAMs and is also phosphorylated by Lck. ZAP-70 can then phosphorylate LAT and SLP-76. This leads to recruitment of multiple effector molecules such as GRB2 family proteins, ADAP, VAV, NCK, PLCγ1 and ITK. ITK phosphorylates PLCγ1 which catalyses production of DAG and IP_3 from PIP_2, leading to the induction of key transcription factors AP-1, NF-κβ and NFAT that regulate cell proliferation and differentiation. ADAP initiates an integrin signalling pathway leading to changes in cell adhesion, and VAV and NCK induce a pathway leading to cytoskeletal changes.

1.3 Immune tolerance and regulation of TCR signalling

It is crucial that lymphocyte activation is tightly regulated in order to avoid autoimmunity and other immunological disorders. The activation of autoreactive immune cells can lead to the development of autoimmune diseases such as multiple sclerosis, type I diabetes, psoriasis and systemic lupus erythematous (SLE). Failure of immune checkpoints can also result in unregulated proliferation and expansion of immune cells, leading to lymphoma or leukaemia (Goodnow, 2007; Brownlie and Zamoyska, 2013). In a healthy body, many immune checkpoints exist to prevent the maturation and activation of self-reactive cells. T cells require multiple signals for full activation, with insufficient signals such as TCR stimulation in the absence of co-stimulatory signals, can lead to cell death or anergy (Schwartz, 2003). Many negative feedback loops also control the extent of TCR signalling (Gaud, Lesourne and Love, 2018). Furthermore, Tregs limit the extent of immune responses in the periphery and can dampen the response (Dario A. A. Vignali, 2008).

1.3.1 Self-reactivity and T cell development

T cell autoreactivity is regulated on many levels starting with development in the thymus, where cells undergo positive and negative selection leading to the release of a select repertoire of T cells. T cell progenitors are produced in the bone marrow, from where they migrate to the thymus to undergo maturation. In the thymus, the T cells undergo recombination of their variable (V), diversity (D) and joining (J) gene segments to form their TCR α and β chains, which are expressed alongside the co-receptors CD4 and CD8 (Schatz and Ji, 2011). The functionality of the newly expressed αβTCR is then tested during positive selection for binding pMHC presented by cortical thymic epithelial cells. Cells that express TCRs that do not mediate positive selection (nearly 90%) are subject to ‘death by neglect’. Next, the cells undergo negative selection to eliminate cells that are strongly autoreactive. Medullary thymic epithelial cells express a range of otherwise tissue-restricted antigens; strong binding to these

leads to cell death or in the case of $CD4^+$ T cells can lead to deviation into $Foxp3^+$ Tregs. (Miosge and Zamoyska, 2007; Klein *et al.*, 2014)

Thymic positive selection requires weak interactions with self-antigen to ensure functionality of the TCR, meaning that T cells are inherently self-reactive. Even in the periphery T cells homeostasis relies on weak interactions with self-pMHC alongside cytokine signals (Tanchot, Lemonnier and Perarnau, 1997; Seddon and Zamoyska, 2003). Therefore, the TCR must be able to differentiate between self-pMHC complexes and foreign peptide, to prevent autoimmunity. The kinetic proofreading model postulates that for signalling to occur, a significant threshold must be crossed in a chain of events before TCR-pMHC dissociation. Several intermediate rate-limiting steps are required between ligand recognition and signal transmission, such as recruitment of active Lck to the TCR by the CD4 and CD8 co-receptors, and phosphorylation the TCR complex and ZAP-70. This allows discrimination between high and low affinity agonists. (Mckeithan, 1995; Stepanek *et al.*, 2014). TCR signalling also appears to be subject to stage-specific tuning, allowing the signalling threshold to be adjusted for positive selection to take place during T cell development, but to allow mature naive T cells to weakly bind self-pMHC for homeostatic proliferation and maintenance (Surh and Sprent, 2008; Cho and Sprent, 2018). Pre-selection thymocytes have been shown to be more responsive to low affinity agonists than mature cells (Davey *et al.*, 1998). Positive selection leads to the selection of responsive, proficient cells that also respond well to foreign peptide (Mandl *et al.*, 2013). The expression of the transmembrane receptor CD5, the level of which is determined during thymic development, correlates with high affinity to self-pMHC, but is also linked to high responsiveness to foreign peptide (Azzam *et al.*, 1998; Klein *et al.*, 2014; Cho and Sprent, 2018).

1.3.2 Regulation of TCR signalling

TCR signalling is regulated through a vast range of control mechanisms and feedback loops (Gaud, Lesourne and Love, 2018). Protein tyrosine phosphorylation is a key property of TCR signalling and cell activation, thus interfering with it is an important regulatory mechanism. Negative regulators of TCR signalling include inhibitory protein tyrosine kinases such as Csk, and protein tyrosine phosphatases, which include cytoplasmic phosphatases such as SHP-1 and PTPN22, and receptor-like phosphatases like CD45 (Veillette, Latour and Davidson, 2002; Hermiston, Xu and Weiss, 2003; Pao *et al.*, 2007). Lipid phosphatases including SHIP1, SHIP2 and PTEN are also important. Following TCR signalling, negative feedback mechanisms are rapidly activated to control extent of signalling. Phosphatases are recruited to the TCR to regulate signalling by dephosphorylating key signalling molecules. For example, PTPN22 has been shown to limit signalling through the TCR in response to weak agonists, without compromising responses to strong agonists (Salmond *et al.*, 2014). The scaffold molecule LAT not only promotes TCR signal propagation, but also controls the formation of a negative signalling complex (Dong *et al.*, 2006). Sustained signalling through the TCR also leads to the upregulation of co-inhibitory receptors such as CTLA4 and PD-1. These inhibitory receptors function by sequestering ligands that bind co-stimulatory receptors, and by recruiting phosphatases or other molecules that negatively regulate TCR signalling (Thaventhiran, 2013). For example, CTLA-4 competes with CD28 for co-stimulatory signals and can also bind the tyrosine phosphatase SHP-1.

1.4 Effector and memory T cell differentiation

1.4.1 T cell fate decisions

An important quality of all lymphocytes is the capability to persist to form a long-lasting memory cell population that protects from subsequent infection. While some T cells differentiate into short-lived effector cells, others become

memory cells. These have traditionally been differentiated by markers such as KLRG1 that is characteristic of short-lived effector cells, and IL-7R that is expressed by memory cells (Kaech *et al.*, 2003). It is commonly accepted that every cell has the potential to either become an effector or a memory cell, and this is determined by a number of signals received by the cells during or after activation (Stemberger *et al.*, 2007). The point at which cell fate is decided is controversial. It has been suggested that asymmetric cell division leads to a 'pre-effector' and a 'pre-memory' daughter cell after the first cell division following activation (Chang *et al.*, 2007). The opposing line of thought suggests that the divide occurs later, with an initial homogeneous pool of cells and gradual acquisition of short-lived effector or memory cell functions. In either case differentiation into effector and memory cells is likely to be influenced by the strength and duration of the initial TCR signal and co-stimulatory signals, as well as the microenvironment during activation and migration into tissues, such as exposure to cytokines, chemokines, nutrients and oxygen (Kaech and Cui, 2012).

1.4.2 Memory cell subsets

T cell memory was previously thought to be divided into 'central memory' (Tcm) and 'effector memory' (Tem), differentiated by the expression of homing receptors to secondary lymphoid organs by the former, or the absence from lymphoid organs and the capacity to rapidly produce effector molecules by the latter (Sallusto, Geginat and Lanzavecchia, 2004). It is however becoming increasingly clear that memory cells exist as more of a continuum and cannot be neatly divided into subgroups (Jameson and Masopust, 2018). Both Tcm and Tem are migratory cells, whereas another more recently discovered group of cells is non-migratory and resides in nonlymphoid tissues, named 'resident memory' (Trm) (Masopust *et al.*, 2001). These cells were initially thought to be part of the Tem population, due to shared characteristics like low expression of lymph node homing receptors CCR7 and CD62L and rapid execution of effector functions, but are now known to be a distinct population crucial for

protective immunity at barrier sites (Schenkel and Masopust, 2014). The circulating Tem pool is heterogeneous as well, and several populations of cells can be differentiated based on the expression of transcription factors and chemokine receptors such as CX3CR1 and CXCR3 (Gerlach *et al.*, 2016). The importance and durability of these different types of memory cells is not fully understood. It is generally thought that $CD8^+$ memory does not require continued exposure to antigen, but cells rely on cytokines such as IL-7 and IL-15 (Surh and Sprent, 2008). This however may hold more true for some types of memory cells than others, and *in vivo* re-exposure to antigen upon secondary or tertiary challenge could be an important factor in memory cell maintenance (Jameson and Masopust, 2018).

1.4.3 Molecular control of memory cell differentiation

Pairs of transcription factors are thought to control $CD8^+$ T cell differentiation. For example T-bet, and the related transcription factor Eomesodermin (Eomes) both play important roles in effector and memory cell differentiation (Pearce *et al.*, 2003; Sullivan *et al.*, 2003). The two transcription factors have partially redundant roles in supporting acquisition of effector cell functions, but their ratio may affect effector/memory cell differentiation. T-bet expression is induced rapidly by TCR signalling and IL-12, with Eomes expression induced slightly later by IL-2 with a further increase in memory cells. The exposure to inflammatory signals, such as IL-12, were shown to cause a gradient in T-bet expression, with high expressing cells becoming short-lived effector cells (Joshi *et al.*, 2007). Contrarily, Eomes expression has been shown to be repressed by IL-12 and instead was shown to increase in memory cells, with Eomes-deficient cells defective in long-term survival (Takemoto *et al.*, 2006; Banerjee *et al.*, 2010). Other pairs of transcription factor which regulate $CD8^+$ T cell differentiation include Id2 an Id3, and the pair Bcl-6 and Blimp1. Some of these transcription factors are expressed by many different types of cells and so the epigenetic landscape may be crucial in determining which genes

are rapidly accessible and transcribed after activation of specific transcription factors.

Cell metabolism is another important determinant of effector versus memory cell differentiation. Activated T cells must support an increase in protein, nucleic acid and phospholipid synthesis, and consequently upregulate amino acid, glucose and transferrin receptors and switch from oxidative phosphorylation to anaerobic glycolysis (Finlay and Cantrell, 2011). Memory cells resemble naive cells in their metabolism but are more poised to faster acquire effector-cell like metabolic profiles upon re-activation. The two mTOR complexes have recently been shown to differentially regulate $CD8^+$ T cell metabolism and memory formation. Several early studies showed that inhibiting the mTOR pathway with rapamycin enhanced memory cell differentiation, partly by affecting levels of T-bet and Eomes (Araki *et al.*, 2009; Rao *et al.*, 2010). More recently, mTORC1 was shown to promote glycolysis and efficient effector cell development from both naive and antigen-experienced cells and inhibited memory formation, whereas mTORC2 enhanced generation of memory (Pollizzi *et al.*, 2015).

1.5 microRNAs and the RNA-induced silencing complex

1.5.1 miRNA biogenesis and function

microRNAs (miRNAs) are short, 22-nucleotide non-coding RNAs that mediate gene silencing by binding their target messenger RNAs (mRNAs), and subsequently promoting their degradation and/or translational repression. miRNAs have been shown to be important for almost every process in the body, from development and cell differentiation to normal organ function and homeostasis. Deletion of the miRNA processing enzyme Dicer is embryonically lethal in mice (Bernstein *et al.*, 2003). Immune cells are also subject to regulation by miRNAs, and miRNA expression is crucial to the normal functioning of the immune system. Deregulation of miRNAs is associated with many pathologies, including cancer, inflammatory disorders

and autoimmunity (Lin and Gregory, 2015; Garo and Murugaiyan, 2016). Consequently, there is potential for miRNAs to be used as biomarkers or therapeutic targets (Luck, Muljo and Collins, 2015; Simpson and Ansel, 2015).

miRNAs are transcribed as a primary miRNA (pri-miRNA) duplex. A pri-miRNA can consist of a single miRNA or a cluster of miRNAs that are transcribed together. The pri-miRNA is processed by the enzymes Drosha and DGCR8 into a pre-miRNA, which is exported to the cytoplasm and cleaved by Dicer into a mature miRNA. In the cytoplasm, one of the strands of the mature miRNA is discarded (passenger strand), whereas the other (guide strand) is loaded on Argonaute (Ago) to form the RNA induced silencing complex (RISC) (Fig.1.2) (O'Connell *et al.*, 2010; Mehta and Baltimore, 2016). It is in this complex that miRNAs interact with their target mRNAs. This binding is mediated by the miRNA seed site, corresponding to nucleotides 2-7 of the 5' end. miRNA target sites are complementary to the miRNA seed and are usually found in the 3' untranslated region (3'UTR) of the target mRNA. A single miRNA can have the potential to target hundreds of genes, even though their effect is usually mild (Selbach *et al.*, 2008). Similarly, one gene can be targeted by multiple miRNAs. miRNAs can be grouped into families that have identical or similar seed sites, often resulting in repression of the same group of target genes. Cooperation of repression can occur with binding to multiple adjacent target sites on a single gene (Na and Kim, 2013; Mehta and Baltimore, 2016).

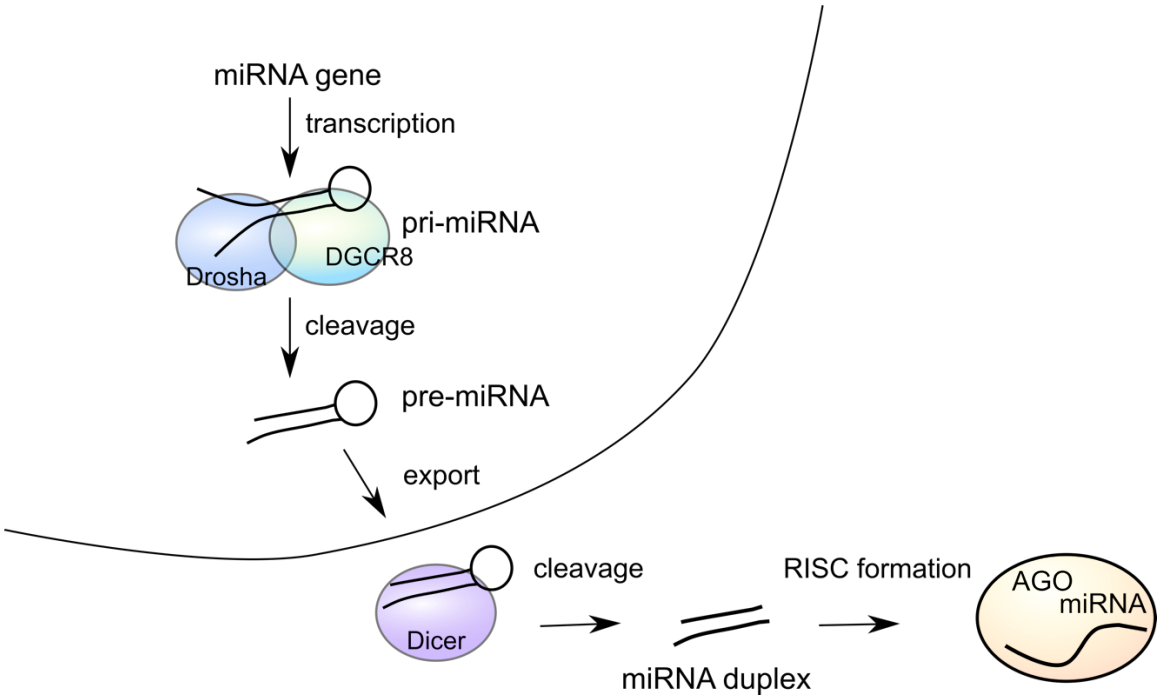

Figure 1.2 miRNA biogenesis pathway
After transcription of pri-miRNAs, these are first processed by Drosha and DGCR8 to pre-miRNA which is exported to the cytoplasm. It is then cleaved by Dicer into a miRNA duplex, from which a single strand is incorporated to RISC.

1.5.2 Ago function and interactions

miRNAs bind to their target mRNAs in the Ago-containing RISC. Ago proteins mediate miRNA target repression directly or through recruitment of other mRNA binding silencing proteins. Four homologues of the Ago protein exist in mammals: Ago 1-4, of which Ago-2 is unique in its ability to directly cleave target mRNAs. Ago proteins alone weight approximately 95kDa and can form small (250-350kDa), medium (600-700kDa) or high (>900kDa) molecular weight complexes by associating with gene silencing proteins (e.g. Dicer, GW182, TRBP), DEAD-box containing proteins (e.g. RNA helicase A), mRNA binding proteins (e.g. poly-A binding proteins), proteins involved in RNA metabolism and ribosomes (Höck *et al.*, 2007; Landthaler *et al.*, 2008).

One of the key interactors of Ago is GW182, which has been shown to be required for the miRNA silencing effect (Behm-Ansmant *et al.*, 2006; Eulalio, Huntzinger and Izaurralde, 2008). Through its N-terminal G (glycine) W (tryptophan)-repeats, GW182 binds to Ago PIWI domain, whereas through its C-terminus it recruits silencing effector proteins (Lazzaretti, Tournier and Izaurralde, 2009; Lian *et al.*, 2009). These mRNA binding proteins include poly(A) binding proteins (PABPs), deadenylases and decapping proteins, which together mediate target gene repression (Fig.1.3). CCR4:NOT deadenylase and DCP1:DCP2 decapping complexes were both shown to be required for target mRNA degradation (Behm-Ansmant *et al.*, 2006). GW182 also plays a role in promoting miRNA stability (Yao *et al.*, 2012). miRNA binding increases the affinity of Ago to GW182, promoting the interaction of the two proteins (Elkayam *et al.*, 2017). GW182 may bind multiple Ago proteins, and potentially cause translational repression of miRNA target sites on same or adjacent mRNAs (Lian *et al.*, 2009; Elkayam *et al.*, 2017).

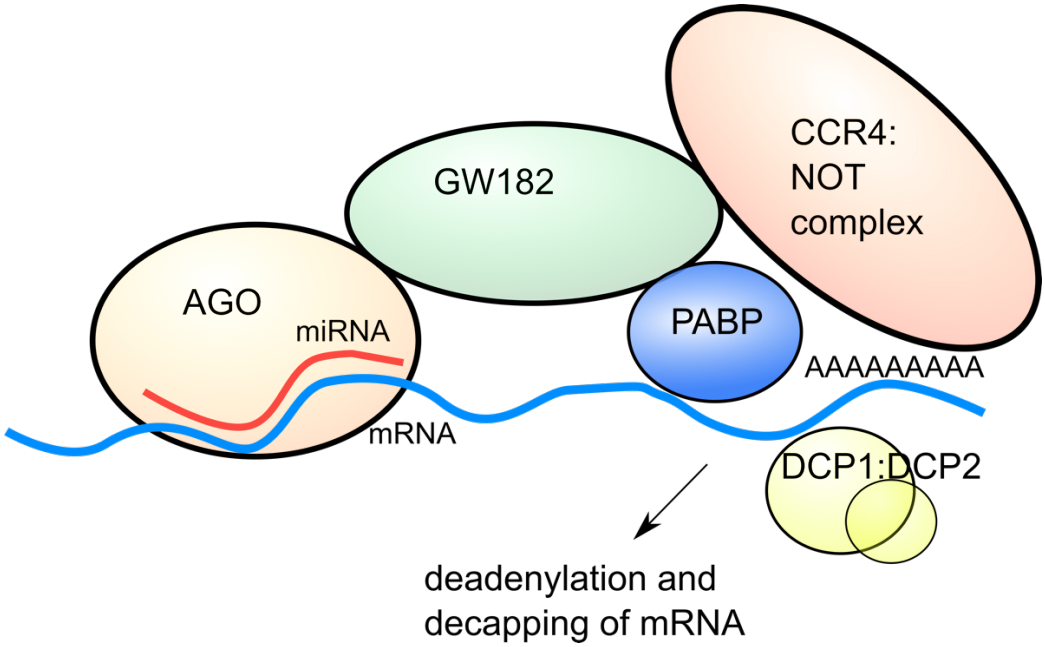

Figure 1.3 RISC and mRNA repression
A representation of RISC and associated proteins causing target mRNA repression. Ago-bound miRNAs bind their target mRNAs through complementarity in the miRNA seed and mRNA 3'UTR. Ago is bound by GW182, which recruits effector molecules such as PABPs, deadenylases (e.g. CCR4:NOT complex) and decapping proteins (e.g. DCP1:DCP2 complex) that bind the mRNA and cause its translational inhibition and/or degradation.

1.6 miRNA function in T cells

1.6.1 Importance of miRNAs for T cell development and function

miRNAs are known to regulate most aspects of T cell biology, from T cell development to cell activation, differentiation and effector and memory cell formation. Deletion of the miRNA biogenesis enzyme Dicer in the T cell lineage causes severe defects in T cell development and greatly reduces mature cell numbers in the periphery (Muljo *et al.*, 2005). The resulting $CD4^+$ T cells are defective in their response to stimulus, characterised by poor proliferation and aberrant cell differentiation and cytokine production (Muljo *et al.*, 2005). Dicer depletion also causes defects in Tregs, leading to immune pathology (Cobb *et al.*, 2006). In $CD8^+$ T cells, Dicer depletion causes stronger T cell activation *in vitro* and higher expression of the cytotoxic effector molecule perforin in CTLs (Zhang and Bevan, 2010; Trifari *et al.*, 2013). The cells initially proliferate more, but cell survival was reduced after two days. *In vivo*, the cells fail to expand and survive, partly due to failure to downregulate CD69 following activation to migrate from lymph nodes into tissues (Zhang and Bevan, 2010). Naive cells have no detectable phenotype, with comparable expression of markers such as CD44 and CD62L (Zhang and Bevan, 2010). Depletion of Ago-2 in T cells does not compromise cell development or homeostasis in the periphery. The proliferation of $CD4^+$ Ago-2 deficient cells was not affected, however as for the Dicer deficient $CD4^+$ T cells, cell differentiation and cytokine production was aberrant (Bronevetsky *et al.*, 2013).

1.6.2 Regulation of miRNA expression and function in T cells through transcriptional regulation and editing of miRNAs and targets

Globally, miRNA expression is downregulated upon T cell activation. Naive and memory cells generally express higher levels of miRNAs compared to effector T cells (Wu *et al.*, 2007). In $CD4^+$ T cells, *in vitro* stimulation with anti-CD3/CD28 was shown to cause downregulation of most miRNAs as early as

4 h after stimulation (Bronevetsky *et al.*, 2013). miRNA expression is regulated transcriptionally, in a similar way to protein-coding genes. In $CD4^+$ T cells, activation caused strong or moderate transcriptional induction, or downregulation of specific miRNAs (Bronevetsky *et al.*, 2013).

RNA editing can also affect miRNA function: modifications at the 5' end can alter the miRNA seed, whereas editing of the 3' end more commonly affects miRNA stability and turnover. Variants of the mature miRNA are named isomirs, and can differ in their sequence or length (Ameres and Zamore, 2013). Isomirs can arise from differential cleavage, RNA editing or non-template nucleotide addition (Gebert and MacRae, 2019). Pri-miRNAs and pre-miRNAs can be targeted by adenosine deaminase acting on RNA (ADAR) or cytidine deaminase acting on RNA (CDAR) proteins, which catalyse the conversion of adenosine to inosine, or cytidine to uracil, respectively. These modifications can alter the cleavage and export of the miRNA precursors, or cause changes in the miRNA seed. Alternative cleavage by Dicer and Drosha can also result in formation of isomirs. In $CD8^+$ T cells, alternative processing by Drosha has been demonstrated for miR-142 and miR-342 (Wu *et al.*, 2009). The shift in Drosha processing generated three different pre-miRNAs from the single miR-142 pri-miRNA. The three miR-142 variants differed in their seed sequence, and most of the predicted targets were different. Interestingly, one variant seemed to be dominant in thymocytes, and another in mature naive $CD8^+$ T cells. Finally, mature miRNAs can be edited through non-template nucleotide addition, such as 3' adenylation or 3' uridylation. Terminal uridylyltransferase 4 (TUT4) mediated uridylation has been shown to cause miRNA downregulation during $CD4^+$ T cell activation (Gutiérrez-Vázquez *et al.*, 2017). The 3' uridylation was observed in naive cells, and following activation the 3' uridylated miRNAs were degraded, alongside downregulation of the TUT4 enzyme.

miRNA function can also be regulated through their target sites. Formation of mRNA 3' UTR isoforms or altering of the 3' UTR can add or remove miRNA

target sites. In $CD4^+$ T cells, activation induced shortening of the 3' UTR of mRNAs was shown to decrease miRNA mediated regulation of some transcripts (Sandberg *et al.*, 2008). High target concentration may result in weaker miRNA activity. Large availability of targets can lead to diminished effect on each individual target (Arvey *et al.*, 2010). By calculating a cellular target-to-miRNA ratio, a trend was found between weaker miRNA activity and higher target concentration (Mullokandov *et al.*, 2012). On the other hand, a different study however found that overexpression of a mRNA with miRNA target sites caused increased RISC association of the miRNA (Flores *et al.*, 2014).

1.6.3 Regulation of Ago and RISC formation during T cell activation

miRNA accumulation can also be controlled at the level of the proteins involved in miRNA biogenesis and function, such as Dicer, Drosha, Ago and GW182. Strong inflammatory signals were shown to downregulate Dicer in CTLs (Trifari *et al.*, 2013). This did not however have a major effect on miRNA expression, with only a slight decrease in some lowly expressed miRNAs in the inflammatory conditions. Global downregulation of Ago proteins has been suggested to contribute to miRNA downregulation during $CD4^+$ T cell activation. Ago proteins were shown to be ubiquitinylated during activation, and the amount of Ago was limiting to for $CD4^+$ T cell miRNA expression, with Ago-2 deficient cells expressing less miRNA (Bronevetsky *et al.*, 2013). Ago degradation was therefore suggested to contribute to the global miRNA downregulation, leading to fast miRNA turnover and remodelling of the miRNA repertoire (Bronevetsky and Ansel, 2013).

Additionally, Ago modifications such as phosphorylation may influence its function and interaction with other proteins. Target engagement was shown to induce phosphorylation of Ago-2 on S824-834, followed by rapid dephosphorylation. Phosphorylation inhibited target mRNA binding, perhaps limiting the length of Ago-target interaction and allowing rapid turnover and

efficient suppression of targets (Golden *et al.*, 2017). Ago-2 phosphorylation on S387 by Akt was shown to promote interaction with LIMD1, which in turn lead to interaction with GW182 (Horman *et al.*, 2013; Bridge *et al.*, 2017). In actively proliferating cells such as cancer cells or activated T cells, Ago is mainly found in a high molecular weight (HMW) RISC, interacting with GW182 and other proteins (Olejniczak *et al.*, 2013). In T cells, the PI3K-Akt-mTOR pathway has been shown to promote expression of GW182 and the formation of HMW RISC in activated T cells. In naive T cells, Ago is predominantly found in low molecular weight (LMW) RISC corresponding to the molecular weight of Ago and non-target bound miRNA (La Rocca *et al.*, 2015). GW182 is not expressed in naive T cells and its expression correlated with HMW RISC formation following activation. Inhibition of PI3K and mTOR caused a reduction in GW182 expression and HMW RISC formation, whereas a constitutively active Akt in a cell line lead to increased HMW RISC formation (La Rocca *et al.*, 2015). The PI3K-Akt-mTOR pathway may therefore promote GW182 expression as well as its interaction with Ago.

Formation of HMW RISC was shown to be crucial for regulation of miRNA suppressive function in T cells. Knocking down GW182 expression in T cells led to decreased miRNA target repression (La Rocca *et al.*, 2015). T cell activation caused a global shift of miRNAs into HMW RISC, irrespective of changes in miRNA expression. miRNAs found in HMW RISC were shown to be more efficient at repressing their targets despite downregulation in their expression. For example, let-7 family miRNAs were shown to be downregulated upon activation, but were more efficient at repressing a target reporter in activated cells (La Rocca *et al.,* 2015). There were individual differences in the extent of recruitment to HMW RISC, allowing for an additional layer of regulation in miRNA function in T cells. Despite global downregulation of miRNAs, some of these may be more functional in activated T cells, where they associate with HMW RISC.

1.7 Key miRNAs and their targets in CD8$^+$ T cells

miRNAs have been shown to regulate most aspects of T cell activation, from TCR signalling to the acquisition of effector functions, cell migration, proliferation and survival, and the differentiation to long-lived memory cells. Key miRNAs and their relevant targets in CD8$^+$ T cells in these processes are summarised in Figure 1.4 and described in the following paragraphs.

Globally, miRNA expression is downregulated during T cell activation, with generally higher expression of miRNAs in naive and memory T cells compared to effector T cells (Wu *et al.*, 2007). Expression studies have identified the most abundant miRNAs in CD8$^+$ T cells. A small number of miRNAs were found to be highly expressed: miR-16, miR-21, miR-142-3p, miR-142-5p, miR-150, miR-15b and let-7f were shown to account for over half the expressed miRNAs in *in vitro* generated CTLs (Wu *et al.*, 2007). During *in vivo* LCMV infection, mR-155 and members of the miR-17~92 cluster were shown to be highly expressed in effector cells compared to naive or memory cells (Wu *et al.*, 2007).

1.7.1 miRNAs and their targets in the TCR signalling pathway

Several miRNAs have been shown to target components of the TCR signalling pathway and affect T cell early activation. miR-181 is a key regulator of TCR signalling threshold and targets many phosphatases associated with the TCR, including Dusp5, Dusp6, Ptpn22 and Shp-2 (Li *et al.*, 2007). Suppression of these phosphatases elevates TCR signalling in developing thymocytes, in which miR-181 expression is high, allowing positive selection to take place. miR-181 is crucial for TCR signal tuning and maintenance of tolerance, with deficiency leads to maturation of autoreactive cells in the thymus (Ebert *et al.*, 2009).

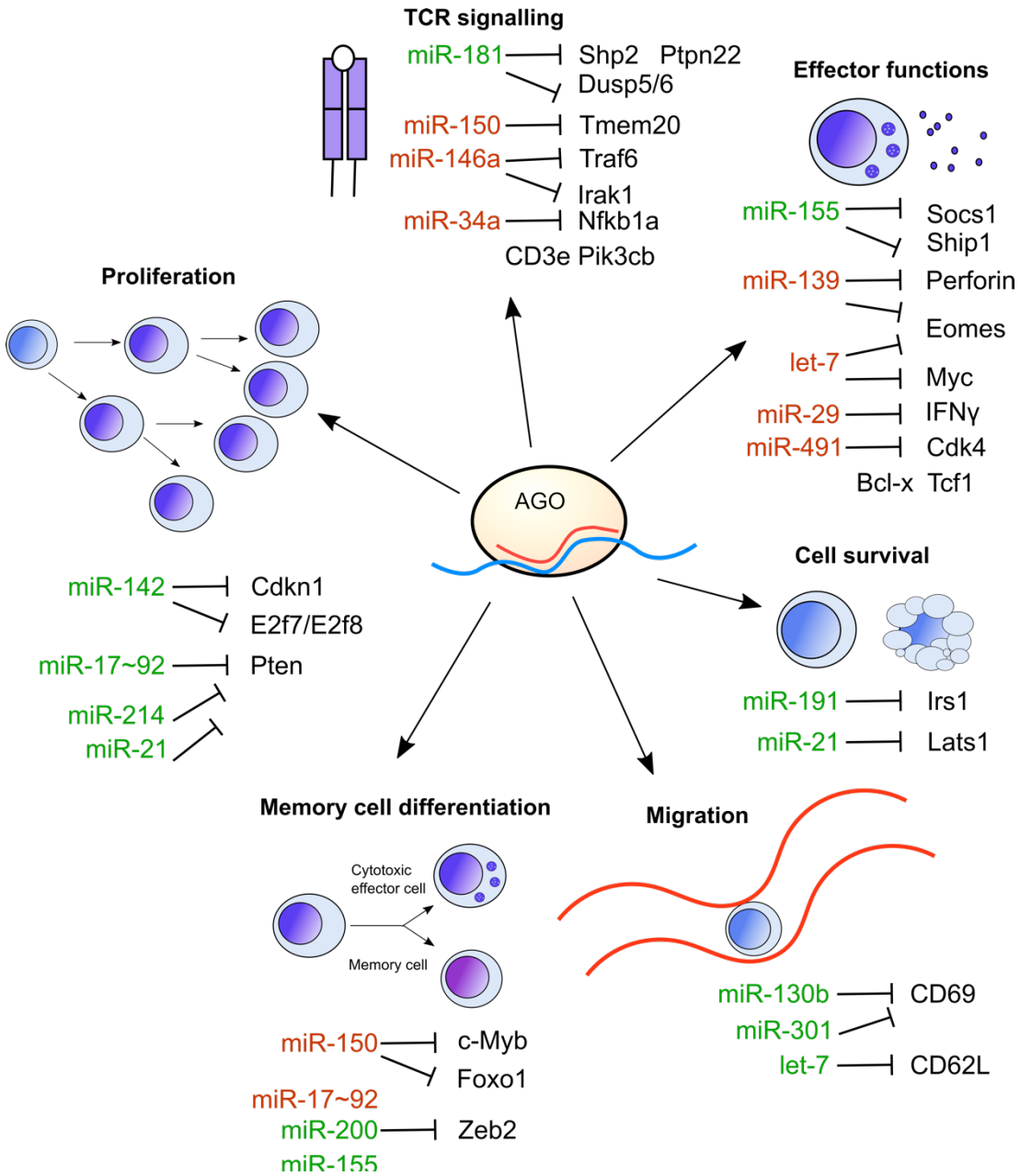

Figure 1.4 miRNAs and their targets in CD8⁺ T cells
A summary of key miRNAs and their target genes in different aspects of CD8⁺ T cell activation and differentiation (TCR signalling, acquisition of effector functions, cell survival, migration, memory cell differentiation and proliferation). When miRNA inhibition of its targets positively affects the described process (e.g. TCR signalling), this miRNA is coloured green, whereas negatively regulating miRNAs are red.

miR-146a is a miRNA that is upregulated by NF-κβ following TCR signalling. It subsequently initiates a negative feedback loop that downregulates NF-κβ through targeting the signal transducer Traf6 and Irak1 (Yang *et al.*, 2012). In the absence of miR-146a, T cells exhibit hyperresponsiveness characterised by increased proliferation, cytokine production and lengthened survival. NF-κβ signalling was recently also shown to be negatively regulated by miR-34a. This miRNAs was shown to be gradually upregulated in activated T cells and targeted multiple components of the NF-κβ signalling pathway, including Nfkb1s, Cd3e and Pik3cb, leading to reduced cytotoxicity (Hart *et al.*, 2019). Finally, miR-150 was recently shown to affect TCR signalling through playing an important role in regulating intracellular Ca^{2+} stores in naive $CD8^+$ T cells (Kim *et al.*, 2017). miR-150 deficiency increased levels of its target Tmem20, leading to an increase in intracellular Ca^{2+}. This caused defects in subsequent T cell activation following stimulation, leading to an anergic phenotype.

1.7.2 Negative regulators of T cell effector functions

T cell activation results in widespread downregulation of miRNAs, which relieves the suppression on transcription factors and molecules needed for effector cell differentiation. For example, miR-139 and the let-7 family have been shown to target key transcription factors needed for effector cell differentiation. miR-139 was shown to target the transcription factor Eomes and the effector molecule perforin in CTLs. Its rapid downregulation upon activation allowed effector cell differentiation, whereas forced expression was disadvantageous for T cell function in infection (Trifari *et al.*, 2013). Members of the let-7 miRNA family have also been shown to be downregulated in $CD8^+$ T cells upon activation, and their forced expression resulted in defects in proliferation and effector function (Wells *et al.*, 2017). In contrast, knockdown of this family was shown to improve effector function and responses *in vivo*. This miRNA family has also been shown to target key transcription factors like Eomes and Myc in $CD8^+$ T cells, as well as components of the mTOR signalling pathway in $CD4^+$ T cells (Marcais *et al.*, 2014; Wells *et al.*, 2017). The miR-

15/16 cluster was also shown to target the mTOR pathway in $CD8^+$ T cells, with deficiency in these miRNAs improving $CD8^+$ T cell effector functions and tumour clearance (Yang *et al.*, 2017).

Other miRNAs have been shown to directly target effector molecules such as cytokines. miR-29a and miR-29b have been shown to be downregulated to allow IFN-γ production in both $CD4^+$ and $CD8^+$ T cells (Ma *et al.*, 2011). miR-29 was shown to directly inhibit IFN-γ mRNA and suppressed responses to intracellular bacteria. Effector functions are also attenuated by the miR-23a~24~27a cluster, that has been shown to target IFNγ and Blimp-1 and reduced $CD8^+$ T cell cytotoxicity (Chandran *et al.*, 2014). The cluster can be induced by transforming growth factor (TGF-β) and was shown to inhibit anti-tumour responses in both human and mouse CTLs (Lin, 2014). Tumour-derived TGF-β has also been shown to cause upregulation of another negative regulator of T cell responses, miR-491 (Yu *et al.*, 2016). This miRNA was shown to inhibit T cell proliferation and effector responses and promote apoptosis through targeting of Cdk4, Bcl-xl and Tcf1, leading to defective anti-tumour responses.

1.7.3 miRNA function in supporting T cell proliferation, survival and acquisition of effector functions

Following engagement of the TCR, $CD8^+$ T cells rapidly begin proliferating and differentiate into cytotoxic effector cells. Several miRNAs are upregulated upon T cell activation and are required for sustained proliferation and cell survival. miR-155 is a key miRNA for T cell activation and function. It is upregulated *in vitro* in a TCR-signal strength dependant manner as well as *in vivo* during LCMV infection (Dudda *et al.*, 2013). miR-155 deficiency causes a failure in T cell expansion and impairs responses to infectious challenge and tumours (Dudda *et al.*, 2013; Lind, Elford and Ohashi, 2013). In contrast, miR-155 overexpression has been shown to enhance $CD8^+$ T cell responses *in vivo* (Gracias *et al.*, 2013). There has been some debate on the targets of miR-155

in $CD8^+$ T cells, but it has been suggested to target components of a number of T-cell signalling pathways in particular those related to cytokine and interferon signalling. The STAT5 signalling pathway has been suggested to be induced by miR-155 through targeting of Socs1 and Ptpn2 (Dudda *et al.*, 2013; Ji *et al.*, 2015). miR-155 has also been suggested to target negative regulators the Akt-dependent pro-survival pathway, specifically Ship1 (Lind, Elford and Ohashi, 2013; Ji *et al.*, 2015). miR-155 has been proposed to mediate its function through the synergistic effect of modest downregulation of many target gene groups, as opposed to having one key target (Gracias *et al.*, 2013).

Another important group of miRNAs for promoting $CD8^+$ T cell proliferation and survival are members of the miR-17~92 cluster. Six miRNAs comprise the cluster: mR-17, miR-18a, miR-19a, miR-20a, miR-19b-1 and miR-92a-1 (Mogilyansky and Rigoutsos, 2013). Clustered miRNAs are transcribed as one unit, but the individual miRNAs are subject to post-transcriptional processing, maturation and stability. These miRNAs are often thought to target same or overlapping mRNAs or pathways, but this is not always the case, and the miRNAs may even antagonise one another. (Lai and Xiao, 2015) The miRNAs of the cluster are strongly induced during $CD8^+$ T cell activation to promote cell cycle progression; deficiency in the cluster results in impaired proliferation and expansion of $CD8^+$ T cells *in vitro* and *in vivo* during LCMV infection (Wu *et al.*, 2012; Khan *et al.*, 2013). The cluster has been suggested to target Pten, Pd1 and Btla, which are negative regulators of the mTOR pathway (Wu *et al.*, 2012). These proteins were found to be less expressed in miR17~92 overexpressing cells, and in particular Pten was found to contain target sites for 5 family members of the cluster. Pten has also been shown to be targeted by other miRNAs in T cells, such as miR-21 and miR-214. The latter has been shown to promote T cell proliferation following activation (Jindra *et al.*, 2010). miR-21 has been shown to improve anti-tumour responses and was also suggested to achieve this through targeting of Pten (He *et al.*, 2017). miR-21 is also induced upon T cell activation and has been suggested to inhibit cell apoptosis through targeting of Lats-1 (Meisgen *et al.*, 2012; Teteloshvili *et al.*,

2017). Another miRNA affecting T cell proliferation is miR-142. Deficiency in this miRNA causes cell cycling defects in thymocytes and mature T cells. miR-142 is thought to promote expression of cell-cycle promoting genes through targets such as Cdkn1b and the atypical E2f transcription factors E2f7 an E2f8 (Sun *et al.*, 2015; Mildner *et al.*, 2017). miR-191 has been shown to target Irs1 and support T cell survival during cytokine-mediated homeostatic maintenance of peripheral T cells, and to further promote survival during effector responses (Lykken and Li, 2016). Finally, miR-31 is another miRNA that is induced following T cell activation. This miRNA has been suggested to promote IL-2 production through inhibition of its suppressor Ksr2 (Xue *et al.*, 2013). However in chronic viral infection this miRNA was shown to contribute to $CD8^+$ T cell exhaustion, through targeting Ppp6c that regulates responsiveness to interferons (Moffett *et al.*, 2017).

1.7.4 The role of miRNAs in $CD8^+$ T cell short-lived effector and memory cell differentiation

Many miRNAs that are downregulated upon activation are re-expressed during the contraction phase of the immune response and memory cell differentiation, as cells cease proliferating and no longer need to produce effector molecules. Some miRNAs that are needed for T cell activation are also important for memory cell formation, such as miR-155. Deficiency causes a failure to expand at peak of infection and impaired memory formation three months later (Dudda *et al.*, 2013). Deficiency has been shown to result in fewer effector - and central memory cells (Gracias *et al.*, 2013) though one study found preferential differentiation to central memory (Tsai *et al.*, 2013). The miR-200 family has been shown to be required for optimal $CD8^+$ T cell memory formation, through targeting the terminal differentiation promoting transcription factor Zeb2 (Guan *et al.*, 2018).

Other miRNAs are required for the initial activation and promote skewing to short-lived effector cells, so their downregulation is crucial for memory cell

differentiation. The expression of the miR-17~92 cluster peaks in actively proliferating cells during day 5 of infection and is then downregulated by day 8 during the contraction phase and memory cell differentiation. Forced expression of the cluster causes skewing to short-lived effector cell differentiation and impairs memory formation (Wu *et al.*, 2012; Khan *et al.*, 2013). Another miRNA that promotes the differentiation of short-lived effector cells is miR-150. This was suggested to be through targeting of c-Myb and Foxo1. Its downregulation appears necessary for efficient memory formation, and miR-150 deficient cells were shown to preferentially differentiate into memory cells (Ban *et al.*, 2017; Chen *et al.*, 2017).

1.8 Aims of the PhD project

$CD8^+$ T cell activation and differentiation is known to be regulated by a network of miRNAs. These miRNAs have generally been identified through studying expression changes of miRNAs, and potential targets have been determined using bioinformatic predictions based on the miRNA seed region. Recent work has shown, that miRNA expression may not be the only determinant of its biological function. Formation of HMW RISC was shown to additionally promote the function of specific miRNAs in activated T cells, irrespective of changes in expression. Furthermore, since miRNAs often have the potential to target hundreds of mRNAs, it is often difficult to decipher the biologically relevant targets from bioinformatic predictions. However, knowing miRNA targets is crucial to understanding their function. Novel biochemical methods that use cross-linking of RNA to proteins, and ligation of miRNAs to their target mRNAs have the potential to directly determine miRNA targets. Therefore, in this project we aimed to study the following questions:

1. Is HMW RISC formed in $CD8^+$ T cells activated with an agonist peptide? What is the role of GW182 in this?
2. Are specific miRNAs associated with HMW and LMW RISC in activated $CD8^+$ T cells? Can we identify biologically active miRNAs from HMW RISC? (Fig.1.5)
3. What are the mRNA targets of these miRNAs?

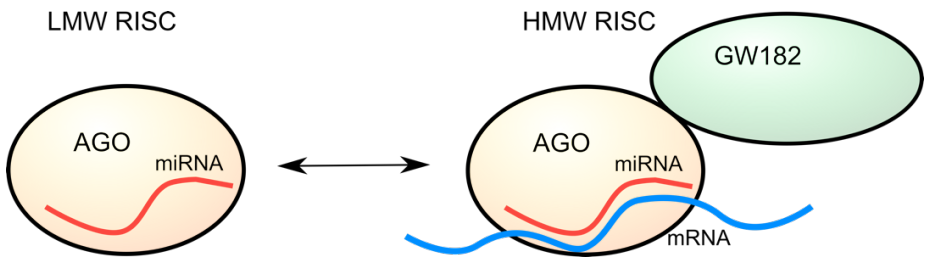

Figure 1.5 miRNA association with LMW and HMW RISC
Activated T cells have been shown to contain both LMW and HMW RISC but miRNAs interacting with target mRNAs were suggested to be predominantly found in the latter. Can we enrich for biologically active miRNAs and their targets by purifying HMW RISC?

CHAPTER 2: Materials and Methods

2.1 List of buffers

Facs buffer (in PBS)

2.5 % FBS
0.05 % sodium azide

WB washing buffer (in PBS)

0.05 % Tween20

WB transfer buffer

24 mM Tris base
192 mM glycine
20 % methanol

CLASH lysis buffer

50 mM Tris/HCl pH=7.8
300 mM NaCl
1% Triton X100
5 mM EDTA
10 % glycerol

Low salt (LS) IP wash buffer

50 mM Tris/HCl pH= 7.5
0.3 M NaCl
5 mM MgCl2
0.5 % Triton x100
2.5 % glycerol

High salt (HS) IP wash buffer

50 mM Tris/HCl pH=7.5
0.8 M NaCl
10 mM MgCl2
0.5 % Triton x100
2.5 % glycerol

Proteinase K buffer

50 mM Tris/HCl pH=7.8
50 mM NaCl

10 mM imidazole
0.1 % NP-40
5 mM EDTA
5 mM beta-Mercaptoethanol

PNK buffer

50 mM Tris/HCl pH=7.5
10 mM MgCl2
0.5 % Triton X100
50 mM NaCl

Elution buffer

4x LDS loading dye diluted in PNK buffer
50mM DTT

Superose 6 lysis buffer

150 mM NaCl
10 mM Tris/HCl pH=7.5
2.5 mM MgCl2
0.01 % Triton x100
1 mM DTT

Superose 6 buffer

150 mM NaCl
10 mM Tris/HCl pH=7.5
2.5 mM MgCl2
0.01 % reduced Triton x100

2.2 Mice

All mice were maintained and bred in pathogen-free conditions at the University of Edinburgh animal facilities in accordance with the UK Home Office and local ethically approved guidelines.

2.2.1 OT-I hom RAG1$^{-/-}$ mice

The OT-I TCR is MHC Class I restricted and binds the N4 peptide (SIINFEKL), corresponding to ovalbumin residues 257-264. RAG1$^{-/-}$ mice are deficient in the Rag-1 recombinase required for T and B cell receptor recombination, thus

only express the transgenic OT-I TCR (Mombaerts *et al.,* 1992; Hogquist *et al.,* 1994). The mice are on the C57BL/6 genetic background.

2.2.2 Ago-2-flag OT-I hom RAG1$^{-/-}$ mice

For some experiments, Ago-2-flag mice were used. These mice have a Flag-purification tag, PreScission cleavage site and 6x His tag inserted at the 5' end of Ago-2, before Exon 1. The knock-in mice were generated at the University of Edinburgh by using gene targeting to insert the tag. For some experiments (where indicated in the figure legends), these mice were used as well as, or instead of the OT-I hom RAG1$^{-/-}$ mice.

2.3 T cell culture

2.3.1 Preparation of single cell suspensions and cell counts

Single cell suspensions were prepared mechanically from mouse lymph nodes using a 70 µm filter. Cells were washed by centrifugation at 300 x g for 5 min in cell culture medium. Cells were grown in Iscove's Modified Dulbecco's Medium (IMDM, Sigma Aldrich) supplemented with 10% Heat inactivated Fetal Calf Serum (FCS, Gibco), 100 U/mL Streptomycin (Gibco), 100 µg/mL penicillin (Gibco), 2 mM L-glutamine (Gibco) and 50 µM β-mercaptoethanol. Cells were counted using CASY cell counter (OMNI Life Science).

2.3.2 OT-I T cell activation and differentiation

To activate OT-I cells, 2 x 10^6 cells/mL were grown in media supplemented with 10 nM N4, T4 or G4 for 2 days. For effector or memory cell differentiation, cells were activated with N4 as before for two days, then resuspended at 2 x 10^5 cells/mL in media supplemented with 20 ng/mL IL-2 (for effector cells, PeproTech) or 20 ng/mL IL-15 (for memory cells, PeproTech).

2.3.3 miRNA inhibition

miRNA inhibitors (miRCURY LNA miRNA power inhibitor with 5'-FAM, Qiagen) were added directly to culture media at the time of activation. 500 nM miRNA inhibitor (mmu-mir-7a-5p) or control inhibitor (negative control A) was added

to naive T cells in cell culture media with N4, and phenotype was assessed after 48 h.

2.3.4 Ago-GW182 blocking peptide

A peptide was designed to bind Ago-2 and block its binding to GW182, based on the known Ago binding motif (Elkayam *et al.*, 2017). The Ago binding motif sequence was fused to a self-translocating peptide sequence, TP2 (He *et al.*, 2013). For a control, key Ago-binding residues were replaced with alanines (Fig.2.1). The peptides were synthesised by Royo Biotech. The peptides were incubated with cell lysates *in vitro* at 10-50 μM.

TP2 + AGO BINDING MOTIF 1
PLIYLRLLRGQFGGVNRTDLDPRVL**S**NSG**W**GQTPIK**Q**N**T**A**W**DTETSPRGER**K**TDC

CONTROL TP2
PLIYLRLLRGQFGGVNRTDLDPRVL**A**NSG**A**GQTPIK**A**N**A**A**A**DTETSPRGER**A**TDC

Figure 2.1 Blocking peptide sequence
The blue part shows the translocating peptide TP2 sequence, followed by two glycines and the Ago binding motif in red. Key residues for Ago-binding have been replaced with alanines for the control peptide (highlighted in green).

2.4 Flow cytometry

Specificity	Conjugate	Clone	Host	Conc.	Supplier
CD8b	PE/Cy7	H35-17.2	Rat	1:400	eBioscience
CD25	APC	PC61.5	Rat	1:200	eBioscience
CD25	Alexa Fluor 488	PC61	Rat	1:200	Biolegend
CD44	APC eFluor 780	IM7	Rat	1:200	eBioscience
CD62L	APC	MEL-14	Rat	1:200	Biolegend
CD69	APC	H1.2F3	Hamster	1:200	Biolegend
CD71	PE/Cy7	RI7217	Rat	1:200	Biolegend
Intracellular stains					
Ki67	FITC	B56	Mouse	1:100	BD Biosciences
IFNγ	Alexa Fluor 488	XMG1.2	Rat	1:400	Biolegend
TNFα	PercP/Cy5.5	MP6-XT22	Rat	1:200	BD Biosciences
Granzyme B	Pacific Blue	GB11	Mouse	1:100	Biolegend
Eomesodermin	eFluor 660	Dan11mag	Rat	1:100	eBioscience
T-bet	PercP Cy5.5 or PE	4B10	Mouse	1:100	eBioscience
IRF4	eFluor 450	3E4	Rat	1:100	eBioscience

Table 2.1 Table of antibodies used for flow cytometry staining.

2.4.1 Surface staining

Flow cytometry staining was undertaken in 96-well round-bottom plates with a minimum of 200,000 cells per well. Washing steps were performed by filling the wells with Phosphate Buffered Saline (PBS) or Facs buffer, and centrifuging the plate at 300 x g for 3 min then discarding the supernatant. Prior to staining, cells were washed in PBS. For staining dead cells, cell pellets were resuspended in LIVE/DEAD Fixable Aqua or Far Red Dead Cell Stain (Thermo Scientific) diluted in PBS at 1:700, and incubated at room temperature for 10 min. The cells were then washed in Facs buffer. For surface staining, antibodies were diluted in Facs buffer then incubated with the cells for 15 min at room temperature (Table 2.1). The cells were then washed in Facs buffer and resuspended in PBS for analysis on MacsQuant Analyzer 10.

2.4.2 Cytokine staining and intranuclear staining

Prior to measuring cytokine production, cells were re-stimulated with N4 in medium containing 2.5 µg/mL Brefeldin A (Cambridge Bioscience) for 4 h. Cells were then centrifuged, washed in Facs buffer and incubated with Fixation buffer (BioLegend) for 20 min at room temperature before washing. Washing steps from here on were performed in Intracellular Staining Permeabilization Wash Buffer (BioLegend) centrifuging at 330 x g for 3 min. Cytokine-specific antibodies were diluted in permeabilization buffer, and incubated with the cells for 20-30 min at room temperature (Table 2.1). The cells were then washed and resuspended in PBS. Intranuclear staining was performed as cytokine staining but using buffers from eBioScience Foxp3 / Transcription Factor Staining Kit (Thermo Scientific).

2.4.3 CellTrace staining for proliferation

To measure cell proliferation, cells were stained with CellTrace Violet (Thermo Scientific) prior to putting in culture. Cell pellets were resuspended in PBS with 1:1000 dilution of CellTrace Violet, and incubated at 37°C for 20 min, protected from light. The cells were then centrifuged at 300 x g for 5 min and resuspended in fresh cell medium for cell culture.

2.5 Western blotting

Specificity	Conjugate	Clone	Host	Conc.	Supplier
Ago-2	-	DO-2 17F1-C1	Mouse	1:4000	InVivo BioTech (custom made)
GW182	-	Polyclonal	Rabbit	1:4000	Bethyl Laboratories
ZAP-70	-	D1C10E	Rabbit	1:4000	Cell Signalling
Secondary antibodies					
Mouse IgG	Alexa Fluor 680	Polyclonal	Goat	1:20,000	Thermo Scientific
Mouse IgG	IRDye 800CW	Polyclonal	Goat	1:20,000	Li-cor
Rabbit IgG	Alexa Fluor 680	Polyclonal	Goat	1:20,000	Thermo Scientific
Rabbit IgG	DyLight 800	Polyclonal	Goat	1:20,000	Thermo Scientific

Table 2.2
Table of antibodies used for western blotting

2.5.1 Cell lysis

Cells were lysed in CLASH lysis buffer containing proteinase inhibitors (cOmplete protease inhibitor cocktail tablets, Roche), and if required, RNase inhibitors (RNasin Ribonuclease inhibitor, Promega). The cells were resuspended in lysis buffer at 1 x 10^8 cells/mL and incubated for 20 min on ice. The lysate was cleared by centrifugation at 13,000 rpm for 10 min. Protein concentration was measured with a spectrophotometric assay (Micro BCA protein assay, Thermo Scientific).

2.5.2 Western blotting

LDS sample buffer (NuPAGE, Thermo Scientific) containing 10% DTT or β-mercaptoethanol was added to the lysate. The lysate was denatured by incubating at 95°C for 10 min. Sample was loaded on a 4-12% Bis-Tris gel (NuPAGE, Thermo Scientific) and ran in MOPS SDS running buffer (NuPAGE, Thermo Scientific) at 150V for 90-120 min, using a mini gel tank (Thermo Scientific). The proteins were then transferred from the gel onto a PVDF membrane (Immobilon-FL, Merck), that had been activated by wetting in methanol. Transfer was performed in transfer buffer for 105 min at 100V, using a wet transfer tank (mini Protean Tetra cell, Bio-rad). After transfer, the

membrane was blocked in Odyssey blocking buffer (Li-cor) for 1 h. Membrane was then incubated overnight at 4°C with a primary antibody in blocking buffer + 0.1% Tween20 (Table 2.2). The membrane was washed in PBS + 0.05% Tween20 for 1 h with several changes of buffer. After washing, the membrane was incubated with the secondary antibody in blocking buffer + 0.1% Tween20 + 0.01% SDS for 30 min at room temperature. The membrane was then washed for another hour and scanned on the Odyssey CLx scanner (Li-cor).

2.6 Immunoprecipitations

3-4 x 10^7 cells per IP were lysed as described for Western blotting. 50-100 µl Protein G Dynabeads (Thermo Scientific) per sample were used for the immunoprecipitations. The beads were washed three times in PBS + 0.01% Tween20 (PBS-T) by adding 1 mL of wash buffer and resuspending the beads, then removing the supernatant on a magnet. For binding antibody to Protein G Dynabeads, the beads were incubated at 4°C on rotation with 5-10 µg anti-Ago-2 or anti-GW182 antibody (Table 2.2), or 5-10 µl mouse IgG or polyclonal rabbit serum for controls, in PBS-T for a minimum of 6 hours. The beads were then washed in PBS-T and lysis buffer, before adding sample lysate. The immunoprecipitations were performed at 4°C overnight on a rotator. The following day the unbound fraction was collected. The beads were then washed once with LS-IP wash, twice with HS-IP wash, once with LS-IP wash and once with PNK buffer. For the HS-IP washes, the beads were incubated with the wash buffer for 5 min on rotation at 4°C. The beads were then resuspended in 50-100 µl LDS sample buffer (NuPAGE, Thermo Scientific) containing 10% DTT or β-mercaptoethanol, and incubated on a shaker at 70°C for 10 min. The eluate was collected by removing the supernatant on a magnet.

2.7 Size exclusion chromatography

2.7.1 Cell lysis

Cells were flash-frozen on dry ice or liquid nitrogen and lysed in 0.5 mL Superose 6 buffer for 20 min. The lysate was cleared by centrifugation at

13,000 rpm and filtering through a 20 µm filter. Protein concentration was measured with Qubit 3.0 fluorometer (Thermo Scientific) using the Qubit Protein Assay kit (Thermo Scientific).

2.7.2 Chromatography

Size exclusion chromatography was performed by Martin Wear at the Edinburgh Protein Production Facility. The sample was loaded on the Superose 6 column, washed with Superose 6 buffer and 0.5 mL fractions were collected.

2.7.3 Protein extraction from fractions

Protein was extracted from the fractions by TCA precipitation. 1 volume of TCA was added to 4 volumes of protein sample and incubated at 4°C for 10 min. The sample was then centrifuged at full speed for 10 min. The supernatant was removed and the pellet was washed by adding 200 µl cold acetone and centrifugation at full speed for 5 minutes. The washing step was repeated once for a total of 2 acetone washes. The pellet was then air dried and resuspended in LDS sample buffer (Thermo Scientific) containing 10% β-mercaptoethanol, and heated at 95°C for 10 min. The samples were then used for western blotting.

2.8 quantitative real-time PCR (qPCR)

2.8.1 RNA isolation

5 x 10^6 cells were resuspended in 0.5 mL Trizol reagent (Thermo Scientific) for RNA purification. RNA was purified by using Direct-zol kit (Zymo Research) following kit instructions. RNA was resuspended in 20-40 µl dH_2O and RNA concentration was measured with Nanodrop 1000 Spectrophotometer (Thermo Scientific).

2.8.2 Reverse transcription

RNA was reverse transcribed by using miScript RT kit (Qiagen). An equal amount of RNA was used for each sample per reaction (minimum 100 ng). The

template RNA was mixed with 5x miScript HiFlex buffer, 10x miScript Nucleics mix, miScript Reverse transcriptase mix and RNase free water. The mixture was then incubated for 60 min at 37°C then for 5 min at 95°C in a thermocycler.

2.8.3 qPCR

For qPCR, the cDNA was diluted 1:10 in dH_2O. For detection of miRNAs, a master mix was prepared from 2x QuantiText SYBR Green PCR Master mix (Qiagen), 10x miScript Universal Primer (Qiagen) and dH_2O. For each miRNA studied, specific miScript Primer Assay (Qiagen) was added. 8 µl of the mix was added to 2 µl cDNA per well in 96 or 384-well plates (LightCycler 480 Multiwell plate, Roche). For detection of mRNA, predesigned qPCR primers were used (IDT) at a final concentration of 500 nM with the 2x QuantiText SYBR Green PCR Master Mix (Qiagen). The plates were run on LightCycler 480 Instrument II (Roche) with the following cycling conditions.

Step	Time	Temperature
PCR initial activation step	15 min	95°C
3-step cycling: (x40)		
Denaturation	15 s	94°C
Annealing	30 s	55°C
Extension	30 s	70°C

2.9 Small RNA library preparation

2.9.1 RNA isolation

For small RNA library preparation, RNA was isolated from Ago-2-IP samples, as well as the IP input and unbound samples. For input samples, cells were resuspended in 0.5 mL QIAzol lysis reagent (Qiagen). For liquid input and unbound samples, 50 µl of sample was resuspended in 650 µl QIAzol. For IP samples, the beads were resuspended in 0.5 mL QIAzol. RNA was isolated using the RNeasy kit (Qiagen), following kit instructions. The RNA samples were eluted in 100 µl dH_2O. The RNA was then ethanol precipitated by adding 2.5 x volume 100% ethanol, 30 µl sodium acetate and 1 µl GlycoBlue Coprecipitant (Thermo Scientific). The samples were incubated overnight at

-20°C. The following day, the samples were centrifuged at full speed for 30 min, then washed twice with 70% ethanol (10 min centrifugation at full speed). The pellets were air-dried on ice then resuspended in 10-15 µl dH_2O and quantified with Qubit 3.0 fluorometer (Thermo Scientific) using the Qubit RNA HS Assay kit (Thermo Scientific).

2.9.2 Adapters and reverse transcription

Small RNA libraries were prepared using the TriLink CleanTag Ligation kit for Small RNA Library Preparation (Catalog #L-3206). When possible, 100 ng of RNA per sample was used for library preparation, as quantified with Qubit. For LMW RISC samples and all IP samples, the maximum amount of sample was used (2 µl, approximately 10-40 ng). The libraries were prepared following kit instructions for the four key steps: 3' Adapter ligation to RNA template, 5' Adapter ligation to tagged RNA template, Reverse Transcription reaction of tagged RNA library, and PCR amplification of RT product, using half-reaction volumes.

2.9.2.1 3' Adapter ligation

2 µl of template RNA was heated at 70°C for 2 min. 3' Adapter was diluted 1:2 for high-input samples (100 ng), and 1:4 for low (40 ng) or 1:8 for very low (<10 ng) input, then used to prepare the following reaction:

Reagent	Amount
RNA template	2 µl
Buffer 1	2.5 µl
RNase inhibitor	0.5 µl
Enzyme 1	0.5 µl
CleanTag 3' Adapter	0.5 µl
	6 µl

2.9.2.2 5' Adapter ligation

The 5' adapter was diluted as the 3' adapter, and heated at 70°C for 2 min. The following mix was then added to the 3' tagged RNA:

Reagent	Amount
3' tagged RNA	6 µl
dH_2O	1 µl

Buffer 2	0.5 µl
RNase inhibitor	0.5 µl
Enzyme 2	1 µl
CleanTag 5’ Adapter	1 µl
	10 µl

The mix was then placed in a thermocycler and heated at 28°C for 1 h, followed by 65°C for 20 min.

2.9.2.3 Reverse transcription

1 µl RT primer (5 µM) was added to tagged library and heated at 70°C for 2 min. For reverse transcription, following mix was added:

Reagent	Amount
RNA (10 µl + 1 µl RT primer)	11 µl
dH_2O	0.96 µl
5x RT buffer	2.88 µl
dNTPs (10mM)	0.72 µl
DTT (100mM)	1.44 µl
RNase inhibitor	0.5 µl
RT Enzyme	0.5 µl
	18 µl

The reaction mix was placed in a thermocycler and incubate at 50°C for 1 h

2.9.2.4 PCR amplification

The following PCR mix was prepared per reaction:

Reagent	Amount
cDNA	18 µl
High Fidelity PCR Master Mix	20 µl
Forward primer	1 µl
Index primer	1 µl
	40 µl

The mix was placed in a thermocycler for the following cycling conditions:

Step	Time	Temperature
PCR initial activation step	30 s	98°C
3-step cycling: (x21)		
Denaturation	10 s	98°C
Annealing	30 s	60°C
Extension	15 s	72°C
Final extension	10 min	72°C

2.9.3 TBE gels and ethanol purification

Following PCR amplification of the RT product, the samples were mixed with DNA loading dye (Gel Loading Dye, blue (6x), NEB) and ran with a digested plasmid ladder (quick load pBR322 DNA MspI digest, NEB) on 6% TBE gels (Thermo Scientific) in TBE running buffer (Thermo Scientific). Gels were ran at 80V for 90 min. The gels were then incubated with 50 mL TBE buffer containing SYBR Gold nucleic acid gel stain diluted 1:10,000 (Thermo Scientific) for 15 min on a plate shaker. The gels were then visualised on the D-Digit gel scanner (Li-cor). The bands corresponding to the tagged library were cut out with a scalpel over Large blue LED transilluminator (IO Rodeo). The gel pieces were shredded by centrifugation through pierced 0.5 mL Eppendorf tubes inside 1.5 mL Eppendorf tubes at 3,000 rpm for 2 min. 300 µl H_2O was added to the gel pieces and the samples were rotated overnight at 4°C. The samples were then centrifuged through spin tube filters (Spin-X Centrifuge tube filters, Corning Costar) for 5 min at full speed. To precipitate the libraries, 2.5 x volume 100% ethanol, 30 µl sodium acetate and 1 µl GlycoBlue Coprecipitant (Thermo Scientific) were added. The samples were ethanol precipitated overnight at -20°C. The tubes were centrifuged at full speed for 30 min, then washed twice with 70% ethanol (10 min centrifugation at full speed). The pellets were air-dried on ice then resuspended in 10-15 µl dH_2O.

2.9.4 Sample preparation for sequencing

The sample concentration was measured with Qubit 3.0 fluorometer (Thermo Scientific) using the Qubit dsDNA HS Assay kit (Thermo Scientific). The samples were also measured on Agilent 2100 Bioanalyzer using the Agilent High Sensitivity DNA kit. 1 ng of input and unbound libraries, and 2 ng of IP libraries were pooled and concentrated to 15 nM in 50 µl for sequencing. The samples were sequenced using NovaSeq 50bp paired end sequencing at Edinburgh Genomics.

2.10 CLASH

2.10.1 Cross-linking

1 x 10^8 cells were washed by centrifugation at 300 x g for 5 min then resuspended in 10 mL PBS. For cross-linking, 5 mL cells were added on a Petri dish and placed on ice. Cross-linking was performed at 400 mJ/cm^2 then twice at 200 mJ/cm^2 using a UV Stratalinker 2400. Cells were collected from the Petri dishes and centrifuged at 300 x g for 5 min.

2.10.2 Cell lysis

Cells were lysed as described for Western blotting, including proteinase inhibitors (cOmplete protease inhibitor cocktail tablets, Roche) and RNase inhibitors (RNasin Ribonuclease inhibitor, Promega) in the CLASH lysis buffer.

2.10.3 Ago-2 Immunoprecipitation

100 µl Protein G Dynabeads (Thermo Scientific) were used per sample. The beads were washed three times in PBS + 0.01% Tween20 (PBS-T) by adding 1 mL of wash buffer and resuspending the beads, then removing the supernatant on a magnet. For binding antibody to Protein G Dynabeads, the beads were incubated at 4°C on rotation with 5-10 µg anti-Ago-2 or anti-GW182 antibody (Table 2.2) in PBS-T for a minimum of 6 hours. The beads were then washed in PBS-T and lysis buffer, before adding sample lysate. The immunoprecipitations were performed at 4°C overnight on a rotator. The following day the unbound fraction was collected. The beads were then washed once with LS-IP wash, twice with HS-IP wash, once with LS-IP wash and once with PNK buffer. For the HS-IP washes, the beads were incubated with the wash buffer for 5 min on rotation at 4°C. These wash conditions were also used for all the following wash steps.

2.10.4 RNase digestion

Following the washing steps, the beads were resuspended in PNK buffer containing RNase. 1 µl RNace-IT ribonuclease cocktail (diluted 1:40, Agilent)

was added to 500 µl pre-warmed PNK buffer. The beads were incubated at 20°C for 7 min with intermittent shaking. Following the incubation, the sample was moved directly on ice and washed as before.

2.10.5 T4 PNK phosphorylation

For the RNA phosphorylation, 80 µl of reaction mix was added onto the beads and incubated 2.5 h at 20°C with intermittent shaking, after which the beads were washed.

Reagent	Amount	Provider
T4 PNK buffer (10x)	8 µl	NEB
rATP (100mM)	0.8 µl	Promega
RNasin ribonuclease inhibitor	2 µl	Promega
T4 PNK (3' phosphatase minus)	4 µl	NEB
dH_2O	65 µl	

2.10.6 Intermolecular ligation

For intermolecular ligation of miRNAs and target mRNAs, 160 µl of reaction mix was added onto each sample and incubated overnight at 16°C with intermittent shaking, after which the beads were washed.

Reagent	Amount	Provider
T4 ligase buffer (10x)	16 µl	NEB
rATP (100mM)	1.6 µl	Promega
RNasin ribonuclease inhibitor	4 µl	Promega
T4 ligase I	8 µl	NEB
dH_2O	130.4 µl	

2.10.7 TSAP phosphorylation

For TSAP phosphorylation, 80 µl of reaction mix was added onto each sample and incubated 45 min at 20°C with intermittent shaking, after which the beads were washed.

Reagent	Amount	Provider
Multicore buffer (10x)	8 µl	Promega
RNasin ribonuclease inhibitor	2 µl	Promega
TSAP	8 µl	Promega
dH_2O	62 µl	

2.10.8 3’ Adapter ligation

For 3’ adapter ligation, 80 µl of reaction mix was added onto each sample and incubated 6 h at 20°C in the dark with intermittent shaking, after which the beads were washed.

Reagent	Amount	Provider
T4 ligase buffer (10x)	8 µl	NEB
PEG 8000 (50%)	16 µl	NEB
3’ CleanTag IR800 (10 µM)	8 µl	TriLink
RNasin ribonuclease inhibitor	2 µl	Promega
T4 RNA ligase K227Q	4 µl	NEB
dH_2O	42 µl	

2.10.9 Elution from beads

After the final wash, the beads were resuspended in 50-100 µl elution buffer and incubated at 70°C for 10 min with constant shaking. The supernatant was then removed from the beads on a magnet and loaded on a protein gel, or kept overnight at -20°C.

2.10.10 Protein gel

Samples were loaded on a 4-12% Bis-Tris gel (NuPAGE, Thermo Scientific) and ran in MOPS SDS running buffer (NuPAGE, Thermo Scientific) at 120V for 90-120 min at 4°C, in a mini gel tank (Thermo Scientific) covered from light. The gel was then either directly scanned on Odyssey CLx scanner (Li-cor) or transferred on a HyBond-N+ membrane (GE Healthcare) for Western blotting. Transfer was performed using transfer buffer (NuPAGE, Thermo Scientific) containing 10% methanol, at 100V for 105 min in the dark.

2.10.11 Elution from gel

After visualisation of gel, RNA-band corresponding to Ago-2 was cut from the gel by using a small scalpel. The gel pieces were shredded by centrifugation through pierced 0.5 mL Eppendorf tubes inside 1.5 mL Eppendorf tubes at 3,000 rpm for 2 min. 300 µl H_2O was added to the gel pieces and the samples were rotated overnight at 4°C. The next day, 300 µl of 2x proteinase K buffer was added to the gel with 2 µl RNase inhibitor (Promega) and 100 µg

proteinase K (Ambion). The samples were incubated at 55°C for 2 h with constant shaking. The mix was supplemented with additional 50 µg proteinase K after 1 h.

2.10.12 RNA extraction

The samples were then centrifuged through spin tube filters (Spin-X Centrifuge tube filters, Corning Costar) for 5 min at full speed. The supernatant was moved to a new tube from which RNA was phenol-chloroform extracted by adding 1/10th volume 3 M sodium acetate (pH=5.5) and equal volume phenol chloroform. The mix was vortexed for 30 s then centrifuged at 10°C for 15 min. The upper layer was moved to a new tube, to which 2.5 x volume 100% ethanol was added with 1 µl GlycoBlue Coprecipitant (Thermo Scientific). The sample was then left to precipitate at -20°C overnight. The samples were centrifuged at full speed for 30 min, then washed twice with 70% ethanol (10 min centrifugation at full speed). The pellet was left to air-dry on ice, then resuspended in 15 µl water.

2.10.13 Library Preparation

RNA libraries were prepared as described for small RNA libraries, using the TriLink CleanTag small RNA library preparation kit. Since the RNA had already been labelled with the 3' Adapter, the protocol was followed from the 5' Adapter ligation step, using a 1:4 dilution of the Adapter. 2.5 µl of RNA was mixed with 2.5 µl buffer 1 (from the 3' Adapter ligation step) then used following the protocol using half reactions. After the PCR amplification, the samples were ran on TBE gels and purified as described for small RNA libraries.

2.10.14 Sample quality control

The sample concentration was measured with Qubit 3.0 fluorometer (Thermo Scientific) using the Qubit dsDNA HS Assay kit (Thermo Scientific). The samples were also measured on Agilent 2100 Bioanalyzer using the Agilent High Sensitivity DNA kit. 1-2 ng of each CLASH library was pooled and sent

for sequencing. The samples were sequenced using NovaSeq 100 bp single end or 75 bp paired end sequencing at Edinburgh Genomics.

2.11 Data analysis

2.11.1 Flow cytometry data

Flow cytometry data were analysed using FlowJo 10 software. Geometric mean fluorescence intensity (gMFI) and percentages of populations were exported and plotted in GraphPad Prism.

2.11.2 Western blot data

Western blot data were analysed using ImageStudioLite (Li-cor). Band signal intensity was calculated using the software by drawing a shape around the band of interest. The median value of the pixels in the background area was subtracted. The signal was then normalised to any loading controls, and adjusted to naive or other control samples.

2.11.3 qPCR data

qPCR data were analysed in Microsoft Excel. Data were first normalised to snRNA U6, then calculated as fold change to naive, using the ΔΔCt value method. Data were plotted in GraphPad Prism.

2.11.4 small RNA library sequencing data

RNA sequencing data were processed by Dr Sujai Kumar to create miRNA count files. Cutadapt (version 1.15) (Martin, 2011) was used to trim the 3' small RNA adapter TGGAATTCTCGGGTGCCA and low quality 3' bases with quality below 20. Only reads with the adapter that were longer than 18 bases were retained. Reads were classified into RNA biotypes by mapping against sets of known mouse RNA sequences using bowtie2 (version 2.3.4) (Langmead and Salzberg, 2012) in the order given below. For example, if a read mapped to a known miRNA sequence then it was called a miRNA and not a YRNA even if it mapped equally well to the YRNA database. The order and sources of the mouse RNA sets are: 1. miRNAs from mmu-hairpin.fa miRBase (version 22)

(Kozomara, Birgaoanu and Griffiths-Jones, 2019); 2. Y_RNAs; 3. tRNAs; 4. rRNAs, all downloaded from the RNAcentral database (Sweeney *et al.*, 2019); 5. protein-coding mRNAs from Gencode version M16 (Frankish *et al.*, 2019); 6. snoRNAs; 7. piRNAs; 8. lncRNAs; 9. other (SRPRNAs, scRNAs, snRNAs, miscRNAs) from RNAcentral. Any reads not belonging to these categories but mapping to the Mouse genome (version GRCm38.p5) were classified as "uncategorized" and the remaining reads as "unmapped". Bowtie2 was used to assign reads to different RNA types to provide an overview of the RNA diversity of the sample. However, to assess the presence and counts of individual miRNAs, we used the more accurate and less redundant miRNA counting tool QuickMIRSeq (Zhao *et al.*, 2017). QuickMIRSeq does its own read trimming and length selection using cutadapt, which we set to trim the 3' adapter TGGAATTCTCGGGTGCCAAGG, the 5' adapter AGATCGGAAGAGCACACGTCT, and choose only reads between 18 and 28 bp in length for assigning to known miRNAs. The default QuickMIRSeq settings were used for identifying mouse miRNAs. The QuickMIRSeq output file miR.filter.Counts.csv was used for all downstream analyses. The Principle Components Analysis (PCA) plot was made using the plotPCA function in DESeq2 (Love, Huber and Anders, 2014) after applying the varianceStabilizingTransformation function to the miRNA count data. The miRNA count files were then uploaded on the Degust (version 3.1.0) (Powell, 2015, DOI: 10.5281/zenodo.3258933) web tool for visualisation of differential expression analysis. The differential analysis was performed using the Voom/Limma method and visualised on Degust.

2.11.5 CLASH data

Bioinformatic analysis of CLASH data was done by Dr Sujai Kumar. CLASH sequencing data quality checks were done the same way as the small RNA sequencing data, with initial trimming with Cutadapt, followed by RNA assignment with bowtie2. Libraries with 75 base paired-end reads were first trimmed as above and then merged using bbmerge.sh (version 37.90) (Bushnell, Rood and Singer, 2017) prior to classification to RNA biotypes.

Chimeric reads were classified as unmapped in the initial quality check because they did not map full-length to any of the RNA biotypes (e.g., miRNA, Y_RNA, tRNA, rRNA, etc.). Chimeric reads were identified using the CLASHchimeras python pipeline (Chhatbar, 2015, DOI: 10.5281/zenodo.57076) using Mouse mature miRNA sequences from miRBase version 22 as the small RNA database, and Mouse protein-coding transcripts from Gencode version M16 as the target RNA database.

2.11.6 Analysis of CLASH chimeric reads

When the pc part of the chimeric read was less than 55 bp long, this was extended to 55 bp for further analysis. Low complexity reads were filtered out by using the DUST module (Morgulis *et al.*, 2006). miRNA seed sites were identified from the protein coding reads by using a script written by Sujai Kumar (*https://github.com/sujaikumar/kleinerna/blob/master/seeds_dust_targetfinder.pl*). MIRZA (Khorshid *et al.*, 2013) was used to assign scores to the pairing between the miRNA and protein-coding parts of each chimera. The TargetScan mouse database version 7.1 (Agarwal *et al.*, 2015) was used to check whether the protein-coding part of the chimera was a known miRNA target according to TargetScan. Gene Ontology (GO) enrichment analysis was performed on the Gene Ontology Research website using a tool from the PANTHER classification system (Mi *et al.*, 2013). Functional annotation of genes was performed using the bioinformatic resource DAVID (v6.8), selecting 1-3 GO terms to describe each gene (Huang, Sherman and Lempicki, 2009).

2.11.7 Statistical analysis

Statistical analysis was performed on GraphPad Prism.

CHAPTER 3:

miRNA expression changes dynamically during CD8$^+$ T cell activation and differentiation

3.1 Introduction

3.1.1 The role of miRNAs in CD8$^+$ T cell activation and differentiation

The expression of miRNAs is dynamically regulated during CD8$^+$ T cell activation and cell differentiation to effector and memory cells. The majority of miRNAs are downregulated upon activation to relieve suppression on molecules required for effector cell differentiation, and expression comes back up in memory cells (Wu *et al.*, 2007; Bronevetsky *et al.*, 2013). miRNAs affect nearly all aspects of T cell activation, from TCR signalling to cell survival and proliferation, and acquisition of effector functions such as cytokine production, cytotoxicity and cell migration. Several key miRNAs regulate these processes, and it has been shown that deficiency or overexpression of single miRNAs can lead to serious defects in T cell activation.

To confirm dynamic regulation of miRNA expression in activated CD8$^+$ T cells and to ask how signalling with different affinity antigens might influence miRNA expression, we measured this in OT-I TCR transgenic cells. OT-I Rag$^{-/-}$ mice are deficient in the Rag1 recombinase required for TCR and BCR recombination, thus only express the transgenic OT-I TCR which is MHC Class I restricted and recognises a fragment of the ovalbumin protein. OT-I cells can be activated *in vitro* using the agonist peptide SIINFEKL (N4), or modified peptides with different affinity to the TCR. The variant peptides SIITFEKL (T4) and SIIGFEKL (G4) bind to the OT-I TCR with weaker affinity compared to N4. Following activation with the N4 peptide, the cells are grown into fully differentiated CTLs by culturing in IL-2, or into memory-like cells by culturing in IL-15. Using this system, we studied the expression of five miRNAs in these cells: miR-155, miR-17, miR-139, miR-150 and miR-181a. These five miRNAs

were chosen because they have been previously shown to have key roles in T cell activation and differentiation (Table 3.1).

3.1.2 Upregulated miRNAs: miR-155 and the miR-17~92 cluster

miR-155 and miR-17, a member of the miR-17~92 cluster, are both upregulated upon T cell activation and promote cell survival and proliferation. miR-155 is indispensable for competent $CD8^+$ T cell mediated immunity: miR-155 deficiency causes an impaired response to infectious challenge or tumours *in vivo*, with a failure to expand and form long-lasting memory (Dudda *et al.*, 2013; Gracias *et al.*, 2013; Lind, Elford and Ohashi, 2013). miR-155 has been suggested to regulate responsiveness to type I interferons during viral infection (Gracias *et al.*, 2013). Additionally, miR-155 has been shown to inhibit suppressors of cytokine signalling, such as Socs1, Ship1 and Ptpn2 (Dudda *et al.*, 2013; Ji *et al.*, 2015). miR-155 inhibition of Socs1 was shown to be dispensable for $CD8^+$ T cell responses to acute viral infection, but was required for the antiviral response in chronic infection (Lu *et al.*, 2015). Recently, miR-155 targeting of Ship1 and subsequent upregulation of Akt signalling, was shown to have far-reaching effects in the epigenetic silencing of transcription factors regulating $CD8^+$ T cell terminal differentiation and functional exhaustion during anti-tumour responses (Ji *et al.*, 2019). Increased Akt signalling promoted expression of Phf19, which in turn enhanced the activity of the epigenetic silencing complex Polycomb repressor complex 2 (PRC2), which inhibited the expression of pro-differentiation transcription factors. This showed how miR-155 indirectly promoted $CD8^+$ T cell anti-tumour function through the Phf19-PRC2 axis.

The miR-17~92 cluster is particularly important for cell proliferation, with miR-17~92 deficient $CD8^+$ cells showing defects in both *in vitro* and *in vivo* expansion (Wu *et al.*, 2012; Khan *et al.*, 2013). The miRNAs of this cluster promote a short-lived effector cell phenotype, with their downregulation required for memory cell differentiation (Wu *et al.*, 2012). The effects of the

cluster are through direct targeting of Pten, and upregulation of the PI3K-Akt-mTOR axis (Wu *et al.*, 2012; Khan *et al.*, 2013).

3.1.3 Downregulated miRNAs: miR-139, miR-150 and miR-181

In contrast to these two miRNAs, many miRNAs are more highly expressed in naive cells, and their downregulation is required for appropriate cell activation and differentiation. For example, miR-139 is strongly downregulated upon activation, to allow expression of its targets Eomes and perforin, that are important for effector cell differentiation and functions (Trifari *et al.*, 2013).

miR-150 is another miRNA that is downregulated upon TCR stimulation (Almanza *et al.*, 2010). This miRNA has been described to have diverse targets and functions in naive $CD8^+$ T cells, activated cells, and memory cells. In naive cells, miR-150 was recently shown to modulate Ca^{2+} levels through suppression of Tmem20. miR-150 deficiency caused an increase in intracellular Ca^{2+} levels, leading to upregulation of NFAT1 and induction of anergy-inducing genes in the absence of TCR stimulation (Kim *et al.*, 2017). This led to defects in cell activation, proliferation and effector differentiation upon antigenic stimulation, a phenotype that had been previously described for miR-150 deficient cells (Smith *et al.*, 2015). Interestingly, miR-150 appears to have a different role in memory cells, with miR-150 deficiency increasing memory cell differentiation *in vitro* and *in vivo*, through modulation of c-Myb and Foxo1 expression (Ban *et al.*, 2017; Chen *et al.*, 2017). Overexpression of this miRNA skewed the cells towards a short-lived effector phenotype (Chen *et al.*, 2017).

Finally, miR-181 plays an important role in the modulation of TCR signalling threshold, by increasing sensitivity to weak agonists. The targets of miR-181 include the phosphatases Shp-2, Ptpn22, Dusp5 and Dusp6, which function to limit TCR signalling (Li *et al.*, 2007). High expression of miR-181 in developing thymocytes allows positive selection against weak self-peptide agonists. Its

expression then decreases in mature T cells to decrease sensitivity to self-peptides. Inhibition of miR-181 impairs T cell development and resulting mature T cells have an increased risk of autoreactivity (Li *et al.*, 2007; Ebert *et al.*, 2009).

miRNA	Direct targets	Overexpression	Inhibition/knockout
miR-155	**Socs1** (Dudda *et al.*, 2013), **Ptpn2, Ship1** (Ji *et al.*, 2015)	Improves effector functions (Gracias *et al.*, 2013)	Impairs responses to infection, tumour (Dudda *et al.*, 2013; Lind, Elford and Ohashi, 2013). Failure to expand and impaired memory formation (Dudda *et al.*, 2013; Gracias *et al.*, 2013)
miR-17~92	**Pten** (Wu et al. 2012)	More proliferation *in vivo*, skewing to short-lived effector phenotype (Wu *et al.*, 2012; Khan *et al.*, 2013)	Impaired cell proliferation *in vitro* and expansion *in vivo* (Wu *et al.*, 2012; Khan *et al.*, 2013)
miR-150	**Foxo1** (Ban *et al.*, 2017), **c-Myb** (Chen *et al.*, 2017), **Cd25** (Trifari *et al.*, 2013), **Tmem20** (Kim *et al.*, 2017)	Reduction in memory formation, short-lived effector phenotype (Chen *et al.*, 2017)	Elevated Ca^{2+} in naive cells (Kim *et al.*, 2017). Defective activation and effector cell differentiation (Smith *et al.*, 2015). Preferential differentiation to memory cells *in vitro* and *in vivo* (Ban *et al.*, 2017; Chen *et al.*, 2017).
miR-181	**Shp-2, Ptpn22, Dusp5, Dusp6** (Li *et al.*, 2007)	Increased TCR-mediated activation (Li *et al.*, 2007)	Diminished TCR signalling and impaired T cell development (Li *et al.*, 2007). Maturation of autoreactive cells (Ebert *et al.*, 2009)
miR-139	**Perforin, Eomesodermin** (Trifari *et al.*, 2013)	Disadvantage during infection, *in vitro* reduction in killing target cells (Trifari *et al.*, 2013)	

Table 3.1 miRNA function and targets in $CD8^+$ T cells
Summary of validated targets and functions derived from overexpression/knockdown studies for miR-155, miR-17~92 cluster, miR-150, miR-181 and miR-139 in $CD8^+$ T cells.

3.2 Results

3.2.1 miRNA expression changes during OT-I $CD8^+$ T cell activation

To study the role of miRNAs in $CD8^+$ T cells, we activated OT-I cells with the agonist peptide N4 and measured the expression of known miRNA regulators of T cell activation during a 6-day time-course. We first assessed the level of activation in these cells following *in vitro* activation with N4 and subsequent supplementation of the cultures with IL-2. Two days after activation with N4, the cells had upregulated surface activation markers CD25 and CD44, had entered cell division as shown by the expression of the proliferation marker Ki67, and had also begun expressing the transcription factor T-bet and the cytotoxic effector molecule Granzyme B (Fig.3.1). After a further 4 days of culture in IL-2, the cells had become fully differentiated CTLs, with increased expression of Granzyme B and the transcription factor Eomes (Fig.3.1E-F). Next, we measured the expression of miRNAs from naive cells, and at different time points following activation with N4. As expected, miR-155 and miR-17 were upregulated upon activation (Fig.3.2A). In particular miR-155 was very strongly induced, with over 100-fold increase in expression in some experiments compared to naive cells. Both miRNAs were up one day after activation, and expression slowly decreased during 6 days of culture, remaining slightly elevated on day 6. In contrast to these two miRNAs, expression of miR-150, miR-139 and miR-181a was downregulated upon activation (Fig.3.2B). The expression of these miRNAs was halved on day 1, and further decreased during the 6 days in culture. Expression of the five miRNAs was therefore shown to dynamically change upon activation, in line with previous work.

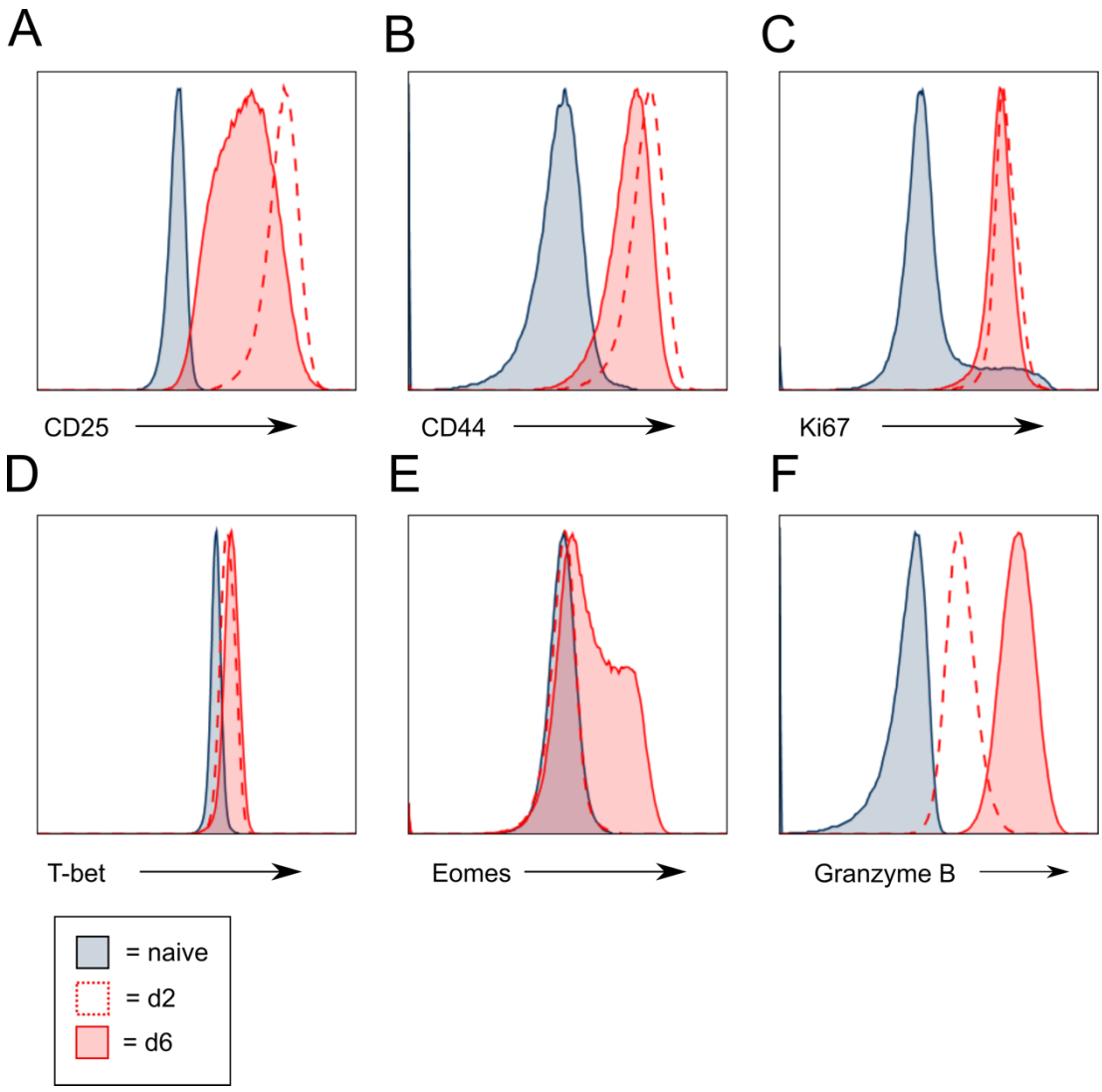

Figure 3.1 Surface molecules, transcription factors and effector molecules are upregulated upon activation of naive OT-I CD8$^+$ T cells with N4
A-F Expression of CD25 (A), CD44 (B), Ki67 (C), T-bet (D), Eomesodermin (E) and Granzyme B (F) measured by flow cytometry in naive OT-I cells (grey), OT-I cells activate with N4 for 2 days (dashed red line), or OT-I cells activated with N4 for 2 days, then cultured in IL-2 for 4 days (solid red line). Graphs are representative of at least 3 independent experiments.

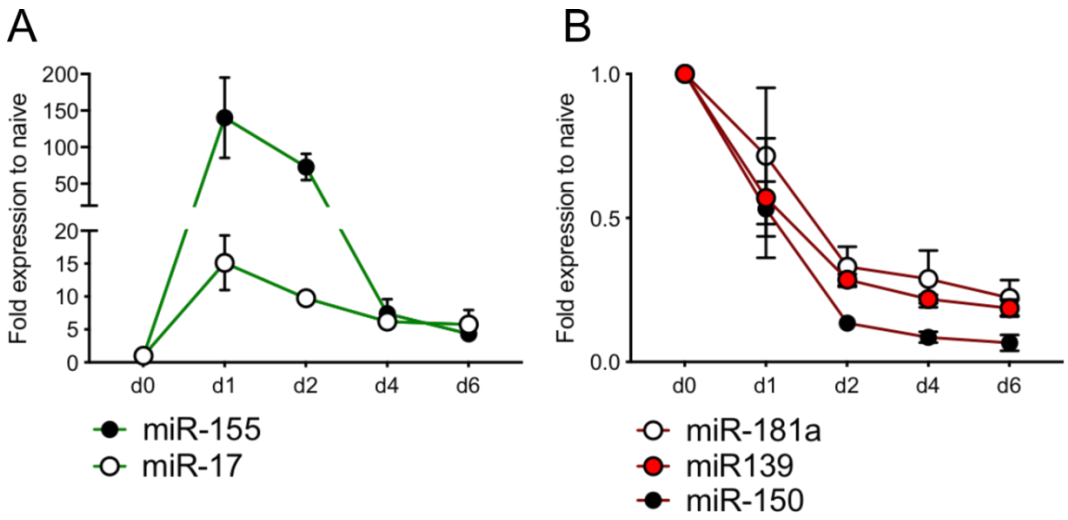

Figure 3.2 miRNA expression changes dynamically upon OT-I CD8$^+$ T cell activation

A-B miRNA expression measured by qPCR during a time-course of OT-I cell activation. Cells were activated with N4 for 2 days then cultured in IL-2 for 4 days. RNA was prepared from snap-frozen cell pellets at the indicated times and analysed by qPCR. miRNA expression was normalised to the internal control, small nuclear RNA U6 (snU6) and is shown as fold expression relative to naive cells. Graphs show mean and standard deviation from 3 independent experiments. Ago-2-flag mice were used for these experiments.

3.2.2 miRNA expression levels depend on the strength of the activating TCR signal

Next, we aimed to determine how the strength of the activating TCR signal affects miRNA expression. OT-I cells were activated with the strong agonist peptide N4 as before, or with the intermediate agonist peptide T4 or weak agonist peptide G4. Cell phenotype was examined 24 h after activation by flow cytometry, and RNA was extracted for qPCR analysis of miRNAs. Flow cytometry confirmed that activation markers such as CD25, CD44 and CD69, and transcription factors T-bet and IRF4 were upregulated with all peptides compared to naive cells (Fig.3.3A-F). N4 caused the strongest upregulation of the activation markers and transcription factors. Activation with T4 resulted in an intermediate phenotype, with slightly reduced expression of the above markers. Cells activated with G4 were clearly less activated; the cells were much smaller in size compared to ones activated with N4 and T4 and the expression of all activation markers was lower (Fig.3.3A-F). miRNA expression also differed between cells activated with N4, T4 or G4. miR-155 was induced by all peptides, with N4 causing the highest upregulation, followed by T4 then G4 (Fig.3.4A). miRNA downregulation was also affected by strength of the activating signal, with stimulation with N4 resulting in strongest downregulation, followed by T4 then G4, which was, in most cases, insufficient to cause downregulation of the measured miRNAs (Fig.3.4B-D). The only statistically significant difference in miRNA expression between the peptide stimulations was expression of miR-139 following activating with N4 vs G4. Statistical significance was not reached in most cases due to high variance in the fold induction of miRNAs from experiment to experiment, but the trend was the same in all three replicates (lowest point in each graph corresponds to the same experiment). These results show that the strength of the initial activating T cell signal affects miRNA up – and downregulation. Cells activated with weaker agonist peptides show a less activated phenotype, corresponding with less pronounced changes in miRNA expression.

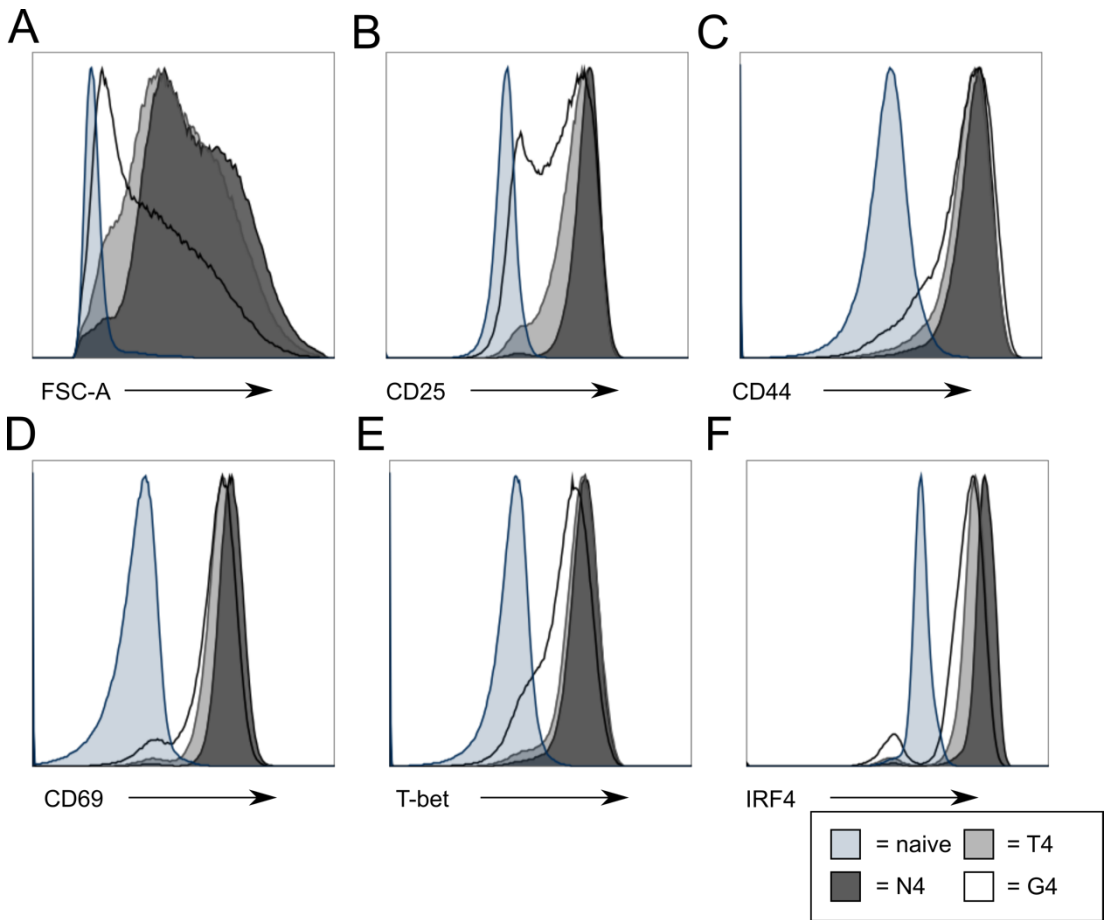

Figure 3.3 Expression of activation markers and transcription factors following CD8$^+$ T cell activation depends on strength of activating signal
A-F Expression of surface markers and transcription factors in naive OT-I cells or following OT-I cell activation with N4, T4 or G4. After 24 h, flow cytometry was used to measure cell size (A), and expression of CD25 (B), CD44 (C), CD69 (D), T-bet (E) and IRF4 (F). Graphs are representative of 3 independent experiments. Ago-2-flag mice were used for these experiments.

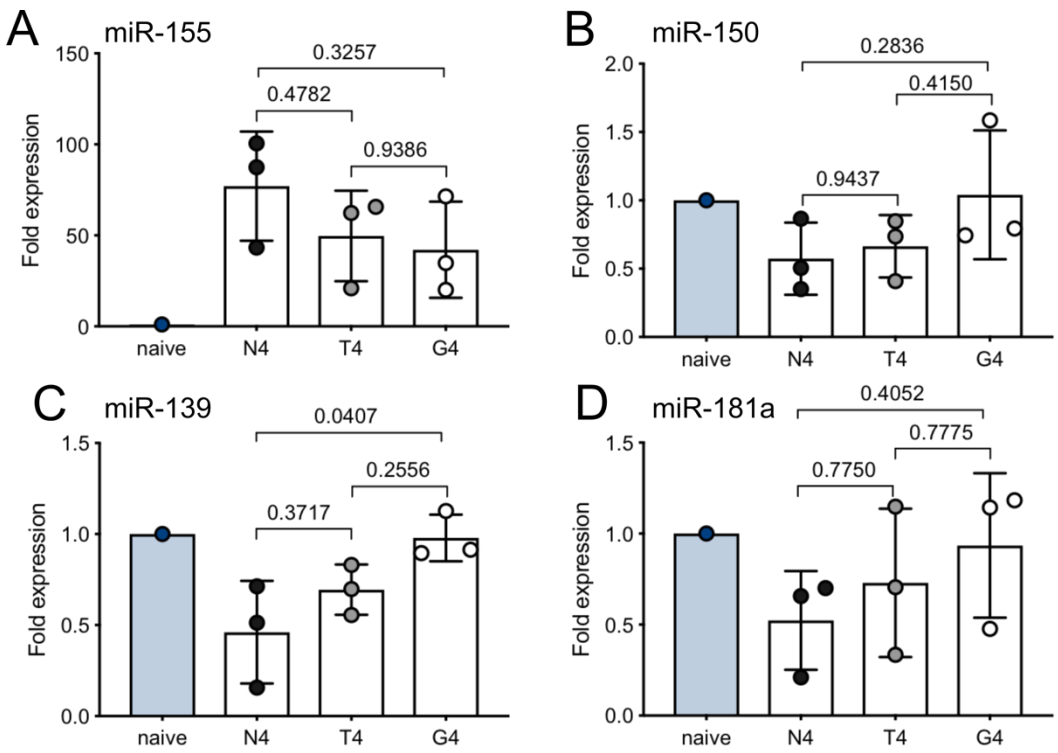

Figure 3.4 miRNA expression depends on strength of activating TCR signal
A-D Expression of miR-155 (A), miR-150 (B), miR-139 (C) and miR-181a (D) measured by qPCR from naive OT-I cells and cells activated for 24 h with N4, T4 or G4. miRNA expression was normalised to snU6 and is shown as fold expression relative to naive cells. The graphs show mean and standard deviation from 3 independent experiments alongside adjusted P values. Statistical analysis was done using an ordinary one-way ANOVA with Tukey's multiple comparisons test, to compare the conditions N4 vs. T4, N4 vs. G4 and T4 vs. G4. Ago-2-flag mice were used for these experiments.

3.2.3 Downregulated miRNAs are re-expressed in memory-like cells

Memory cells, similar to naive cells, have been previously shown to have an increased global expression of miRNAs compared to effector cells. We wanted to determine how the expression of miRNAs changes during *in vitro* differentiation of effector cells grown in IL-2, or memory-like cells differentiated in IL-15. OT-I cells were activated with N4 for 2 days, then cultured with IL-2 or IL-15 for 4 days. Effector or memory phenotype was confirmed by flow cytometry on day 6. Cells grown in IL-2 expressed more CD25, CD44 and the cytotoxic molecule Granzyme B, and produced proinflammatory cytokines IFNγ and TNFα upon re-stimulation with N4 (Fig.3.5A-F). IL-15 grown cells expressed lower levels of activation markers, produced less Granzyme B and proinflammatory cytokines, and expressed the secondary lymphoid organ homing receptor CD62L (Fig.3.5A-F). miRNA expression was measured in fully differentiated effector and memory-phenotype cells on day 6. The expression of miR-155 and miR-17 did not significantly differ between the effector and memory-like cells. Both miRNAs were induced by N4 and expression gradually reduced in culture with both IL-2 and IL-15. The expression of these miRNAs remained higher than in naive T cells for both effector and memory-like cells on day 6 (Fig.3.6A-B). miR-150, miR-139 and miR-181a were previously shown to be downregulated upon activation with N4, and to further decrease in expression in culture with IL-2 (Fig.3.2). Culture in presence of IL-15 resulted in re-expression of these miRNAs after the initial downregulation caused by activation. After 4 days of culture with IL-15, the expression of these miRNAs had returned to levels comparable to naive cells (Fig3.6C-E). These results show that there is differential regulation of miRNA expression in *in vitro* differentiated effector and memory-like cells.

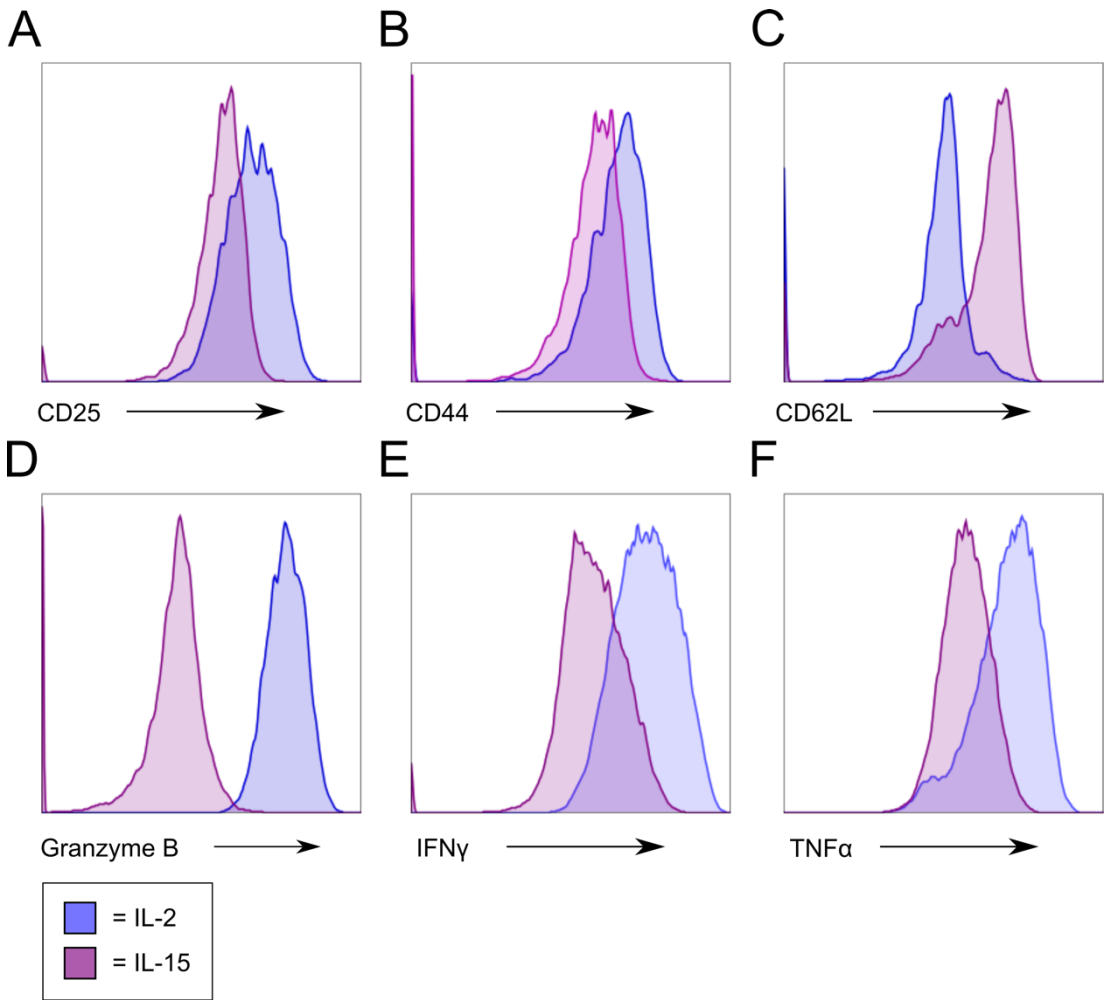

Figure 3.5 Addition of cytokines to culture media can be used to differentiate effector or memory-like cells *in vitro*

A-F Expression of surface markers and effector molecules in OT-I cells activated in N4, then cultured in IL-2 for 4 days for differentiation to effector cells, or cultured in IL-15 for 4 days for memory-like cells. On day 6, expression of C25 (A), CD44 (B), CD62L (C) and Granzyme B (D) was measured by flow cytometry. Expression of IFNγ (E) and TNFα (F) was measured following 4 h re-stimulation with N4 in the presence of Brefeldin A. Graphs are representative of 4 independent experiments. Ago-2-flag mice were used for these experiments.

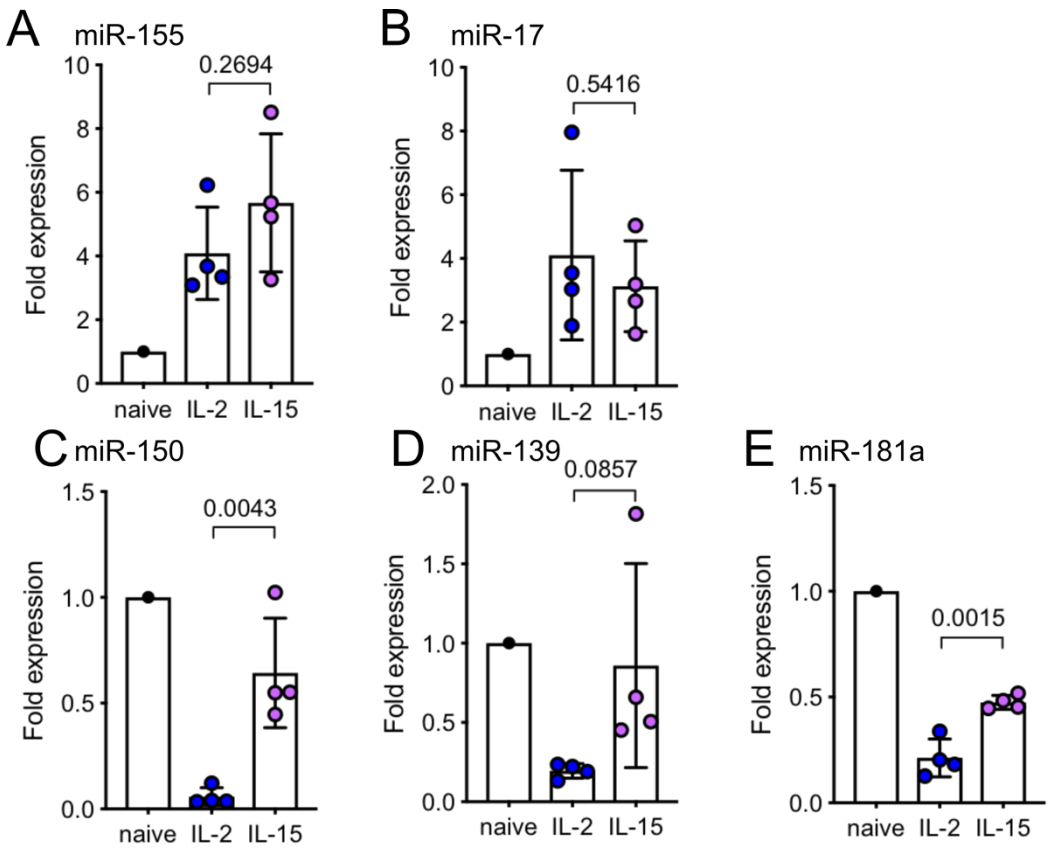

Figure 3.6 Differentiation to effector or memory-like cells alters miRNA expression

A-E Expression of miR-155 (A), miR-17 (B), miR-150 (C), miR-139 (D) and miR-181a (E) was measured by qPCR from naive cells, and on day 6 from IL-2 and IL-15 differentiated cells. Expression was normalised to snU6 and is shown as fold expression relative to naive cells. The graphs show mean and standard deviation from 4 independent experiments alongside adjusted P values. Statistical analysis was done using an unpaired two-tailed student's t-test comparing the IL-2 and IL-15 conditions. Ago-2-flag mice were used for these experiments.

3.3 Discussion

3.3.1 Regulation of miRNA expression

The expression of the five studied miRNAs changed dramatically upon $CD8^+$ T cell activation, depending on the strength of the activating signal and cytokines guiding cell differentiation. As previously reported, miR-155 and miR-17 were strongly induced upon activation. These, alongside other miRNAs of the 17~92 cluster and miR-21 are among the few miRNAs have been shown to be upregulated in activated T cells, with the majority of miRNAs downregulated (Wu *et al.*, 2007; Bronevetsky *et al.*, 2013). This was the case for miR-150, miR-139 and miR-181a, which all decreased in expression. miRNA expression can be regulated on the transcriptional level, through post-transcriptional regulation of miRNA processing or by mature miRNA homeostasis, stability and loading onto RISC. Transcription factors can affect the expression of specific miRNAs, for example Myc and NF-κβ have been shown to bind miRNA promoters, with miRNAs often forming reciprocal negative feedback loops (Chang *et al.*, 2008; Boldin and Baltimore, 2012). Globally, miRNA turnover has been shown to be accelerated in activated $CD4^+$ T cells with continuous production of new miRNAs and Ago-proteins coupled with degradation (Bronevetsky *et al.*, 2013).

3.3.2 The effect of TCR signal strength on miRNA expression

The strength of the activating TCR signal was shown to influence the extent of miRNA up-and downregulation. The cells activated with T4 showed intermediate changes in expression, whereas those activated with the weakest agonist G4 were similar to naive cells in their miRNA expression. This trend was clear for all the miRNAs studied, even though statistical significance was only reached in the case of miR-139. The cells activated with G4 exhibited a much less activated phenotype, compared to cells activated with N4 and T4. This presented as smaller cell size and lower expression of activation markers and the transcription factors T-bet and IRF4. This phenotype could be the

cause or the effect of the reduced miRNA downregulation. The activating signals provided by G4 may not be sufficient to activate the pathways normally leading to changes in miRNA expression. The altered miRNA expression could also subsequently contribute to the less activated phenotype of the cells activated with T4 or G4. For example, failure to downregulate miR-139 could lead to inhibition of its described targets Eomes and perforin, required for CTL function. Contrarily, failure to upregulate miR-155 could lead to increased expression of its targets, such as inhibitors of cytokine signalling. miR-155 expression has previously been shown to be stronger with N4 compared to T4, in agreement with our findings (Dudda *et al.*, 2013). This has been shown to be biologically relevant in the context of tumour clearance, in a study that compared miR-155 expression in OT-I T cells isolated from N4 and T4 expressing B16 tumours. OT-I cells from the T4-tumours had lower expression of miR-155 compared to cells from N4 tumours, and low levels of miR-155 expression were shown to correlate with bigger tumour volume for the T4-tumours consistent with reduced effector function in cells with lower miR-155 expression (Martinez-Usatorre *et al.*, 2019).

As well as the regulation of miRNA expression by TCR signal strength (as shown for miR-155), miRNAs can also influence the strength of TCR signalling. High levels of miR-181 in immature thymocytes increase TCR signalling through inhibition of phosphatases, allowing positive selection to take place (Li *et al.*, 2007). In naive mature T cells miR-181 levels are decreased to adjust the threshold of TCR signalling and allow discrimination between strong and weak agonists. We showed that expression of miR-181 further decreases upon T cell activation, depending on the activating peptide.

3.3.3 miRNA expression during effector and memory cell differentiation

Various miRNAs have been shown to influence $CD8^+$ T cell effector and memory cell differentiation. Expression of miR-155 is important for both effector functions and for mounting long-lasting memory (Dudda *et al.*, 2013;

Gracias *et al.*, 2013). miR-17~92 cluster is also required for effector cell responses, however its overexpression leads to skewing to a short-lived effector phenotype compromising memory formation (Wu *et al.*, 2012; Khan *et al.*, 2013). Similarly, overexpression of miR-150 has been shown to compromise $CD8^+$ T cell memory (Chen *et al.*, 2017).

During *in vitro* activation of OT-I cells, upregulation of miR-155 and miR-17 appeared to be transient, with levels slowly returning to baseline when cells were kept in culture, either with IL-2 or IL-15. This suggests that during *in vitro* activation, these miRNAs are important for the early events upon activation, causing inhibition of factors normally prohibiting cell proliferation and effector function. miR-139, miR-150 and miR-181a were downregulated upon activation and remained low in effector cells cultured in IL-2. However, culture in IL-15 lead to re-expression of these miRNAs. Memory cells have been previously shown to have a similar miRNA profile to naive cells (Wu *et al.*, 2007). The inhibition of the targets for these miRNAs was therefore potentially required to maintain the effector phenotype, but no longer needed when the cells acquired a memory-like phenotype. miR-155, miR-17 and miR-150 have all been described complex roles in effector and memory cell differentiation *in vivo* which are probably not recapitulated in the *in vitro* system based on signals from IL-2 versus IL-15. Differential expression of miRNAs has been previously studied in IL-2 and IL-15 differentiated $CD8^+$ T cells (Almanza *et al.*, 2010). In line with our results, the expression of miR-150 but not miR-155 was shown to increase with IL-15. From their findings the authors suggested that a $miR\text{-}150^{high}$, $miR\text{-}155^{low}$ phenotype guides the cells towards a central memory phenotype. *In vivo* studies have however since showed that miR-150 overexpression causes a short-lived effector phenotype and miR-155 deficiency impairs memory formation, highlighting the fact that miRNA expression in an *in vitro* setting may not always be representative of its biological function (Dudda *et al.*, 2013; Chen *et al.*, 2017).

miRNA function is regulated not only through their expression, but also through changes in the formation of RISC and expression of miRNA-associated proteins. To further understand the role of miRNAs in T cell activation, we next studied changes in the expression of RISC-interacting proteins and miRNA association with RISC.

CHAPTER 4:

CD8$^+$ T cells form a HMW RISC upon activation containing Ago-2 and GW182

4.1 Introduction

miRNAs bind and suppress their target mRNAs in the Ago-containing RISC. RISC is guided by the miRNA to its target mRNA through sequence-complementarity between the miRNA seed region and the mRNA 3' UTR. This leads to suppression of target gene expression, either by mRNA degradation or translational repression (O'Connell *et al.*, 2010). Ago proteins are a core component of RISC and mediate target suppression either directly or through recruitment of other mRNA silencing effector molecules. Four Ago proteins exist in mammals, Ago-1-4, all of which bind miRNAs and can repress their target genes. Ago-2 differs from the other three by its endonucleolytic activity that allows direct cleavage of target mRNAs (Tuschl *et al.*, 2004).

Ago forms large multi-protein complexes with its interactors to mediate miRNA target suppression. A key interactor is GW182, that binds Ago PIWI region through its N-terminal GW-repeats (Lian *et al.*, 2009; Elkayam *et al.*, 2017). Knock-down of GW182 has shown that this interaction is essential for miRNA suppressive function (Eulalio, Huntzinger and Izaurralde, 2008; Lian *et al.*, 2009). GW182 functions as a scaffold protein recruiting RNA metabolism factors to RISC through its C-terminal domains. These GW182-binding proteins include poly(A) binding proteins (e.g. PABPC1), deadenylases (e.g. PAN2/3, CCR4/NOT), decapping proteins (e.g. DCP1/2) and exonucleases (XRN1), which together cause miRNA target gene silencing (Fabian and Sonenberg, 2012). GW182 is part of the TNRC6 (trinucleotide repeat-containing protein 6) family of proteins encompassing TNRC6A (also known as GW182), TNRC6B and TNRC6C. The three paralogues share a conserved domain structure: all three proteins can bind Ago and have redundant functions in mediating miRNA silencing (Lazzaretti, Tournier and Izaurralde, 2009). Furthermore, several isoforms of GW182 exist. In mice, two alternatively

spliced isoforms are predicted; a full-length protein of 203kDa and a shorter splice-variant at 150kDa, missing the first five exons (Fig.4.1). Both isoforms contain the domains required for Ago binding and miRNA target silencing. The human protein has also been described to have at least three isoforms, named GW220/TNGW1, GW195 and GW185 after their molecular weights (Castilla-Llorente *et al.*, 2012). GW220 and GW195 transcripts contain additional exons at the N-terminus compared to GW182. GW220 and GW182 appear to be functionally similar, with both isoforms inducing mRNA degradation and translational repression to a comparable extent (Li *et al.*, 2008).

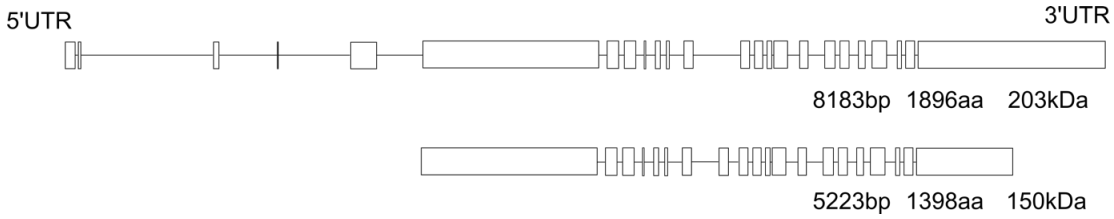

Figure 4.1 GW182 isoforms
A graphical representation of the two isoforms from the GW182 gene in mouse. The blocks represent exons and the lines introns. The length of the introns has been reduced 10-fold for better visualisation of the exons.

In T cells, GW182 expression has been shown to be induced upon activation (La Rocca *et al.,* 2015). The other two GW182 paralogues TNRC6B and TNRC6C are also expressed in T cells. Analysis of existing proteomics data from P14 $CD8^+$ T cells (Howden *et al.* 2019) indicated that expression of all three paralogues increases during $CD8^+$ T cell activation, with a drastic 38-fold increase in copy number of GW182, and a more modest 5-fold and 3-fold change for TNRC6B and TNRC6C, respectively. TNRC6B was however the most abundant isoform in activated T cells with an average of ~16,000 copies in activated cells, compared to ~6,000 average copies of TNRC6A. However, it has been previously shown, that knock-down of GW182 but not TNRC6B or TNRC6C in T cells compromised miRNA suppressive function (La Rocca *et al.* 2015). In naive T cells, in which GW182 is not expressed, Ago is predominantly found in LMW RISC (La Rocca *et al.*, 2015). Upon activation, TCR signalling leads to GW182 protein upregulation, interaction with Ago and formation of HMW RISC. miRNAs that were associated with HMW RISC were shown to

have an increased suppressive capacity compared to those found in LMW RISC (La Rocca *et al.*, 2015). Association with different Ago-complexes may therefore regulate miRNA function. We aimed to further study the formation of HMW and LMW RISC in activated $CD8^+$ T cells, and to characterise the interaction between Ago-2 and GW182, a key component of HMW RISC.

4.2 Results

4.2.1 Ago-2 expression during $CD8^+$ T cell activation

To measure Ago-2 expression during $CD8^+$ T cell activation, OT-I T cells were activated with N4 for 2 days, then the cultures were supplemented with IL-2 for 4 days. Cells were collected for western blotting (WB) before activation, on day 1 (d1) and d2 after adding N4, then 2 and 4 days after addition of IL-2 (d4 and d6). Ago-2 expression was quantified using ZAP-70 as a loading control. The expression of most proteins increases upon $CD8^+$ T cell activation due to an increase in global protein production and cell size. As expected, the total amount of Ago-2 per cell increased after activation, as did that of ZAP-70 (Fig.4.2A). When loading was normalised by adding the same concentration of protein per well for each of the samples, the relative abundance of Ago-2 was found to be gradually decreasing after activation, during 6 days of culture (Fig.4.2B-C). This decrease was only statistically significant on day 6 ($p=0.045$) most likely due to the high variance arising from pooled data from three independent experiments.

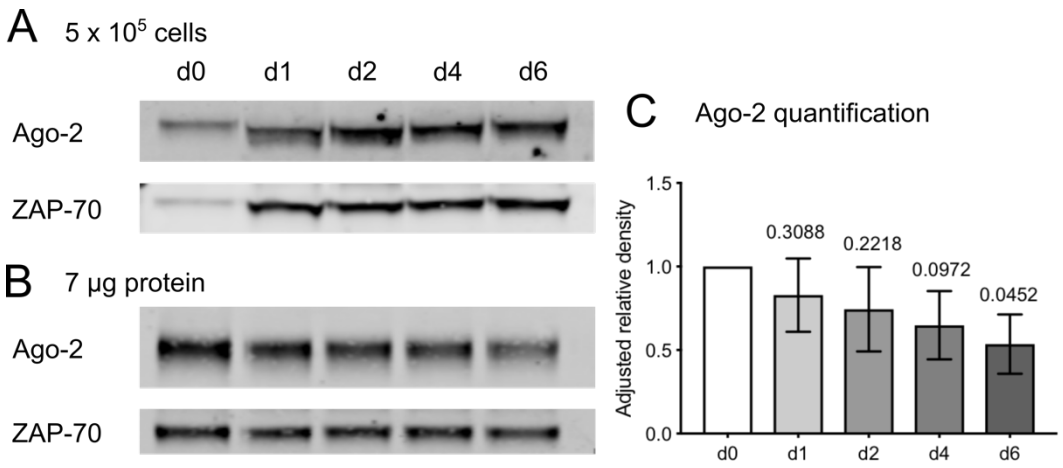

Figure 4.2 Ago-2 is expressed in naive and activated $CD8^+$ T cells
A-C OT-I cells were activated with N4 for 2 days then cultured with IL-2 for 4 days. Cells were lysed and 5 x 10^5 cells (A) or 7 µg of protein (B) were loaded for western blotting. Relative abundance of Ago-2 was quantified from B by measuring band intensity of Ago-2 normalised to the loading control ZAP-70. The relative abundance is shown in C as expression relative to naive cells. The graph is showing the mean and standard deviation from three biological replicate experiments. Statistical analysis was performed by doing a one sample t-test comparing each activated time-point to the hypothetical mean 1. Ago-2-flag mice were used for 2 out of 3 of these experiments.

4.2.2 GW182 expression in $CD8^+$ T cells and its interaction with Ago-2

GW182 has been previously shown to be a key interactor of Ago and an important component of RISC. We therefore aimed to confirm the expression of GW182 in OT-I T cells and to study the dynamics of its interaction with Ago-2 following T cell activation. First, we measured the expression of Ago-2 and GW182 mRNA. RNA was extracted from naive cells, and at different timepoints after activation with N4. Ago-2 mRNA expression remained unchanged during 6 days of culture (Fig.4.3A). However, GW182 mRNA was upregulated at 24 hours, and remained higher at later time-points compared to naive cells (Fig.4.3B). We also confirmed expression of GW182 in activated cells by immunoprecipitation (IP) of GW182 or Ago-2 from d6 activated cells. In the input lysate, probing with anti-GW182 antibody revealed several bands around the correct molecular weight. In the GW182 IP with the same antibody there was enrichment of two clear bands, both between 150-250 kDa (Fig.4.3C). The mouse GW182 isoforms have predicted molecular weights of 150 kDa and 203 kDa, whereas the human protein has at least three isoforms at 220, 195 and 182 kDa. The two bands may therefore correspond to the 203 kDa large isoform and a previously uncharacterised isoform, or the shorter 150 kDa isoform running at a higher molecular weight than expected. The other bands seen in the WB of the total input lysate could be non-specific interactions with the polyclonal anti-GW182 rabbit antibodies. The two bands also co-immunoprecipitated with Ago-2 in the Ago-2 IP, further supporting that these are genuine GW182 isoforms (Fig.4.3C). Alignment of the protein sequence of GW182 with its two paralogues TNRC6B and TNRC6C showed poor conservation of the region recognised by the GW182 antibody, making it unlikely that these would be bound by the antibody.

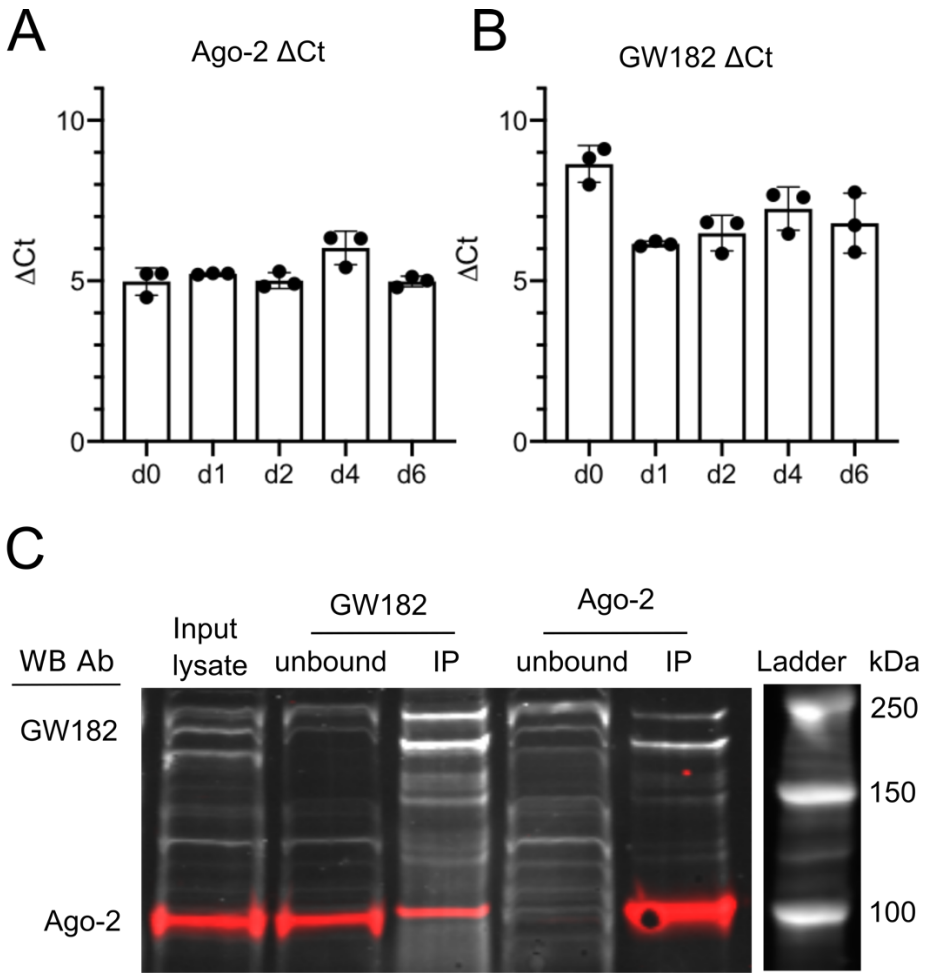

Figure 4.3 GW182 is expressed and binds Ago-2 in activated CD8⁺ T cells
A-B Ago-2 and GW182 mRNA expression during OT-I T cell activation measured by qPCR from samples taken at indicated time-points. The Ct values were normalised to snRNA U6 to obtain delta Ct values. The graph is showing mean and standard deviation from three technical replicates. Data are representative of two independent experiments.
C Western blot showing Ago-2 and GW182 expression in input lysate, GW182 and Ago-2 IPs and unbound fractions from d6 activated CTLs. GW182 was immunoprecipitated with a rabbit polyclonal antibody and Ago-2 was immunoprecipitated with a mouse monoclonal antibody. The input, IP and unbound samples were run on a gel for western blotting, probed again with the same GW182 and Ago-2 antibodies and fluorescently labelled secondary antibodies, then visualised on a western blot imaging scanner. Data are representative of two biological replicates. Ago-2-flag mice were used for these experiments.

After confirming the expression of GW182 and its association with Ago-2 in activated $CD8^+$ T cells, we followed this interaction during a time-course of T cell activation with the aim to determine the stoichiometry of binding between GW182 and Ago-2 in naive and activated cells. We undertook a series of Ago-2 and GW182 IPs to confirm that the binding of the two proteins was specific to activated cells. Ago-2 IP efficiently pulled down Ago-2 from both naive and activated cells, as almost no Ago-2 was detected in the WB of the unbound fraction (Fig.4.4A). GW182 was not detected in the Ago-2 IP from naive cells but could be pulled down in the Ago-2 IP from activated cells. Next, we immunoprecipitated GW182. In naive cells, the GW182 IP potentially pulled down a small amount of the longer isoform, not detected from the Ago-2 IP (Fig.4.4A). All Ago-2 however remained in the GW182 unbound fraction, confirming that the interaction was specific to activated cells. In activated cells, Ago-2 distributed between GW182-bound and unbound fractions.

The amount of GW182 that co-immunoprecipitated with Ago-2 was quantified from a time-course of cell activation (Fig.4.4B). The amount of GW182 relative to Ago-2 was at its highest soon after activation, on d1-d2 (Fig.4.4C). The interaction was however detectable during 6 days in culture. Two isoforms could be detected, with the shorter isoform being predominant in the Ago-2 IP on d4-d6 (Fig.4.4C). Both isoforms could be detected equally from the GW182 IP on day 6, suggesting Ago-binding of one isoform may specifically be reduced (Fig.4.4A). Based on the previous results, not all Ago-2 was engaged in a complex with GW182 in activated cells, and we next attempted to determine what this proportion was. We quantified Ago-2 from GW182 IP bound and unbound fractions and showed that approximately 40% of Ago-2 was bound to GW182 with 60% remaining unbound (Fig.4.4D, E). The amount of GW182-bound Ago-2 appeared at its highest at earlier timepoints, but this trend was however not replicated in a repeat experiment. Unfortunately, due to the background noise of the anti-GW182 antibody we were unable to do the reciprocal calculation and accurately quantitate the proportion of GW182 that is associated with Ago-2 at these times.

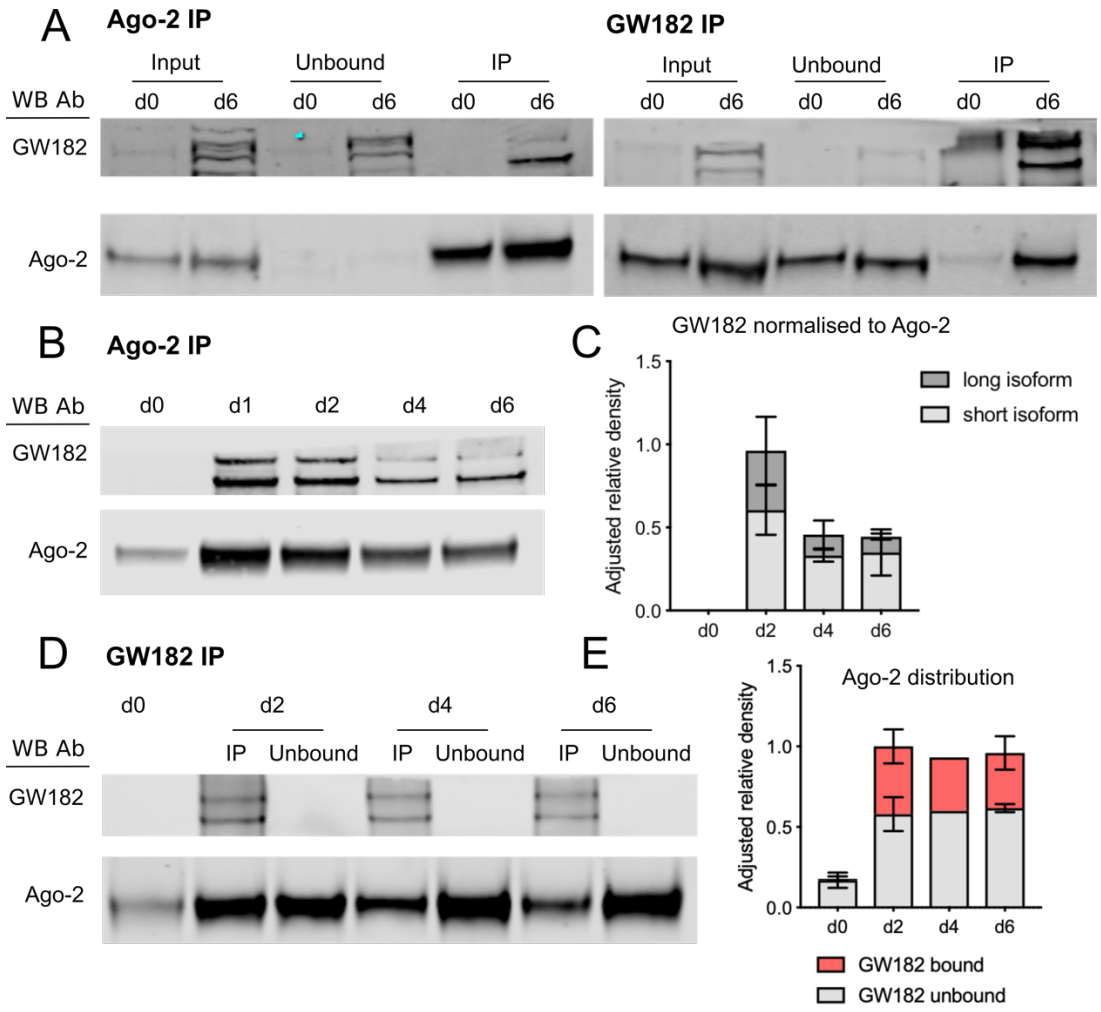

Figure 4.4 Dynamics of Ago-2 and GW182 interaction upon T cell activation
Immunoprecipitations using a polyclonal rabbit GW182 antibody and a monoclonal mouse Ago-2 antibody. All WBs were probed with the same antibodies that were used for the IPs. Ago-2-flag mice were used for these experiments apart from D-E.
A Ago-2 and GW182 were immunoprecipitated from naive and d6 activated cells. Input lysate, unbound fraction, and eluted IP samples are shown on a WB probed with the Ago-2 and GW182 antibodies.
B-C Ago-2 was immunoprecipitated from OT-I T cell lysates taken at the indicated time points. The eluted IP samples are shown on a WB probed with Ago-2 and GW182 antibodies (B). GW182 relative abundance was quantified by measuring GW182 band intensity (as sum of the two bands) relative to Ago-2 band intensity and is shown normalised to expression on d2 (C). The proportions of the two GW182 bands were also calculated. Mean and standard deviation from two independent experiments are shown.
D-E GW182 was immunoprecipitated from lysates taken at the indicated time-points. The unbound fraction was used for an Ago-2 IP. The eluted IP fractions are shown on a WB probed with Ago-2 and GW182 antibodies (D). Amount of Ago-2 found in GW182 IP or Ago-2 IP from GW182 unbound fraction was quantified and is shown normalised to expression on d2 (E). Mean and standard deviation from two independent experiments is shown.

4.2.3 Formation of HMW and LMW RISC during $CD8^+$ T cell activation

Ago-2 has been previously shown to form a HMW RISC containing GW182 in activated T cells. We wanted to see if the GW182-bound Ago-2 corresponded to HMW RISC. Size exclusion chromatography was used to separate protein complexes by size from naive and d2 activated OT-I T cells. Large complexes were eluted in the first fractions, followed by intermediate sized complexes and lastly uncomplexed proteins. Proteins were precipitated from the different size fractions, and Ago-2 was detected by WB. In naive cells, Ago-2 was found predominantly in LMW fractions, whereas in activated cells it could be detected from both low and high MW fractions (Fig.4.5A-B). In fact, Ago-2 could be detected from a range of fractions from low to intermediate to high.

GW182 was previously reported to be an important component of HMW RISC in activated T cells. To confirm interaction of Ago-2 with GW182 in HMW RISC, Ago-2 was immunoprecipitated from the fractions. Based on the WB, we pooled fractions corresponding to 'HMW', 'intermediate' and 'LMW' complexes in activated cells, and 'LMW' in naive cells. GW182 was shown to co-immunoprecipitate with Ago-2 from the HMW complex, whereas a weak signal was seen from the intermediate complexes, and no signal from the LMW complex from either the naive or the activated cells (Fig.4.5C). These findings confirm that Ago-2 is found in a non-GW182 bound LMW RISC in naive cells. LMW complex is also present in activated cells, but Ago-2 but can additionally form larger complexes, including a GW182 containing HMW RISC.

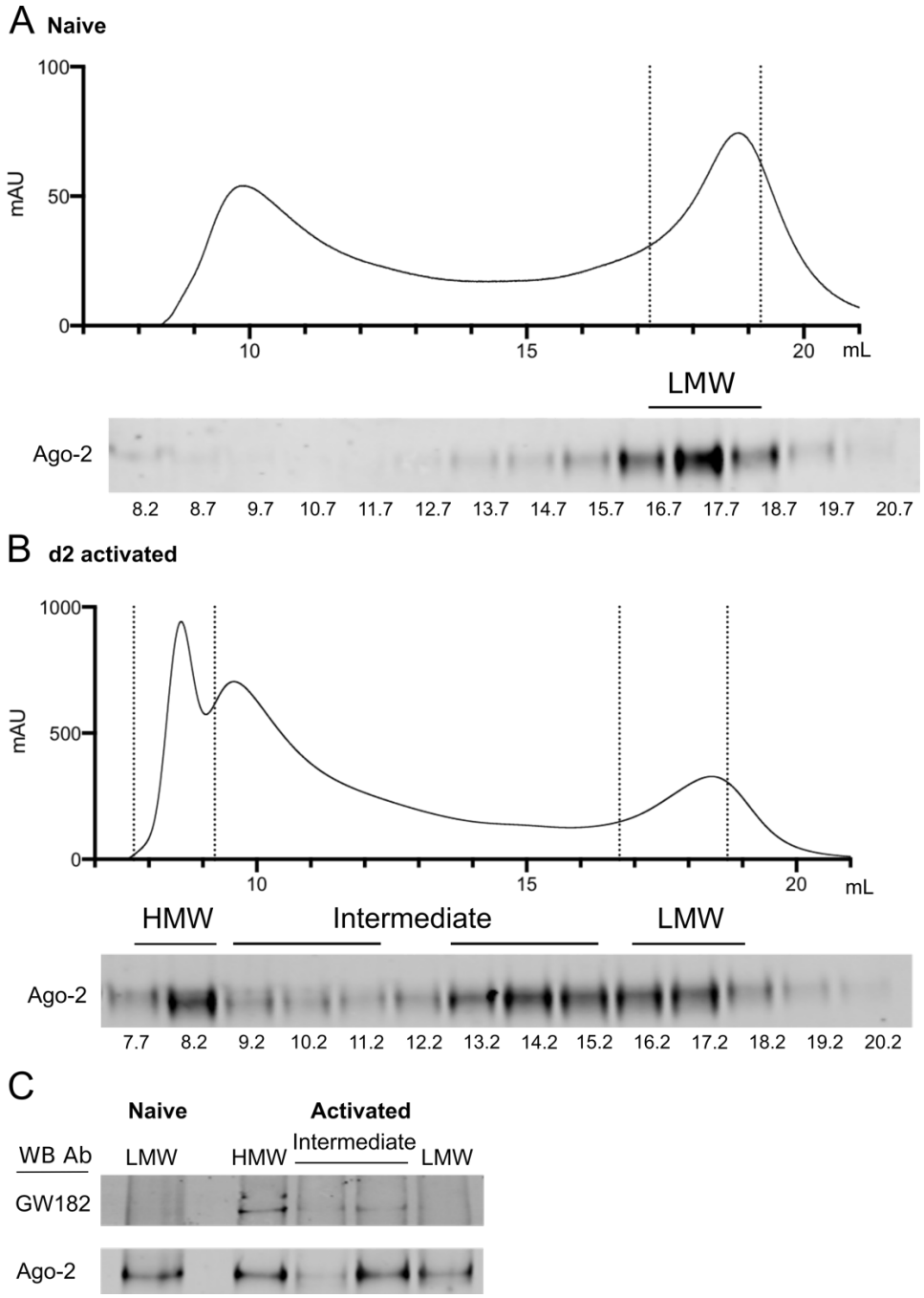

Figure 4.5 Ago-2 forms HMW RISC with GW182 in activated CD8$^+$ T cells
A-B Protein elution curves and WB from size exclusion chromatography fractions. Fractions were obtained by running naive or d2 activated cell lysate through a Superose 6 gel filtration column. 0.5 mL fractions were eluted from the column and protein content was measured by absorption at 280 nm (shown in milli-Absorption Units). Protein was precipitated from the fractions and used for western blotting to detect Ago-2. Dashed lines in A and B indicate location of HMW and LMW Ago-2 in the elution profile, corresponding to the WB.
C Ago-2 was immunoprecipitated from HMW, intermediate and LMW fractions, pooled together as indicated in the WBs in A-B. The eluted IP samples are shown on a WB probe with Ago-2 and GW182 antibodies. Ago-2-flag mice were used for this experiment.

4.2.4 Blocking Ago-GW182 binding with a peptide

To determine whether the interaction between Ago and GW182 was required for T cell activation, we attempted to block their binding. We designed a peptide based on the Ago binding sequence of GW182. GW182 has been described to have three Ago binding sites, motif 1, motif 2 and the hook motif (Elkayam *et al.*, 2017). Each of these peptide motifs was previously shown to bind Ago *in vitro* and could displace other peptides from Ago in titration experiments. We designed our peptide based on motif 1. To get the peptide into our cells, we linked the Ago binding motif sequence to the sequence of a described translocating peptide TP2. This translocating peptide sequence was shown to transport molecular cargo across cell membranes through spontaneous translocation (He *et al.*, 2013). We named this the GW TP2 peptide, and also designed a control peptide with key Ago binding residues mutated to alanine residues (Fig.2.1). To test the function of the peptides, we made lysates from d2 activated OT-I T cells and and incubated these with the peptides during an Ago-2 IP for 6 h, with the intention to displace GW182 from Ago-2. After the 6 h IP, we eluted the samples and visualised these on a WB probed with Ago-2 and GW182 antibodies. GW182 co-immunoprecipitated with Ago-2 as expected, but addition of the GW TP2 at 10 μM or 50 μM did not reduce the amount of co-immunoprecipitating GW182 (Fig.4.6). No GW182 could be detected from the unbound fractions.

Potentially, the peptide was not strong enough to displace GW182, as it had previously only been shown to displace other short peptides (Elkayam *et al.*, 2017). It is possible that the concentration of the peptide may not have been high enough to displace GW182, or addition of the TP2 sequence may have altered the binding of the peptide. Since we did not see any reduction in Ago-2 and GW182 binding *in vitro*, we did not expect the peptide to have a significant effect when delivered to live cells, thus decided not to pursue this approach further at this time.

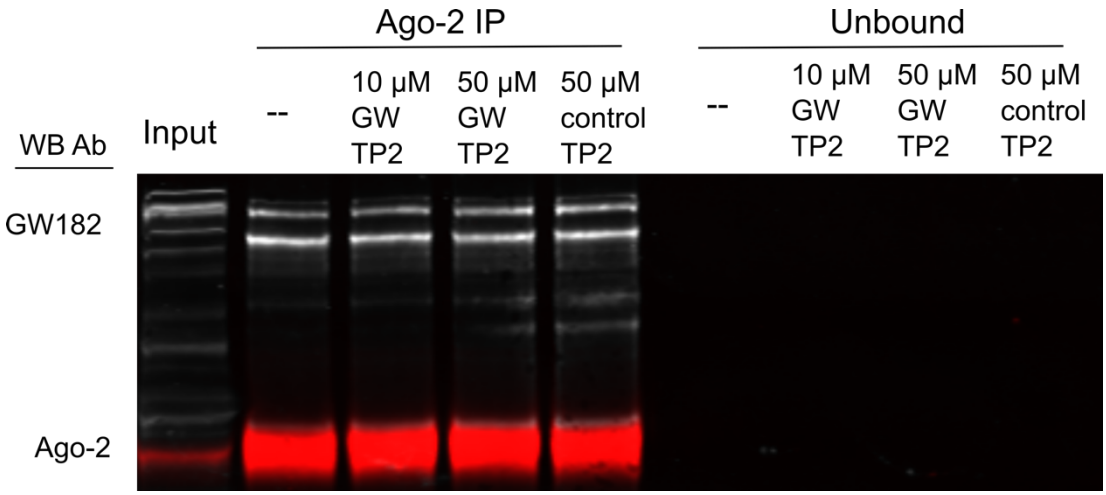

Figure 4.6 GW TP2 does not block Ago-2 and GW182 binding in an Ago-2 IP
Ago-2 IPs and unbound fractions from d2 activated OT-I T cells shown on a western blot probed with Ago-2 and GW182 antibodies. GW TP2 or control TP2 were added directly to the lysates and incubated for 6 h during Ago-2 IP with magnetic beads.

4.3. Discussion

4.3.1 Summary of findings

These experiments show that GW182 is not expressed, or is very weakly expressed, in naive $CD8^+$ T cells but is upregulated upon activation. The protein was quickly recruited to RISC after activation and remained bound to Ago-2 during 6 days of culture. In activated cells, Ago-2 was found associated and non-associated with GW182. Approximately 40% of Ago-2 was found to be engaged with GW182 in activated cells, with 60% remaining unbound. Size exclusion chromatography also confirmed the presence of a GW182-non-associated LMW RISC, and a GW182-associated HMW RISC in activated cells.

4.3.2 Changes in Ago expression

The availability of miRNA-associated protein machinery changes upon T cell activation. In $CD4^+$ T cells, a previous study showed ubiquitination and degradation of all Ago proteins upon cell activation, which was suggested to cause global downregulation of miRNAs (Bronevetsky *et al.*, 2013). In $CD8^+$ T cells, a gradual decrease in the relative amount of Ago-2 per cell could be noted in the 6 days following activation, with statistical significance reached on day 6. However, unlike shown for $CD4^+$ T cells, the protein was not completely degraded as it could still be readily detected from both naive and activated cells. Since we did not measure expression in $CD4^+$ T cells, it is unclear whether this is a difference between the types of T cells, or a difference in experiments, for example the method of activation (cognate peptide versus anti-CD3/28 antibody). Other studies have also shown expression of Ago-2 in both naive and activated T cells (composed of a mix of $CD4^+$ and $CD8^+$ cells) (La Rocca *et al.*, 2015).

4.3.3 Ago-interacting proteins and RISC composition

Association of Ago-2 with other proteins changes dramatically upon T cell activation. We showed that in agreement with previous work, Ago-2 binds GW182 in activated cells (La Rocca *et al.*, 2015). Two isoforms of GW182 co-immunoprecipitated with Ago-2, with the shorter isoform being the predominant one. Several isoforms of GW182 have been reported in human cells and these were shown to have redundant functions (Li *et al.*, 2008; Castilla-Llorente *et al.*, 2012). The longest human isoform, GW220 contains N-terminal polyQ-repeats not present in the other isoforms, and it has been suggested these may influence protein-protein interactions, and could play a role in the localisation of RISC in processing bodies (P-bodies) versus the cytoplasm (Castilla-Llorente *et al.*, 2012). These polyQ repeats are also conserved on the 203 kDa mouse GW182, but not the 150 kDa isoform.

Approximately 40% of Ago-2 was bound to GW182 in activated cells, with the rest remaining unbound. Ago-2 IP from size fractionated samples showed that GW182-unbound Ago-2 was predominantly found in LMW or intermediate size complexes, whereas GW182-bound Ago-2 formed HMW RISC. Some GW182 signal could also be detected from the intermediate size complexes, suggesting these may be smaller complexes composed of only Ago-2 and GW182, whereas HMW RISC contains additional proteins. These intermediate complexes could be precursors of the HMW RISC, or a separate complex composed of different proteins. Different sized Ago-complexes have been previously separated by sucrose gradients, and proteomic analysis of these showed differences in the protein composition of these complexes (Höck *et al.*, 2007). RISC-associated proteins can for example include Dicer, mRNA metabolism factors and ribosomal proteins. Dicer was found to associate with a low density Ago complex, in which miRNA loading to RISC occurs. This complex was separate from the effector miRNA complexes to which Ago was recruited after miRNA loading (Höck *et al.*, 2007; Landthaler *et al.*, 2008). Proteins involved in gene silencing, mRNA binding and RNA metabolism were

found in intermediate to large Ago-complexes (Höck *et al.*, 2007). Larger Ago complexes were also shown to co-sediment with ribosomal proteins and polysomes (Landthaler *et al.*, 2008). Depletion of ribosomal proteins has been shown to reduce miRNA mediated suppression, and lead to a shift of miRNA targeted transcripts from monosomes to polysomes (Janas *et al.*, 2012). The GW182 containing HMW RISC separated by size exclusion chromatography was also shown to contain RNA metabolism factors such as PABP1 and ribosomal proteins and rRNA (La Rocca *et al.*, 2015).

4.3.4 Regulation and function of different RISC complexes

Mitogenic stimuli such as growth factors and glucose have been shown to regulate the formation of LMW and HMW RISC in immortalised IL-3 dependent haematopoietic cells and mouse embryonic fibroblasts. Withdrawal of growth factors or glucose resulted in decreased expression of GW182 and formation of a LMW RISC, whereas reintroduction led to reincorporation of miRNA-Ago complexes to functional HMW RISC (Olejniczak *et al.*, 2013). As opposed to *de novo* synthesis of a HMW RISC, this complex was shown to be formed from LMW RISC following specific signalling, demonstrating the dynamic nature of these associations. In Drosophila, mitogenic signals were also shown to alter RISC composition. A constitutively expressed RISC named G-RISC was shown to be composed of Ago-1 and GW182. Mitogenic signals led to the formation of an alternative complex named P-RISC, that associated with polysomes and did not include GW182. The authors suggested that both complexes caused mRNA translational repression through different means, G-RISC inhibiting translation initiation, and P-RISC elongation (Wu, Isaji and Carthew, 2013).

In T cells, TCR signalling causes upregulation of GW182 and formation of HMW RISC, possibly through the mTOR pathway (La Rocca *et al.*, 2015). These changes in RISC composition are likely to have important consequences for miRNA function. Most miRNAs are downregulated upon T

cell activation. However, the specific induction of GW182 and the formation of HMW RISC upon cell activation suggests that miRNA function is not shut down. Instead, miRNA function might indeed increase irrespective of expression changes, if recruited to HMW RISC, which contains GW182 and other silencing effector proteins. To further understand the role of HMW RISC in activated T cells, we next isolated HMW and LMW RISC bound miRNAs and measured their distribution between the two complexes.

CHAPTER 5:

Specific miRNAs are enriched in HMW RISC irrespective of changes in expression

5.1 Introduction

After confirming the formation of HMW RISC and LMW RISC in activated $CD8^+$ T cells, we aimed to identify which miRNAs are associated with the two complexes. We attempted to determine whether miRNAs were evenly distributed between HMW and LMW RISC in activated cells or whether specific miRNAs were found enriched within HMW RISC. In Chapter 3 we noted drastic changes in miRNA expression upon T cell activation and wanted to see how these related to miRNA distribution between HMW and LMW RISC. It was previously reported, that while majority of miRNAs were downregulated upon T cell activation, their occupancy in HMW RISC increased in activated cells, compared to naive cells (La Rocca *et al.*, 2015). This study also suggested that the shift to HMW RISC varied for individual miRNAs. Many miRNAs that were downregulated upon activation, were found in HMW RISC in activated cells and were shown to be actively suppressing their targets. These included miRNAs of the let-7 family and miR-15/16 family, that were shown to have an increased ability to suppress a reporter construct in activated cells despite downregulation in expression. Consequently, instead of miRNA expression changes, presence in HMW RISC may be more predictive of miRNA biological function. We therefore aimed to identify the involvement of miRNAs in regulating activated $CD8^+$ T cells by measuring differential miRNA abundance in naive versus activated cells, along with miRNA distribution between HMW RISC and LMW RISC in activated cells.

5.2 Results

5.2.1 Generation of small RNA libraries from HMW and LMW RISC

To identify which miRNAs were associated with Ago-2 in naive and activated cells, we activated OT-I cells with N4 for 2 days and collected samples for Ago-2 IPs. Ago-2 was immunoprecipitated from three biological replicates of naive cells, and for two of these we had a corresponding activated sample. In addition, two replicates of Ago-2 IPs from activated cells were also included from a separate experiment. Ago-2 was efficiently immunoprecipitated from all the input lysates (Fig.5.1A-B). GW182 co-immunoprecipitated with Ago-2 from activated, but not naive cells, as expected (Fig.5.1A-B). As a control, we performed an IP from activated cells with mouse IgG antibody. As expected, Ago-2 was found in the input, but remained in the unbound fraction following IgG IP (Fig.5.1B). Similarly, no GW182 was pulled down from the IgG IP.

We also wanted to separate HMW and LMW RISC in the activated cells, to identify which miRNAs were associated with each. Three more biological replicates of day 2 activated cells were prepared for size exclusion chromatography to separate HMW and LMW RISC. Following the size separation, protein was precipitated from the fractions and used for a WB to detect Ago-2. This showed presence of Ago-2 in high, intermediate and low molecular weight fractions (Fig.5.1C). The HMW and LMW fractions were pooled and Ago-2 was immunoprecipitated from these. A small amount of immunoprecipitated material was used for a WB, and as expected, GW182 co-immunoprecipitated with Ago-2 from the HMW but not LMW fractions (Fig.5.1D).

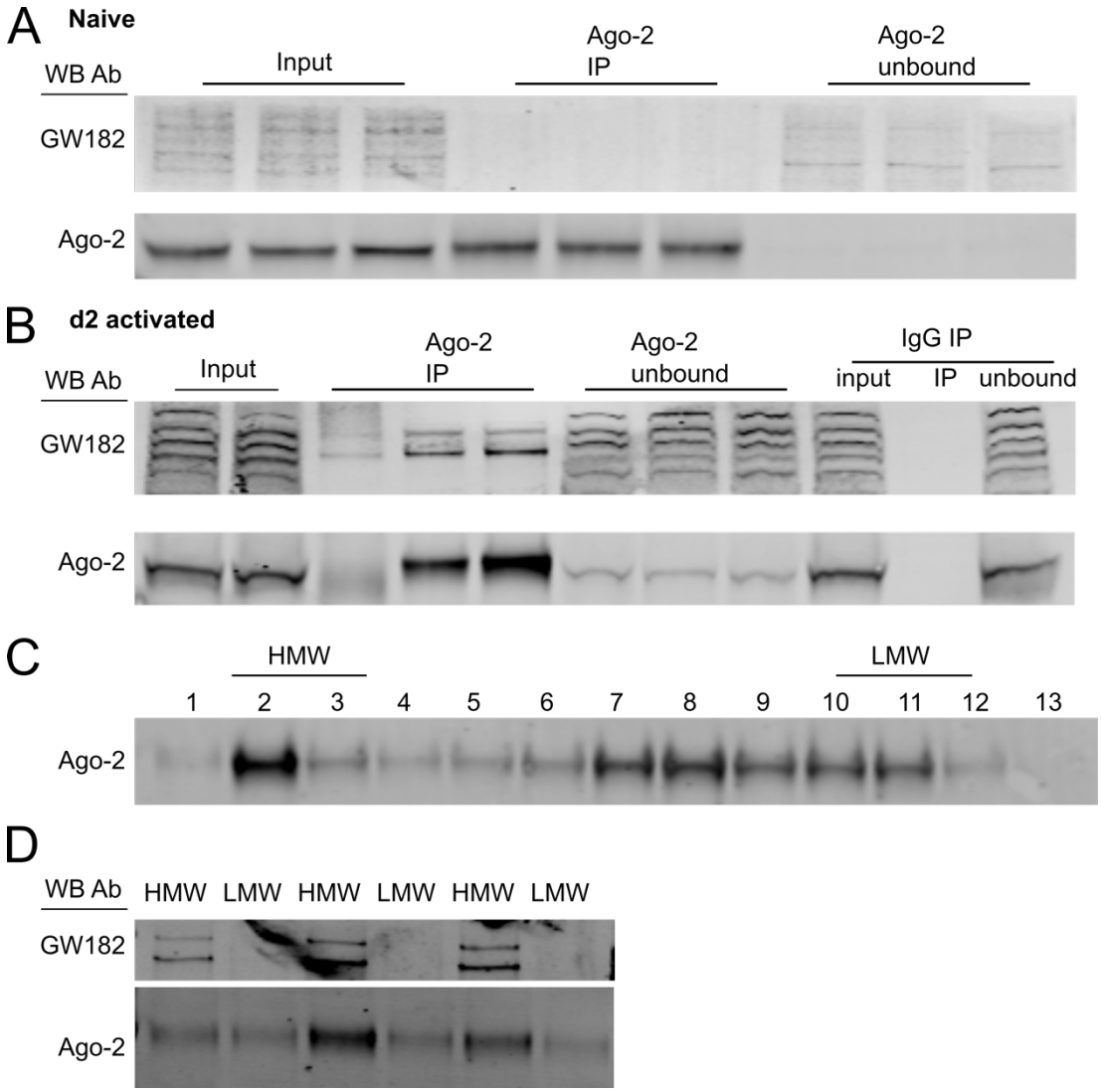

Figure 5.1 Ago-2 IPs from naive cells, activated cells, HMW RISC and LMW RISC

A-B WBs from input, Ago-2 IP and unbound fractions from naive and d2 activated OT-I cells. Blots probed with Ago-2 and GW182 antibodies. Three biological replicates are shown for naive and activated cells.

C WB from protein precipitated from size exclusion fractions. Blot probed with Ago-2 antibody. One replicate is shown as representative of all three.

D Ago-2 IP from the pooled HMW (lanes 2-3) and LMW (lanes 10-12) fractions shown in C. WB probed with Ago-2 and GW182 antibodies. All three biological replicates are shown.

Ago-2-flag mice were used for the size fractionated samples.

Next, we isolated RNA that was present in the cell input, the Ago-2 IP and the Ago-2 unbound fraction from naive cells and activated cells. For the size fractionated samples, we also isolated RNA from the from the HMW and LMW fractions prior to the Ago-2 IP (input), the Ago-2 IP and then Ago-2 unbound fractions. Once RNA was purified from all of the Ago-2 IPs, as well as the input for each IP and the unbound fractions, small RNA libraries were prepared from each sample. 3' and 5' adapters were ligated to the RNA, which was then reverse transcribed and amplified by PCR. The prepared input, Ago-2 IP and unbound libraries were pooled and run on TBE gels (Fig.5.2A). PCR products of the miRNAs with adapters ran at approximately 145 bp, and an adapter dimer band could be seen just below. The input and unbound libraries contained several bands of different sized RNAs, whereas the Ago-2-IP samples were enriched for miRNAs (Fig.5.2A). A distinct small RNA band could be seen for all the Ago-2 IPs, including the HMW and LMW RISC samples (Fig.5.2B). The IgG IP control sample did not have this band, and instead mostly contained adapter dimers (Fig.5.2B). The small RNA band at 145 bp was cut from each set of samples. Following gel purification, the samples were combined to make a final pool. The samples were measured on a Bioanalyzer to confirm the expected size (Fig.5.2C). The libraries were then sent for sequencing.

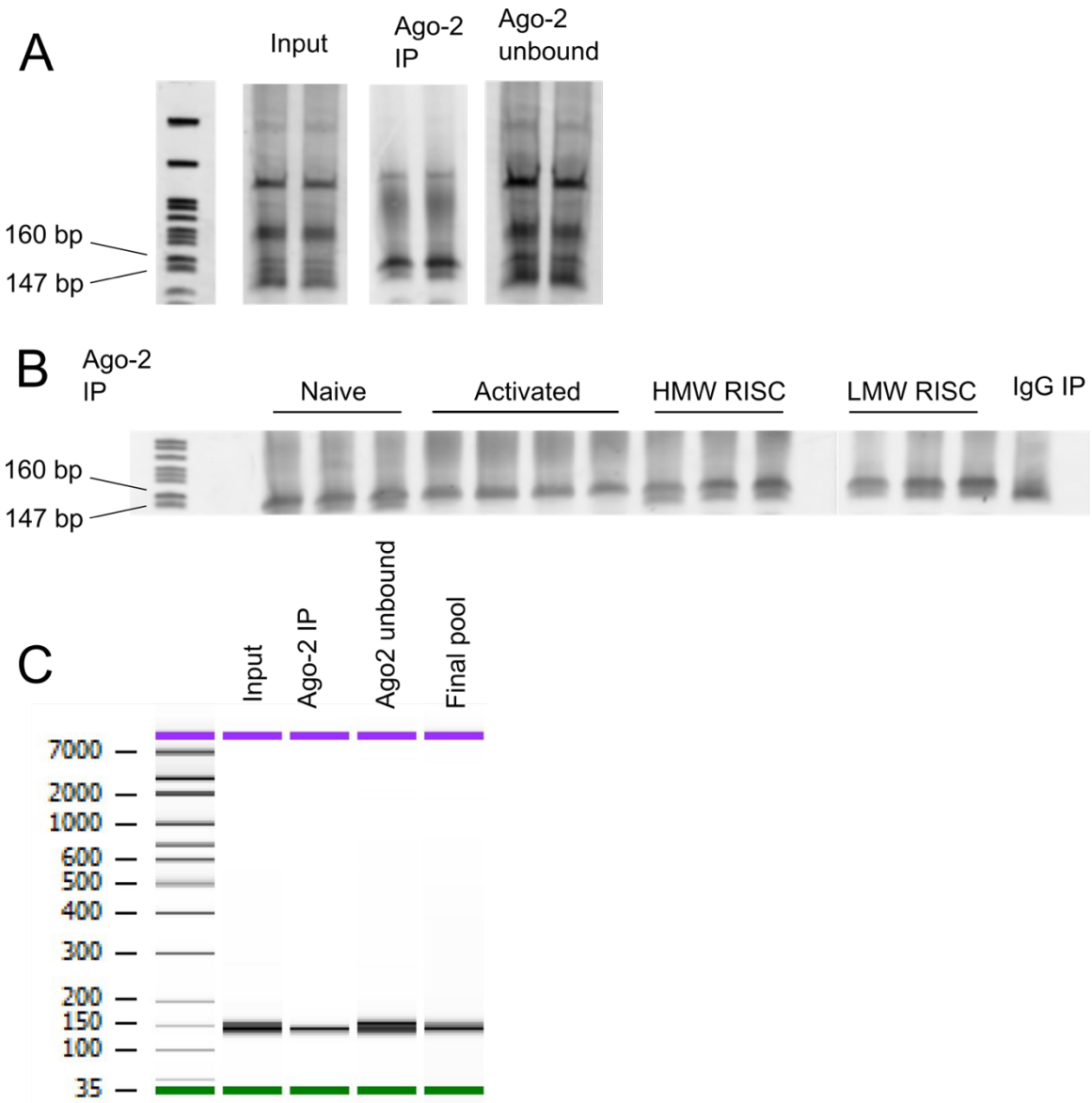

Figure 5.2 Generation of small RNA libraries from Ago-2 IPs
ATBE gels showing small RNA libraries made from the input, Ago-2 IP and unbound samples that have been pooled together from naive and activated cells and HMW and LMW RISC. The miRNA band is seen at 145 bp.
B TBE gels showing each individual Ago-2 IP sample and the IgG IP control.
C Bioanalyzer measurement of pooled input, Ago-2 IP and unbound samples, and final pool containing all samples.

5.2.2 miRNAs are enriched following Ago-2 immunoprecipitation

To determine the predominant RNA biotypes found in the samples, the sequencing reads were mapped to known mouse RNA families. The naive and activated input samples were similar in RNA content, containing approximately 40% miRNAs, with ribosomal (rRNA) and transfer RNAs (tRNA) being the next most abundant groups (Fig.5.3A). The other RNA detected contained some protein coding reads and long-non-coding RNAs, though most had been eliminated during size selection of libraries. Activated cells contained more rRNAs whereas naive cells were more enriched in tRNAs (Fig.5.3A). HMW and LMW RISC input samples contained fewer miRNA reads compared to the total unfractionated input, approximately 25% for HMW and only 5% for LMW (Fig.5.3A). The rest of the reads in the HMW sample were mostly ribosomal and in the LMW sample they were tRNAs (Fig.5.3A). miRNA reads were strongly enriched in all Ago-2 IP samples, making up 80-95% of all reads, whereas the unbound fractions contained only 5-20% miRNAs (Fig.5.3B-C). The unbound fractions contained mostly rRNA and tRNA (Fig.5.3C). The control IgG-IP contained only 5% miRNAs, whereas the IgG unbound fraction contained 40% miRNAs, similar to the activated input sample (Fig.5.3B-C).

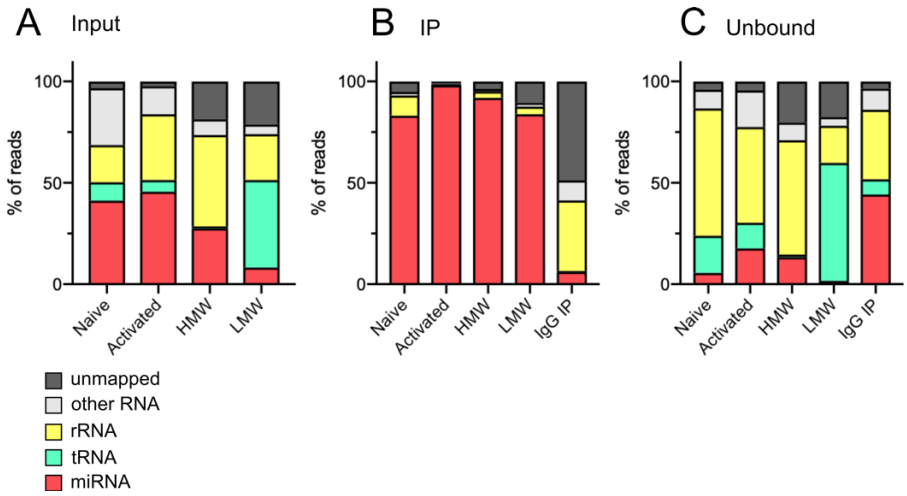

Figure 5.3 RNA composition of libraries
A-C RNA biotypes in input (A), Ago-2 IP (B) and unbound (C) samples. Proportion of reads corresponding to miRNAs, tRNAs, rRNAs, other types of RNAs (including protein coding reads and uncategorised RNA) or unmapped reads is shown.

Next, the miRNA content in each sample was compared by principal component analysis (PCA). Naive samples clustered together to one side of the plot, with the naive input, Ago-2 IP and unbound samples all forming their own small cluster (Fig.5.4). For the activated samples, even though two separate experiments were pooled, the miRNA expression profile appeared to be similar for all these. Total Ago-2-IP from activated samples clustered together with HMW Ago-2 IP samples, and LMW Ago-2 IP samples clustered next to these. IgG IP sample did not cluster with any other samples. However, the IgG unbound sample clustered together with the activated input samples as expected.

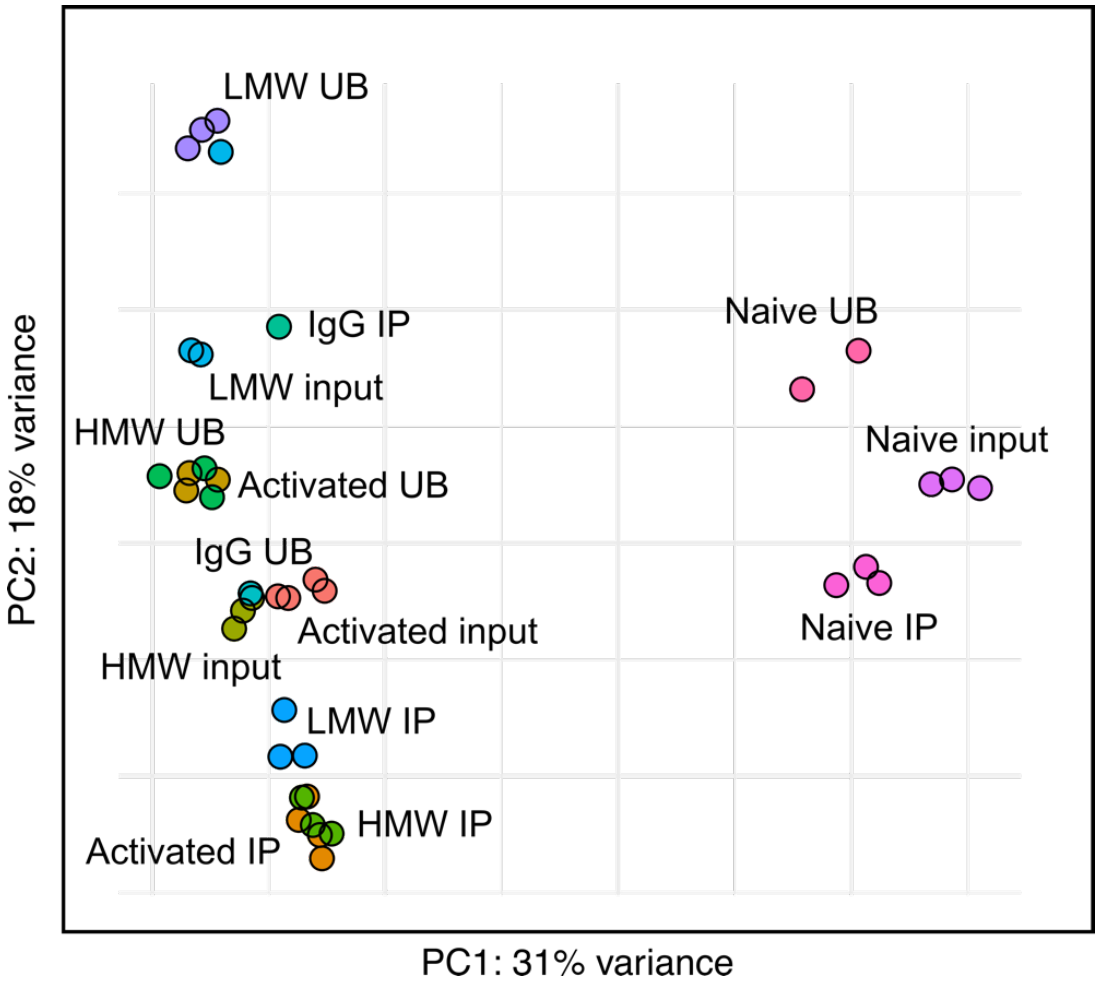

Figure 5.4 Principal component analysis of miRNAs in all sequencing samples. The PCA plot was created on DESeq2 from miRNA read count data.

5.2.3 Specific miRNAs are not enriched in Ago-2 unbound fractions

To get a global picture of the miRNA profile in the cells, we compared the miRNA reads in the input, Ago-2 IP and unbound samples. RISC association has been suggested to be a better determinant of miRNA suppressive function than total miRNA expression (Flores *et al.*, 2014). We looked for the presence of non-Ago-2 bound miRNAs, by looking for the enrichment of specific miRNAs in the input or unbound samples compared to the Ago-2 IP. The average expression (AveExpr) of miRNAs is shown as the average read counts per million (CPM) of miRNA across all samples on a log2 scale (Fig.5.5). This was used as an approximate measure of the general abundance of the miRNAs. To compare miRNA expression between the Ago-2 IP and the input and unbound fractions, fold change differential expression was calculated. miRNAs with a high average expression were enriched in the Ago-2 IP compared to both the input and the Ago-2 unbound samples (Fig.5.5A-B). It was previously shown in human monocytic THP-1 cells and human embryonic kidney 293T cells, that only the most abundant miRNAs in the cell mediated significant target suppression (Mullokandov *et al.*, 2012). Most suppression was found for miRNA expressed at above 1000 CPM, and no suppression was found for those expressed at less than 100 CPM (Mullokandov *et al.*, 2012). Very few miRNAs were significantly enriched in the input or unbound samples compared to Ago-2 IP at AveExpr > 6, which corresponds to 64 CPM (2^6). This suggests that most miRNAs in the cell are found in a complex with Ago-2.

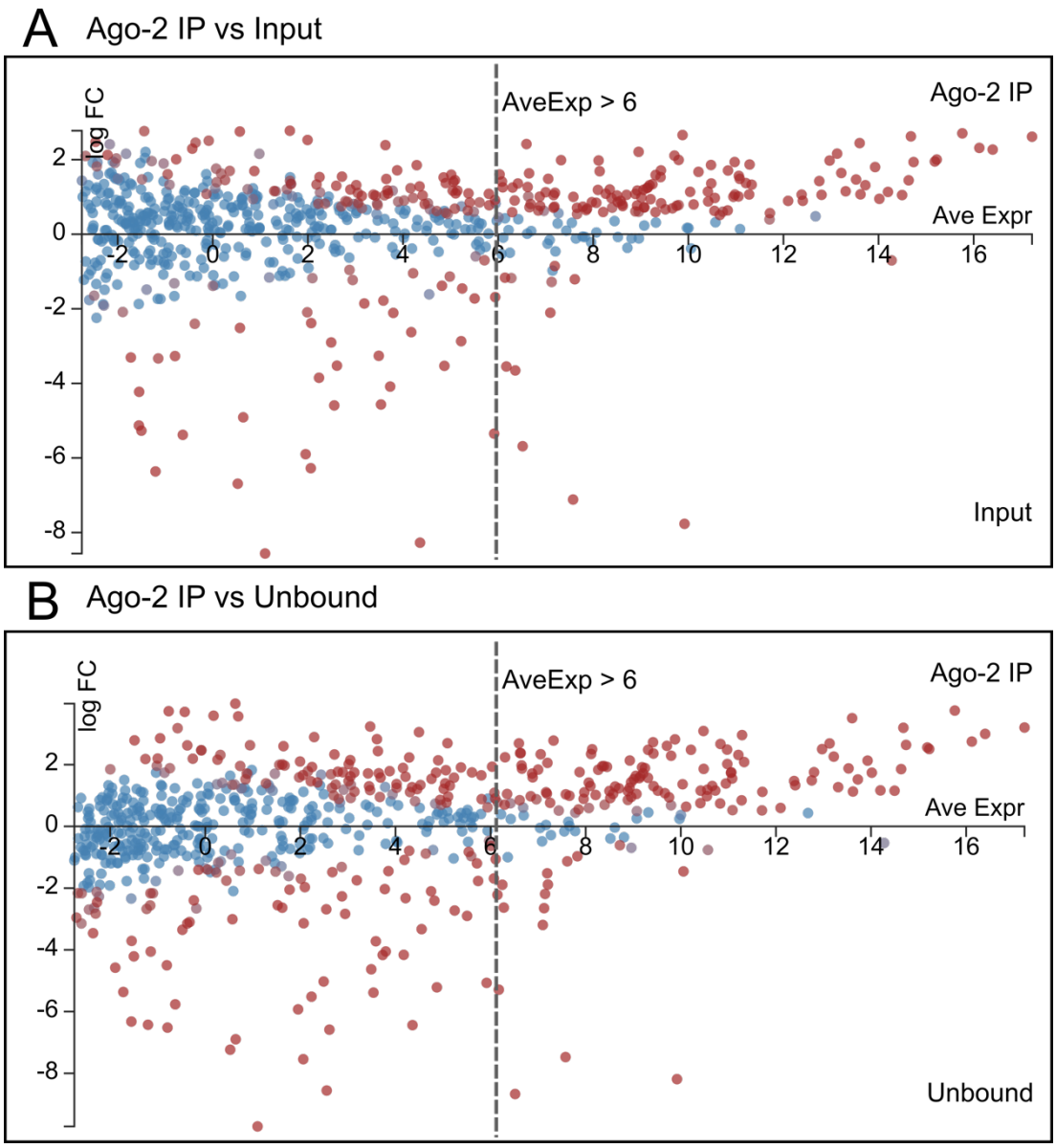

Figure 5.5 Most miRNAs are enriched in Ago-2 IP compared to input and unbound samples

A-B Differential expression of miRNAs in d2 activated OT-I cell Ago-2 IPs versus input and unbound samples. x-axis shows average expression (log2(CPM)), y-axis shows log2 fold change in Activated Ago-2 IP relative to Activated input (A) or Activated unbound (B). Average expression is average CPM across naive and activated Ago-2 input, IP and unbound samples, on a log2 scale. Dashed lines show miRNAs with AveExpr > 6. miRNAs with FDR < 0.01 are highlighted in red.

5.2.4 T cell activation induces dynamic changes in miRNA expression

Next, we compared miRNAs from the naive and activated cells, in both the input and the Ago-2-IP. As expected, T cell activation induced many changes in miRNA expression, with most miRNAs differentially expressed between the naive and activated cells (Fig.5.6A-B). We listed the miRNAs with the largest fold difference between the naive and activated cells, only including miRNAs with a high average expression (AveExpr > 10 (CPM > 1024)) and a significant change in expression, defined as low false discovery rate (FDR < 0.01) (Table 5.1). Many of the same miRNAs were found to be significantly changed in the input and Ago-2 IP samples. Previously described T cell regulators such as miR-155, miR-21 and members of the miR-17~92 cluster were amongst the most upregulated miRNAs in both the input and the Ago-2 IP. Other miRNAs that were enriched in the activated cells in both the input and the Ago-2 IP included miR-298, miR-182, miR-148, miR-186, miR-191 and miR-7. The miRNAs that were most downregulated upon activation included miR-150 and miR-181 in both input and Ago-2 IP. Let-7 family members and miR-26 were also enriched in the input and Ago-2 IP in naive cells compared to activated cells. These findings confirm dynamic changes in miRNA expression upon activation, apparent in both total input RNA and Ago-2 bound RNA. These results also correlate with findings in Chapter 3, showing upregulation of miR-155 and miR-17, and downregulation of miR-150 and miR-181.

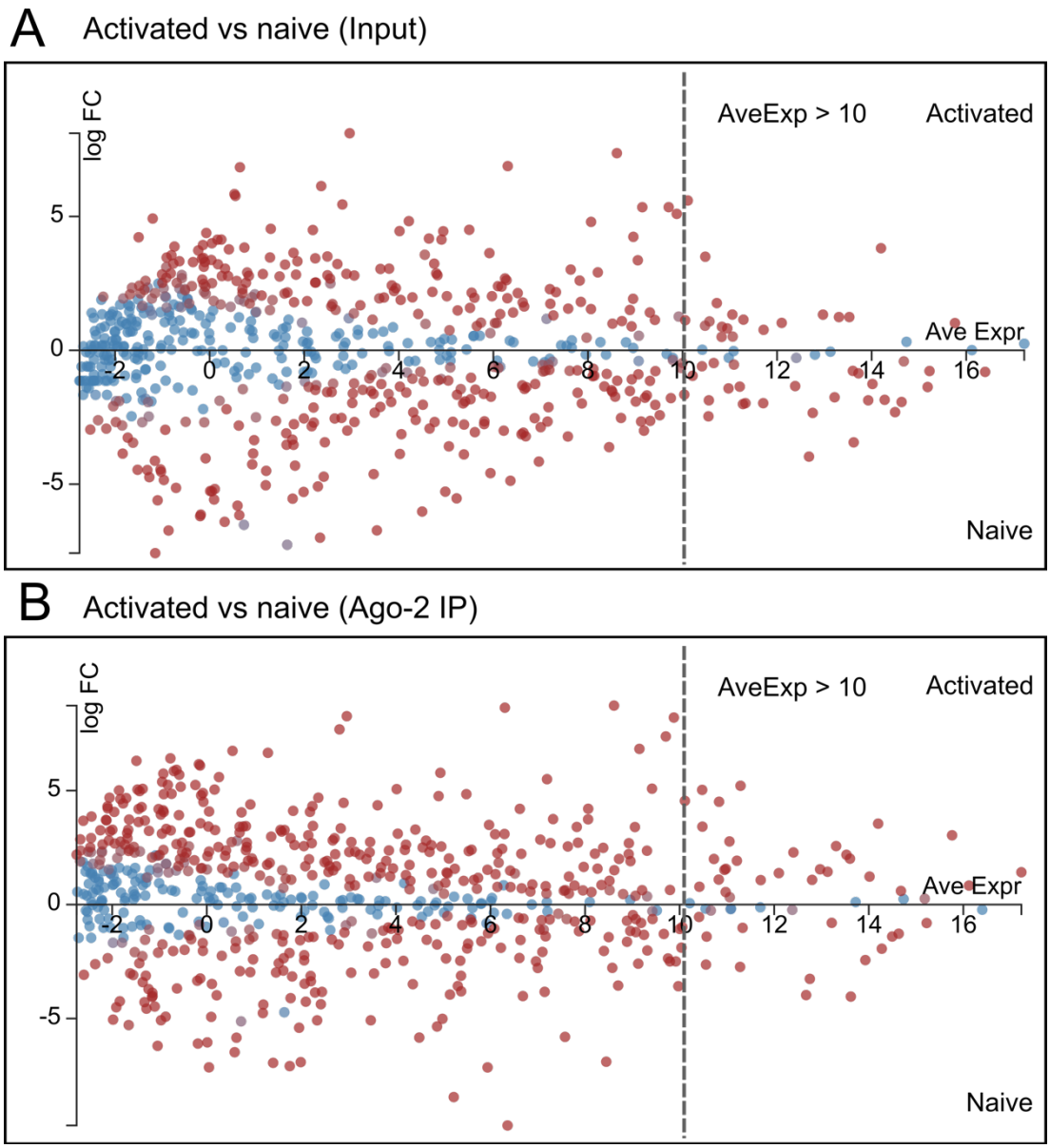

Figure 5.6 Differential expression of miRNAs between naive and d2 activated cells

Average expression and log2 fold change in Activated input relative to Naive input (**A**) or Activated Ago-2 IP relative to Naive Ago-2 IP (**B**). Average expression is average CPM across naive and activated Ago-2 input, IP and unbound samples, on a log2 scale. Dashed lines show miRNAs with AveExpr > 10, shown in Table 5.1. miRNAs with FDR < 0.01 are highlighted in red.

Upregulated miRNA	FC	FDR	Downregulated miRNA	FC	FDR
Input			**Input**		
miR-298-5p	5.60	9.71E-14	miR-150-5p	-3.97	6.64E-13
miR-155-5p	3.81	5.76E-12	miR-181a-5p	-3.44	9.71E-14
miR-182-5p	3.50	7.06E-12	miR-29a-3p	-2.47	3.85E-12
miR-148a-3p	1.76	1.53E-06	let-7b-5p	-2.34	5.27E-10
miR-186-5p	1.34	7.14E-09	miR-26a-5p	-2.31	9.71E-14
miR-98-5p	1.33	6.86E-07	miR-181b-5p	-2.01	2.36E-11
miR-7a-5p	1.24	4.52E-07	miR-142a-3p	-1.97	1.26E-10
miR-191-5p	1.24	2.52E-08	miR-140-3p	-1.97	6.52E-12
miR-17-5p	1.15	1.33E-04	miR-26b-5p	-1.93	3.97E-13
miR-342-5p	1.12	8.74E-04	let-7c-5p	-1.87	3.75E-09
miR-423-5p	1.08	6.21E-03	miR-181c-5p	-1.87	1.52E-09
miR-423-3p	1.02	1.34E-06	miR-142a-5p	-1.85	1.26E-07
miR-21a-5p	1.02	9.23E-05	miR-378a-3p	-1.76	6.58E-12
miR-20a-5p	0.92	8.00E-03	miR-1839-5p	-1.65	8.19E-10
miR-20b-5p	0.88	2.15E-04	miR-101b-3p	-1.42	5.92E-08
Ago-2 IP			**Ago-2 IP**		
miR-17-5p	5.21	2.87E-15	miR-181a-5p	-4.04	6.29E-17
miR-20a-5p	5.03	2.78E-13	miR-150-5p	-3.97	4.21E-15
miR-298-5p	4.55	5.16E-16	let-7b-5p	-3.26	7.21E-15
miR-20b-5p	4.51	8.42E-16	miR-181b-5p	-2.74	8.42E-16
miR-155-5p	3.55	8.17E-14	miR-181c-5p	-2.63	3.32E-14
miR-182-5p	3.42	2.26E-14	let-7c-5p	-2.44	2.10E-13
miR-21a-5p	3.04	2.71E-13	miR-142a-5p	-1.94	4.69E-09
miR-186-5p	2.77	1.64E-15	miR-1839-5p	-1.89	5.55E-13
miR-191-5p	2.57	4.83E-15	miR-423-5p	-1.41	2.11E-05
miR-24-3p	2.29	4.06E-14	miR-26a-5p	-1.40	1.10E-12
miR-7a-5p	2.18	8.44E-13	miR-26b-5p	-1.28	9.09E-13
miR-93-5p	2.01	1.06E-12	miR-669p-5p	-1.07	1.84E-07
miR-148a-3p	2.00	6.80E-09	miR-140-3p	-1.02	1.57E-09
miR-19b-3p	1.92	1.14E-09	miR-342-5p	-0.99	2.10E-04
miR-22-3p	1.57	8.39E-09	let-7a-5p	-0.81	8.18E-07

Table 5.1 miRNA enrichment in naive and activated cells
Differentially expressed miRNAs between naive and d2 activated cells, ranked by log2 fold change (FC). Table shows the top 15 miRNAs with biggest fold change difference between naive and activated cells, in the input and Ago-2 IP samples. Table includes miRNAs with AveExpr > 10 and FDR < 0.01. Average expression is log2 of average CMP across naive and activated Ago-2 input, IP and unbound samples.

5.2.5 Specific enrichment of miRNAs in HMW and LMW RISC

Next, we wanted to see if miRNAs were differentially associated with HMW and LMW RISC in the activated cells. The fold change differential expression of miRNAs between HMW and LMW RISC was plotted against the average expression of these miRNAs (Fig.5.7A) and -log10 FDR (Fig.5.7B). Many miRNAs were found to be differentially associated with one complex or the other. We wanted to focus our attention to the miRNAs with a relatively high average expression, and a significant difference in fold change expression between HMW and LMW RISC across the three replicates. The average expression limit was set to 6, corresponding to 64 CPM, as it was previously suggested that miRNAs with lower than 100 CPM expression did not cause significant suppression of targets (Mullokandov *et al.*, 2012). We however kept miRNAs with a low-to-average expression (64-1024 CPM, AveExpr 6-10), since we hypothesised these may play a biological role if enriched in HMW RISC. miRNAs with low average expression (AveExpr < 6) and those with FDR > 0.01 were filtered out. This left 50 HMW RISC and 42 LMW RISC enriched miRNAs. These miRNAs were ranked by the fold change difference between HMW and LMW RISC (Table 5.2). The most enriched miRNAs in HMW RISC included miR-378c, let-7g, miR-210, miR-34a and miR-7a. Other highly enriched miRNAs included those from the miR-17~92 cluster. In the LMW RISC, the differential expression analysis showed enriched of miR-211, miR-486b, miR-150, miR-320 and miR-181. Interestingly, the 5p strand of miR-210 was enriched in LMW RISC, whereas the 3p strand was found in HMW RISC.

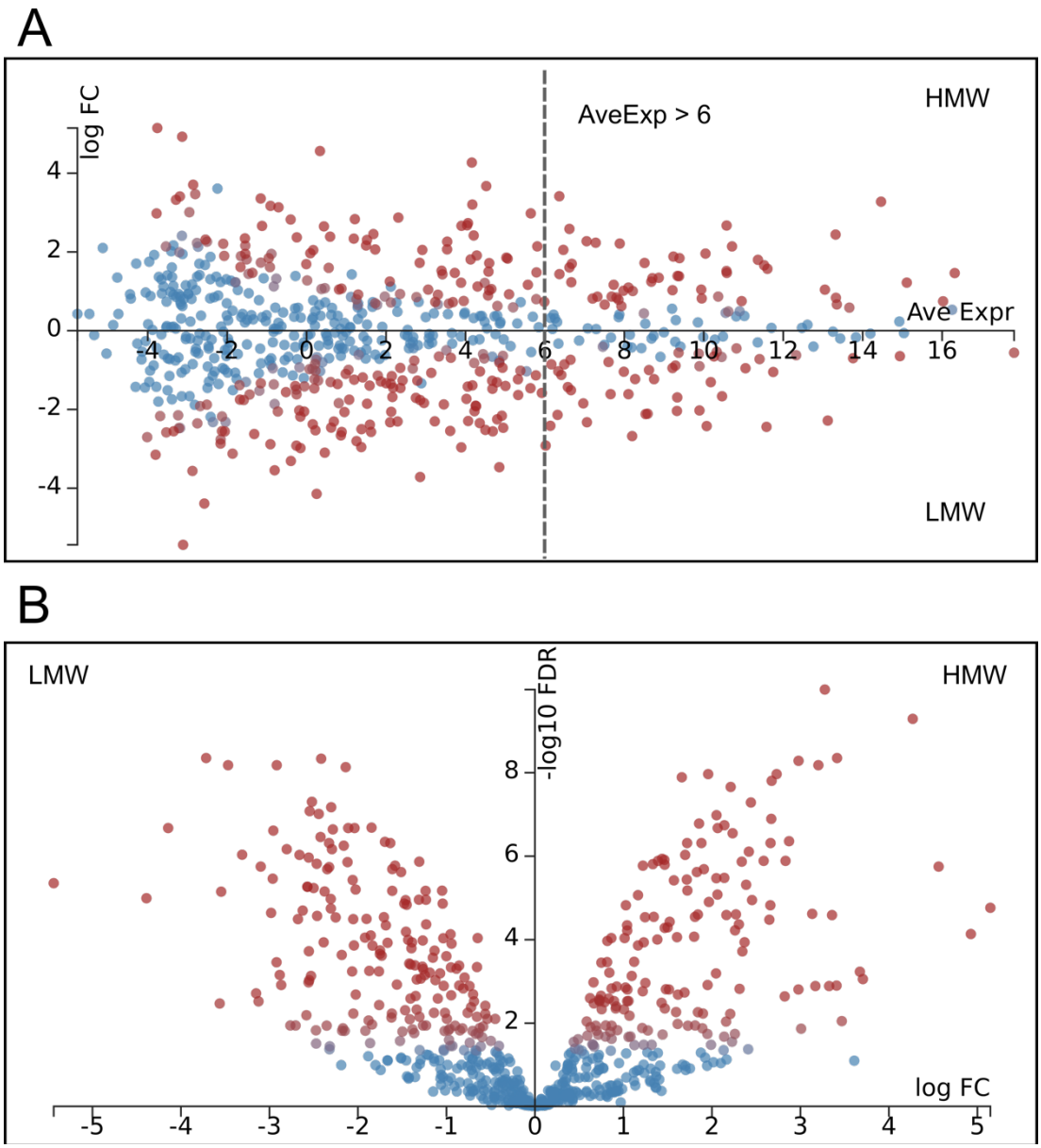

Figure 5.7 Differential expression of miRNAs in HMW and LMW RISC
A miRNA average expression and log2 fold change in HMW RISC Ago-2 IP relative to LMW RISC Ago-2 IP. Average expression is average CPM across Ago-2 IP from naive, activated, HMW and LMW RISC samples, on log2 scale. Dashed line shows miRNAs with AveExpr > 6, shown in Table 5.2. miRNAs with FDR < 0.01 are highlighted in red.
B log2 FC as above, plotted against negative log10 of FDR. Plot includes all miRNAs irrespective of average expression. miRNAs with FDR < 0.01 are highlighted in red.

HMW enriched			LMW enriched		
miRNA	FC	FDR	miRNA	FC	FDR
miR-378c	3.41	4.45E-09	miR-211-5p	-2.92	6.61E-09
let-7g-5p	3.28	1.02E-10	miR-486b-5p	-2.68	3.21E-05
miR-210-3p	2.67	1.28E-07	miR-150-5p	-2.44	9.71E-08
miR-34a-5p	2.58	1.29E-06	miR-320-3p	-2.42	3.47E-07
miR-7a-5p	2.44	5.17E-08	miR-181a-3p	-2.42	4.62E-09
miR-18a-5p	2.27	2.47E-05	miR-210-5p	-2.33	1.83E-06
miR-140-5p	2.23	2.82E-07	miR-142a-5p	-2.28	2.28E-07
miR-28a-5p	2.21	2.19E-08	miR-126a-5p	-2.14	7.36E-09
miR-20b-5p	2.14	3.30E-06	miR-151-3p	-2.12	1.38E-06
miR-185-5p	2.05	1.04E-07	miR-342-3p	-2.11	2.12E-07
miR-148b-3p	1.96	1.08E-08	miR-192-5p	-2.04	2.12E-07
miR-31-5p	1.88	4.84E-07	miR-146b-5p	-2.03	6.28E-06
miR-106a-5p	1.84	2.49E-05	miR-99b-5p	-1.85	2.07E-07
miR-17-5p	1.80	8.49E-05	let-7d-3p	-1.69	4.54E-07
miR-15a-5p	1.72	4.84E-07	miR-423-5p	-1.67	1.19E-04
miR-378a-5p	1.70	9.32E-07	miR-1981-5p	-1.61	6.75E-06
miR-423-3p	1.66	1.29E-08	miR-130b-5p	-1.61	2.03E-06
miR-296-5p	1.61	8.72E-05	miR-92b-3p	-1.51	2.39E-06
miR-24-3p	1.57	3.79E-06	miR-16-2-3p	-1.43	1.01E-04
miR-20a-5p	1.51	1.56E-03	miR-30e-3p	-1.31	1.35E-06

Table 5.2 miRNA enrichment in HMW and LMW RISC
Differentially expressed miRNAs between HMW and LMW Ago-2 IP, ranked by log2 fold change (FC). Table shows the top 20 miRNAs with biggest fold change difference between HMW and LMW RISC. Table includes miRNAs with AveExpr > 6 and FDR < 0.01. Average expression is log2 of average CPM across Ago-2 IP from naive, activated, HMW and LMW RISC samples.

We were also interested in the most abundant miRNAs found in HMW RISC, based on ranking by CPM, irrespective of the differential expression compared to LMW RISC. These overlapped with those that were in general abundant in the total Ago-2 IP from activated cells, as expected. The most abundant miRNA was miR-92a, followed by miR-21, and miR-155 in fifth place (Table 5.3). Many miRNAs from the let-7 family were found to be abundantly present in HMW RISC. For these abundant miRNAs, we calculated the ratio of the miRNA found in HMW RISC compared to LMW RISC as the fraction of the normalised read count (CPM) of the miRNA in HMW RISC over the sum of the read count in both complexes (HMW CPM / (HMW CPM + LMW CPM)). From these highly abundant miRNAs, miR-210-3p, miR-7a, miR-17 and let-7g were also among the most enriched in HMW RISC based on the ratio (Fig.5.8).

miRNA	CPM
miR-92a-3p	216175
miR-21a-5p	108585
let-7f-5p	92421
let-7i-5p	63530
miR-155-5p	57648
let-7g-5p	42637
let-7a-5p	37837
miR-25-3p	31307
let-7d-5p	30486
miR-7a-5p	24932
miR-16-5p	16660
miR-93-5p	16606
miR-191-5p	16289
miR-103-3p	15466
miR-26b-5p	15418
miR-26a-5p	13306
miR-30d-5p	11916
miR-98-5p	10729
miR-17-5p	9124
miR-210-3p	8805

Table 5.3 Most abundant miRNAs in HMW RISC
The top 20 most abundant miRNAs in HMW RISC Ago-2 IP ranked by average CPM in three biological replicates.

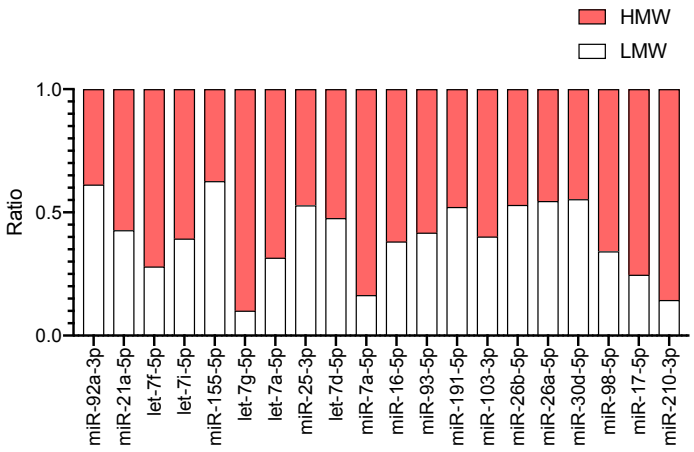

Figure 5.8 Ratio of miRNAs in HMW and LMW RISC
Ratio is calculated as miRNA average CPM in HMW Ago-2 IP samples over the sum of the read count in both HMW and LMW Ago-2 IP (HMW CPM / (HMW CPM + LMW CPM). Ratio is shown for the top 20 most abundant miRNAs in HMW RISC shown in Table 5.3.

5.2.6 miRNA expression changes cannot predict association with HMW or LMW RISC

We saw significant changes in miRNA expression upon activation, as well as differences in association with HMW and LMW RISC within activated cells. Next, we wanted to see how miRNA up - and downregulation correlated with subsequent association with HMW and LMW RISC in the activated cells. To get a global picture of miRNA expression changes in respect to HMW/LMW RISC association, we filtered out very lowly expressed miRNAs (AveExpr < 2, CPM < 4) and split the miRNAs into two groups: miRNAs with significant (FDR < 0.01) upregulation upon activation and miRNAs with significant downregulation, based on differential expression between naive Ago-2 IP and activated Ago-2 IP samples. We ended up with 227 miRNAs, 122 of which were significantly upregulated and 105 downregulated. We then calculated the ratio of the miRNAs in HMW RISC versus LMW RISC. For each miRNA, the ratio of the normalised read count (CPM) in HMW RISC over total CPM was calculated, with upregulated and downregulated miRNAs considered separately. On average, upregulated miRNAs were found equally distributed between HMW and LMW RISC (average proportion in HMW RISC: 52%) (Fig.5.9A). Downregulated miRNAs were also divided between both complexes; however, these were on average slightly more present in LMW RISC (average proportion in HMW RISC: 41%) (Fig.5.9C). We then ranked the miRNAs based on the level of up -or downregulation, to see if stronger upregulation correlated with higher occupancy in HMW RISC, and vice versa, stronger downregulation with higher occupancy in LMW RISC. There appeared to be no such correlation, with miRNAs apparently distributing to HMW and LMW RISC irrespective of changes in expression (Fig.5.9B,D). Some highly upregulated miRNAs were found in LMW RISC, and some strongly downregulated miRNAs were found in HMW RISC. We then examined both the up-and downregulated miRNAs with the highest occupancy in HMW RISC (Table 5.4). The most HMW RISC enriched miRNAs were miR-671, miR-669f, miR-466f, miR-210-3p and miR-147 for the upregulated, and miR-5099,

miR-387c, miR-6240, miR-28a and miR-378a for the downregulated. In addition, miR-210-3p, miR-34a, miR-7a, miR-378 and let-7 family miRNAs stood out, as they had already been identified in the differential expression analysis.

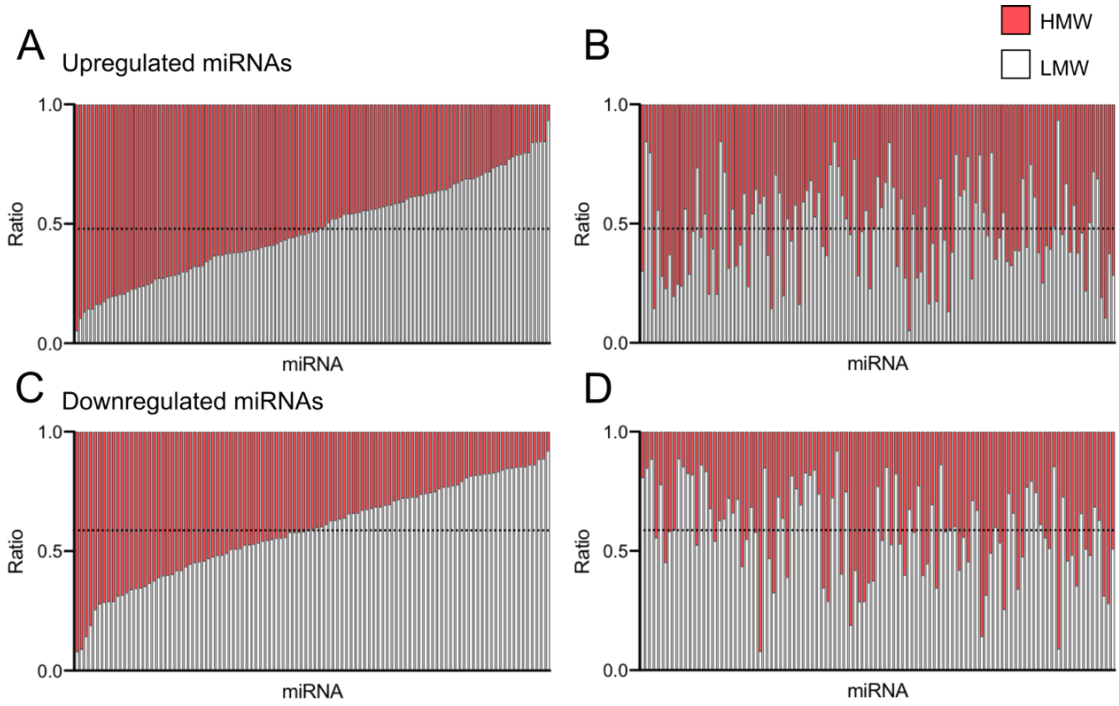

Figure 5.9 miRNA expression changes do not correlate with distribution to HMW and LMW RISC
Ratio of upregulated (**A-B**) and downregulated (**C-D**) miRNAs in HMW and LMW RISC. Ratio is calculated as miRNA average CPM in HMW Ago-2 IP samples over the sum of the read count in both HMW and LMW Ago-2 IP (HMW CPM / (HMW CPM + LMW CPM). Analysis includes miRNAs with AveExpr > 2. Average expression is log2 of average CPM across Ago-2 IP from naive, activated, HMW and LMW RISC samples. Upregulated miRNAs are those with significant enrichment in activated Ago-2 IP compared to naive Ago-2 IP (FDR < 0.01), downregulated miRNAs are significantly enriched in naive Ago-2 IP versus activated Ago-2 IP (FDR < 0.01). Each bar represents a single miRNA. A and C ranked by proportion of miRNA in HMW RISC. B and D are ranked by fold change upregulation or downregulation, with biggest fold change first. Dashed lines show average proportion of miRNAs found in LMW RISC.

Upregulated		Downregulated	
miRNA	Ratio (%)	miRNA	Ratio (%)
miR-671-5p	95	miR-5099	92
miR-669f-5p	89	miR-378c	91
miR-466f	87	miR-6240	86
miR-210-3p	86	miR-28a-5p	81
miR-147-3p	86	miR-378a-5p	74
miR-34a-5p	84	let-7f-5p	72
miR-7a-5p	84	miR-669a-3p	71
miR-466a-5p	82	miR-297b-3p	71
miR-140-5p	81	miR-1839-5p	71
miR-18a-5p	80	miR-15b-5p	69
miR-363-5p	80	let-7a-5p	68
miR-20b-5p	79	miR-466i-3p	67
miR-5104	79	let-7e-5p	66
miR-148b-3p	78	miR-669p-5p	66
miR-31-5p	77	miR-322-5p	65
miR-330-5p	77	miR-500-3p	65
miR-326-3p	76	miR-195a-5p	63
miR-106a-5p	76	let-7j	62
miR-17-5p	75	miR-378d	61
miR-423-3p	75	miR-466d-3p	60

Table 5.4 Up- and downregulated miRNAs with highest ratio in HMW RISC
Upregulated and downregulated miRNAs ranked by the proportion of miRNA found in HMW RISC. Ratio is calculated as miRNA average CPM in HMW Ago-2 IP samples over the sum of the read count in both HMW and LMW Ago-2 IP (HMW CPM / (HMW CPM + LMW CPM)x100). Analysis includes miRNAs with AveExp > 2. Average expression is log2 of average CPM across Ago-2 IP from naive, activated, HMW and LMW RISC samples. Upregulated miRNAs are those with significant enrichment in activated Ago-2 IP compared to naive Ago-2 IP (FDR < 0.01), downregulated miRNAs are significantly enriched in naive Ago-2 IP versus activated Ago-2 IP (FDR < 0.01).

Next, to better to visualise miRNA expression changes alongside distribution to HMW and LMW RISC, we plotted the miRNAs with both a significant change in expression, and in distribution between HMW/LMW RISC (FDR < 0.01), excluding miRNAs with very low average expression (AveExp < 2). This divided the miRNAs into four quadrants: upregulated miRNAs in HMW RISC or LMW RISC, and downregulated miRNAs in HMW RISC or LMW RISC (Fig.5.10A). Out of a total of 145 miRNAs with significant changes in both expression and HMW/LMW RISC distribution, 49 were upregulated and found predominantly in HMW RISC, 32 were upregulated but found mostly in LMW RISC, 18 were downregulated and found in HMW RISC, and 46 were downregulated and enriched in LMW RISC. Interestingly, we noted that members of a particular miRNA family were often associated specifically with HMW or LMW RISC. For example, members of the miR-17~92 cluster and the two paralogous clusters, miR-106b~25 and miR-106~363, were all upregulated and almost exclusively found enriched in HMW RISC, with the exception of miR-92a (Fig.5.10B). Similarly, members of the miR-449 family, which contains miR-34a, were found upregulated and in HMW RISC (Fig.5.10C). Downregulated miRNAs found in HMW RISC were the smallest group of the four quadrants. The let-7 family of miRNAs was downregulated upon activation, but interestingly many members of this family were enriched in HMW RISC, with some enriched in LMW RISC (Fig.5.10D). Similarly, miRNAs of the miR-378 family were downregulated but enriched in HMW RISC (Fig.5.10E). For each quadrant, we listed the miRNAs with the biggest fold difference between HMW and LMW RISC, including only those with AveExpr > 6 (Table 5.5). As well as the miRNA families discussed above, the upregulated miRNAs found in HMW RISC included many miRNAs already identified in the previous analyses, such as miR-210-3p, miR-7a and miR-34a, whereas the downregulated included miR-28a. Many miRNAs were found upregulated but enriched in LMW RISC. Notably, this group included miR-155**,** one of the most strongly upregulated miRNAs (Table 5.5). Finally, many downregulated miRNAs were found enriched in LMW RISC, such as miR-211, miR-486b and miR-181a.

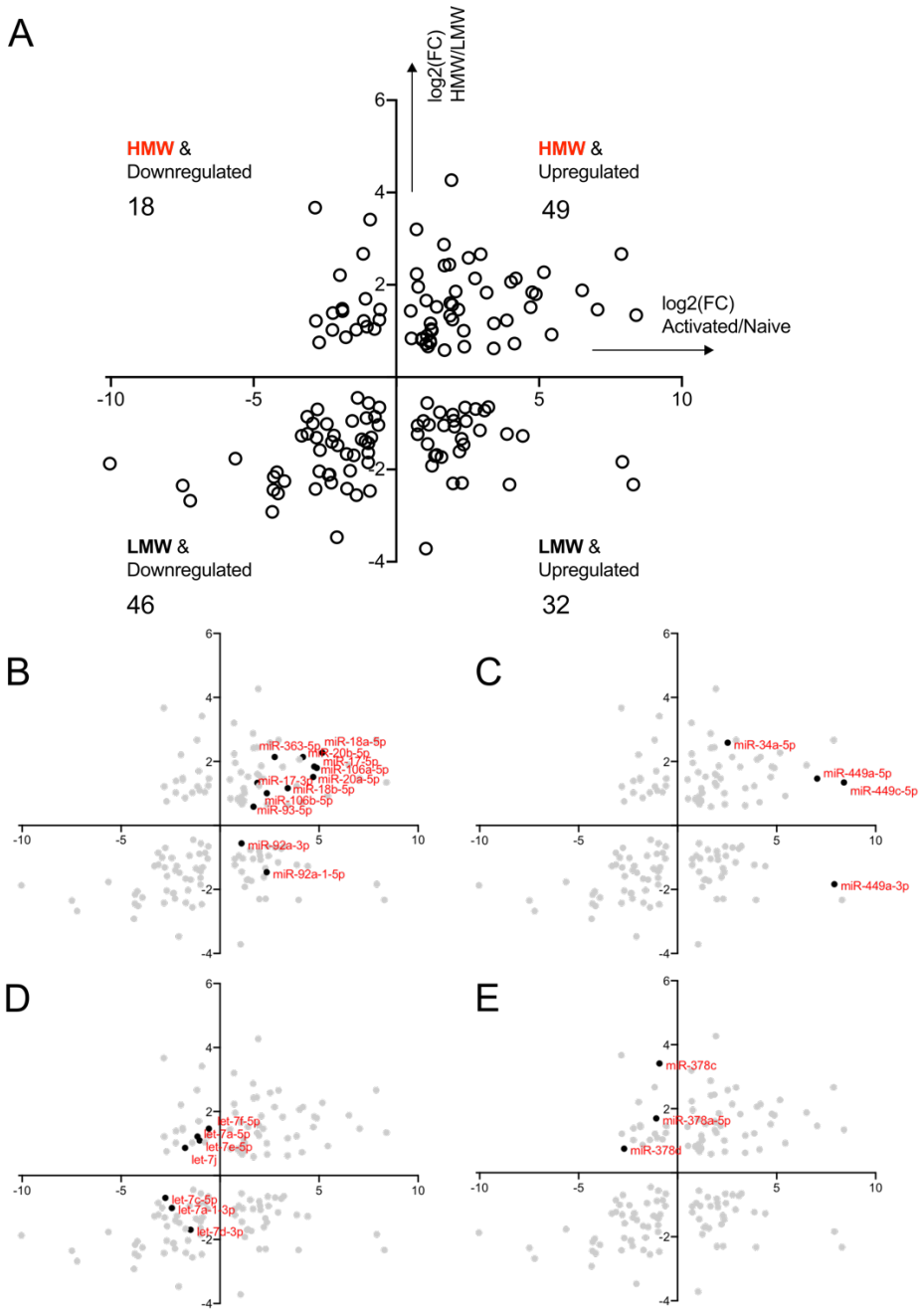

Figure 5.10 Upregulated and downregulated miRNA families enriched in HMW and LMW RISC

A shows log2 fold change differential expression between naive and activated Ago-2 IP (x-axis) and HMW and LMW Ago-2 IP (y-axis). Upregulated miRNAs are those with significant enrichment (FDR < 0.01) in activated Ago-2 IP compared to naive Ago-2 IP, downregulated miRNAs are significantly enriched in naive Ago-2 IP versus activated Ago-2 IP and these are separated into HMW Ago-2 IP enriched and LMW Ago-2 IP enriched miRNAs. Figure includes miRNAs with AveExpr > 2. Average expression is log2 of average CPM across Ago-2 IP from naive, activated, HMW and LMW RISC samples. **B-E** highlight members of miR-17~92 cluster and related families (B), miR-449/34 family (C), let-7 family (D) and miR-378 family (E).

Downregulated/HMW RISC			Upregulated/HMW RISC		
miRNA	Expression	HMW/ LMW	miRNA	Expression	HMW/ LMW
miR-378c	-0.92	3.41	miR-210-3p	7.88	2.67
miR-28a-5p	-1.97	2.21	miR-34a-5p	2.53	2.58
miR-378a-5p	-1.08	1.70	miR-7a-5p	1.85	2.44
let-7f-5p	-0.57	1.46	miR-18a-5p	5.17	2.27
miR-1839-5p	-2.22	1.39	miR-140-5p	0.71	2.23
miR-15b-5p	-0.59	1.24	miR-20b-5p	4.18	2.14
let-7a-5p	-1.14	1.22	miR-148b-3p	0.76	1.96
let-7e-5p	-1.03	1.09	miR-31-5p	6.51	1.88
miR-669p-5p	-1.40	1.03	miR-106a-5p	4.75	1.84
let-7j	-1.77	0.87	miR-17-5p	4.88	1.80
Downregulated/LMW RISC			**Upregulated/LMW RISC**		
miRNA	Expression	HMW/ LMW	miRNA	Expression	HMW/ LMW
miR-211-5p	-4.34	-2.92	miR-210-5p	8.30	-2.33
miR-486b-5p	-7.22	-2.68	miR-130b-5p	2.21	-1.61
miR-150-5p	-4.30	-2.44	miR-183-5p	3.87	-1.23
miR-320-3p	-2.83	-2.42	miR-146a-5p	0.75	-1.05
miR-181a-1-3p	-1.72	-2.42	miR-24-2-5p	1.67	-1.04
miR-142a-5p	-2.28	-2.28	miR-504-5p	1.14	-1.03
miR-151-3p	-2.37	-2.12	miR-186-5p	2.44	-0.95
miR-342-3p	-2.34	-2.11	miR-182-5p	3.09	-0.72
miR-192-5p	-2.70	-2.04	miR-155-5p	3.22	-0.65
miR-146b-5p	-1.62	-2.03	miR-92a-3p	1.08	-0.56

Table 5.5 Upregulated and downregulated miRNAs enriched in HMW and LMW RISC

Table shows log2 fold change differential expression between naive and activated Ago-2 IP (Expression, FDR < 0.01) and HMW and LMW Ago-2 IP (HMW/LMW, FDR < 0.01), ranked by FC enrichment in HMW or LMW RISC. Upregulated miRNAs are those with significant enrichment in activated Ago-2 IP compared to naive Ago-2 IP, downregulated miRNAs are significantly enriched in naive Ago-2 IP versus activated Ago-2 IP and these are separated into HMW Ago-2 IP enriched and LMW Ago-2 IP enriched miRNAs. Table includes miRNAs with AveExpr > 6. Average expression is log2 of average CPM across Ago-2 IP from naive, activated, HMW and LMW RISC samples.

Finally, we decided to focus on the RISC distribution of miRNAs known to regulate T cell responses, the expression of which was studied in Chapter 3. miR-155 and miR-17 were shown to be strongly induced upon activation by qPCR measurements (Fig.3.2). The sequencing data also showed upregulation of these miRNAs, both in the input and the Ago-2-IP (Fig.5.11A-B). Interestingly miR-155 was found enriched in LMW RISC despite very strong upregulation (Fig.5.11A). However, looking at the CPM in each sample, it was also found in HMW RISC in high abundance. miR-17 was found enriched in HMW RISC, as shown previously for most of the miRNAs from this cluster (Fig.5.10, 5.11B). miR-139, miR-150 and miR-181a were previously shown to be downregulated (Fig.3.2). Again, the sequencing results correlated with this, showing downregulation in both input and Ago-2-IP for all three miRNAs (Fig.5.11C-E). miR-150 and miR-181a were enriched in LMW RISC, with miR-139 equally distributed between the complexes (Fig.5.11C-E). However, as these miRNAs were strongly downregulated upon activation, the amount of miRNA remaining in the activated cells was quite low, particularly for miR-139.

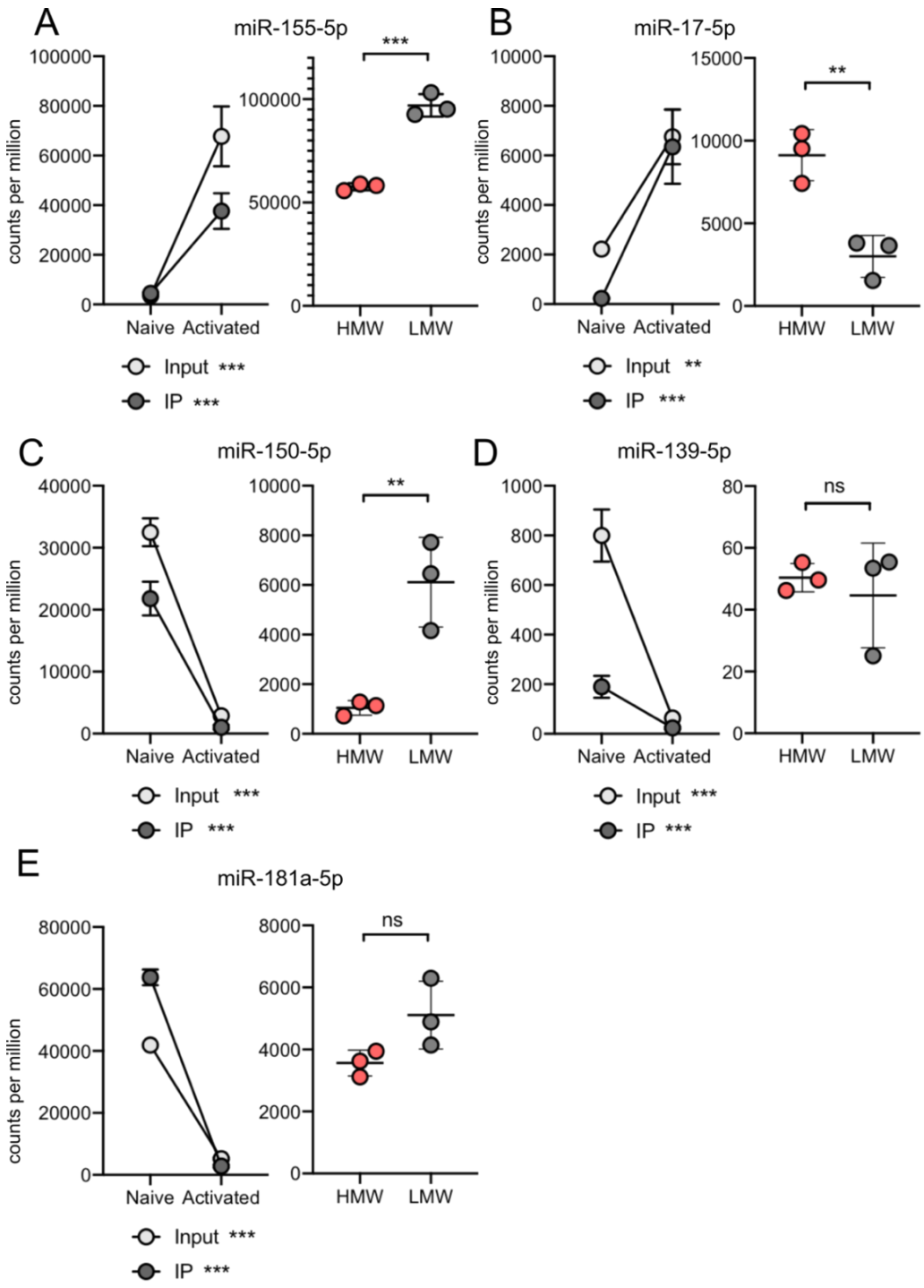

Figure 5.11 Expression and HMW/LMW association of miRNAs known to regulate T cells

A-E Expression is shown as CPM of miRNA in naive and activated input and Ago-2 IP samples. HMW/LMW association is shown as CPM of miRNA in HMW and LMW Ago-2 IP. The mean and standard deviation of three biological replicates are shown. Statistical analysis is done using a two-tailed unpaired student's t-test. (*) p-value < 0.05, (**) p-value < 0.01, (***) p-value < 0.001.

3.2.7 miR-7a inhibition affects CD8+ T cell activation

We wanted to focus our attention to specific miRNAs that were found enriched in HMW RISC. Many miRNAs were consistently found enriched in HMW RISC in the different analyses. These included the upregulated miRNAs miR-17~92, miR-210-3p, miR-7a and miR-34a, and the downregulated miRNAs miR-378, let-7 and miR-28a. We decided to confirm the upregulation of miR-7a and miR-210-3p by qPCR, during a 6-day activation time-course of OT-I cells. Both miRNAs were upregulated by d2, as shown by both qPCR and sequencing data (Fig.5.12). miR-7a expression was induced early, by d1 and remained up during 6 days of culture. miR-210 expression was upregulated slightly later, with maximal induction on d2.

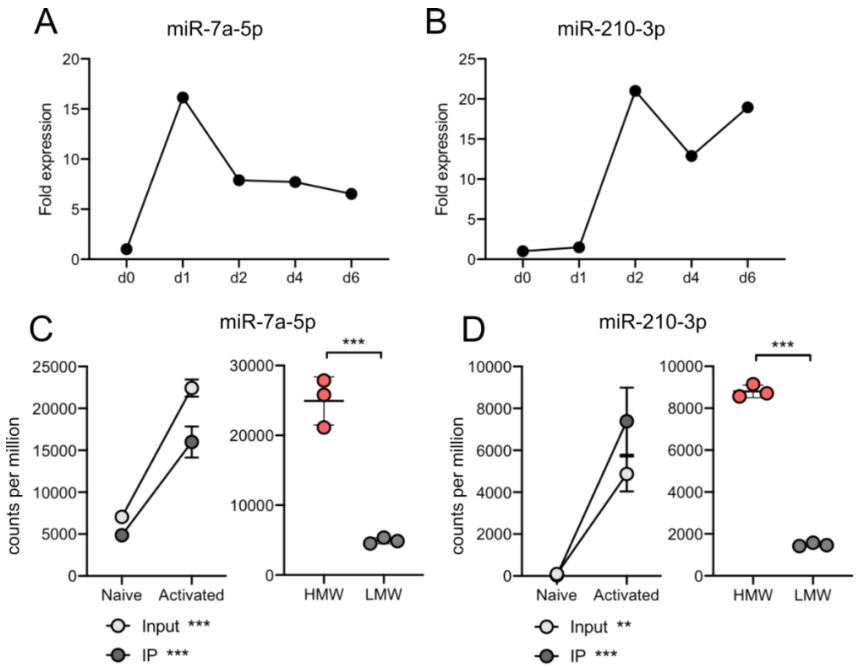

Figure 5.12 miR-7a and miR-210-3p are upregulated upon T cell activation and are enriched in HMW RISC

A-B miRNA expression measured by qPCR during a time-course of OT-I T cell activation. Cell were activated with N4 for 2 days then cultured in IL-2 for 4 days. Expression was normalised to snU6 and is shown as fold expression relative to naive cells. Figure is showing a single experiment.

C-D miRNA expression and HMW RISC association from sequencing data, shown in in counts per million of miRNA. miRNA in naive and activated input and Ago-2 IP samples. HMW/LMW association is shown as counts per million of miRNA in HMW and LMW Ago-2 IP. Statistical analysis is done using a two-tailed unpaired student's t-test. (**) p-value < 0.01, (***) p-value < 0.001.

We decided to focus on the role of miR-7a in $CD8^+$ T cells, as this miRNA had not been previously described in T cells, despite being a well-known tumour-suppressive miRNA. Expression of miR-7a was inhibited with an antagomir linked to a 5'FAM (fluorescein) tag. For a negative control, an inhibitor with no known targets in the mouse genome was used. The inhibitors have locked nucleic acid (LNA) and phosphorothioate (PS) modifications to protect them from enzymatic degradation and can be added directly to culture medium without the need for transfection reagents, and are instead taken up by the cells by gymnosis. The inhibitors were added to OT-I cells with 10 nM N4 and left for 2 days to monitor their unassisted uptake by the cells. On d2, the fluorescence of the cells was measured using flow cytometry. The cells receiving the control or the miR-7a inhibitor became brightly fluorescent, suggesting the inhibitor had been taken up (Fig.5.13A). We next measured the effect of the inhibitors on the cell number and on cell viability, in cells activated with 10 nM or 1 nM N4 for 2 days. Reducing the concentration of activating peptide resulted in fewer cells per well on d2 (Fig.5.13B). Slightly fewer cells were also recovered from the wells receiving the inhibitors, with a decrease with miR-7a inhibition in particular (Fig.5.13B). Cell viability was not affected by the inhibitors (Fig.5.13C). We next measured cell proliferation following miR-7a inhibition. While the control inhibitor had no effect on cell proliferation, miR-7a inhibition lead to a slight decrease in proliferation (Fig.5.14). All the cells had entered the cell cycle, but fewer cells had undergone the final divisions, resulting in a lower overall proliferation index with both 10 nM and 1 nM N4. Lastly, we studied the effect of miR-7a inhibition on the cell phenotype. We measured the expression of the surface markers CD25 (IL-2 receptor), CD44 and CD71 (transferrin receptor) on d2. The expression of all three markers was increased in cells receiving the miR-7a inhibitor compared to the control inhibitor (Fig.5.15).

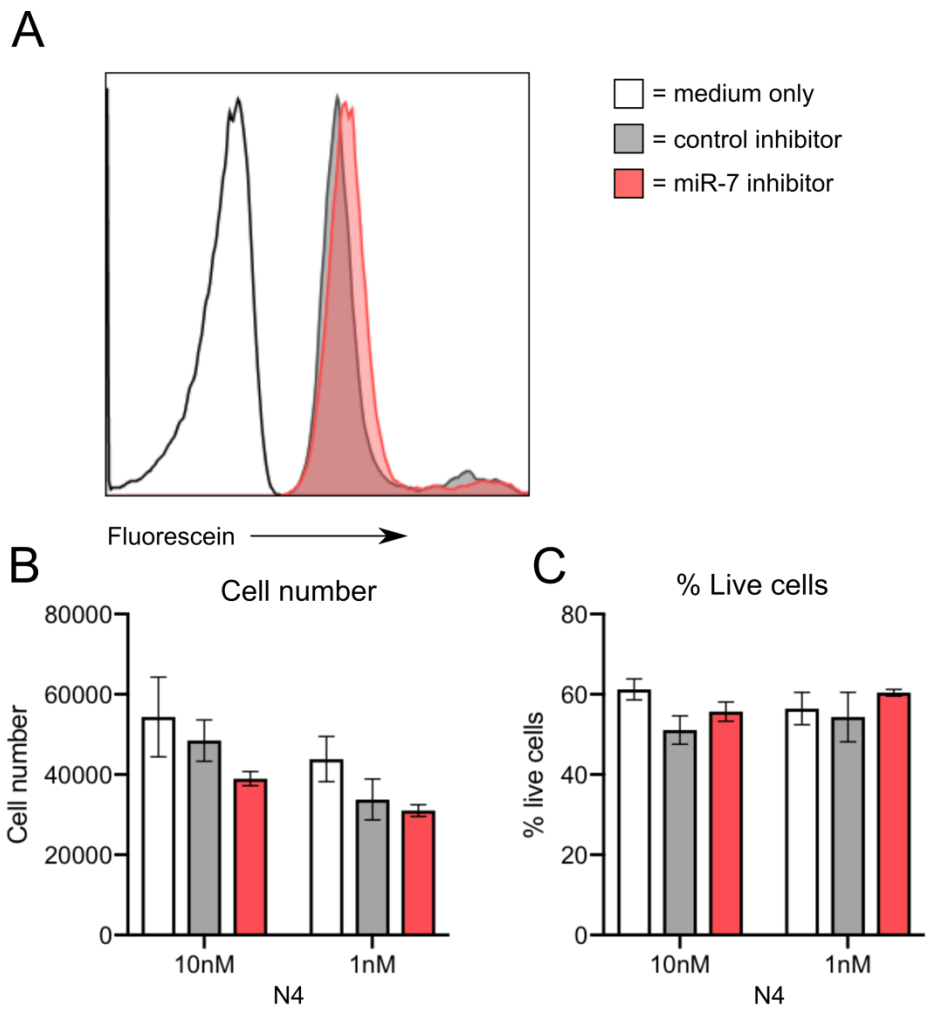

Figure 5.13 miR-7a inhibitor is taken up by $CD8^+$ T cells and does not reduce cell viability

A-C Cells were activated with 10 nM or 1 nM N4 and cultured with no inhibitors, with a negative control inhibitor, or a miR-7a inhibitor for 2 days.

A Fluorescence intensity from inhibitor 5'FAM-tag, measured by flow cytometry on d2.

B-C Total cell number per well (B) and proportion of live cells (C) measured by flow cytometry of Live/Dead stained cells on d2.

The figure shows the mean and standard deviation of two biological replicates within one experiment. This is representative of two independent experiments.

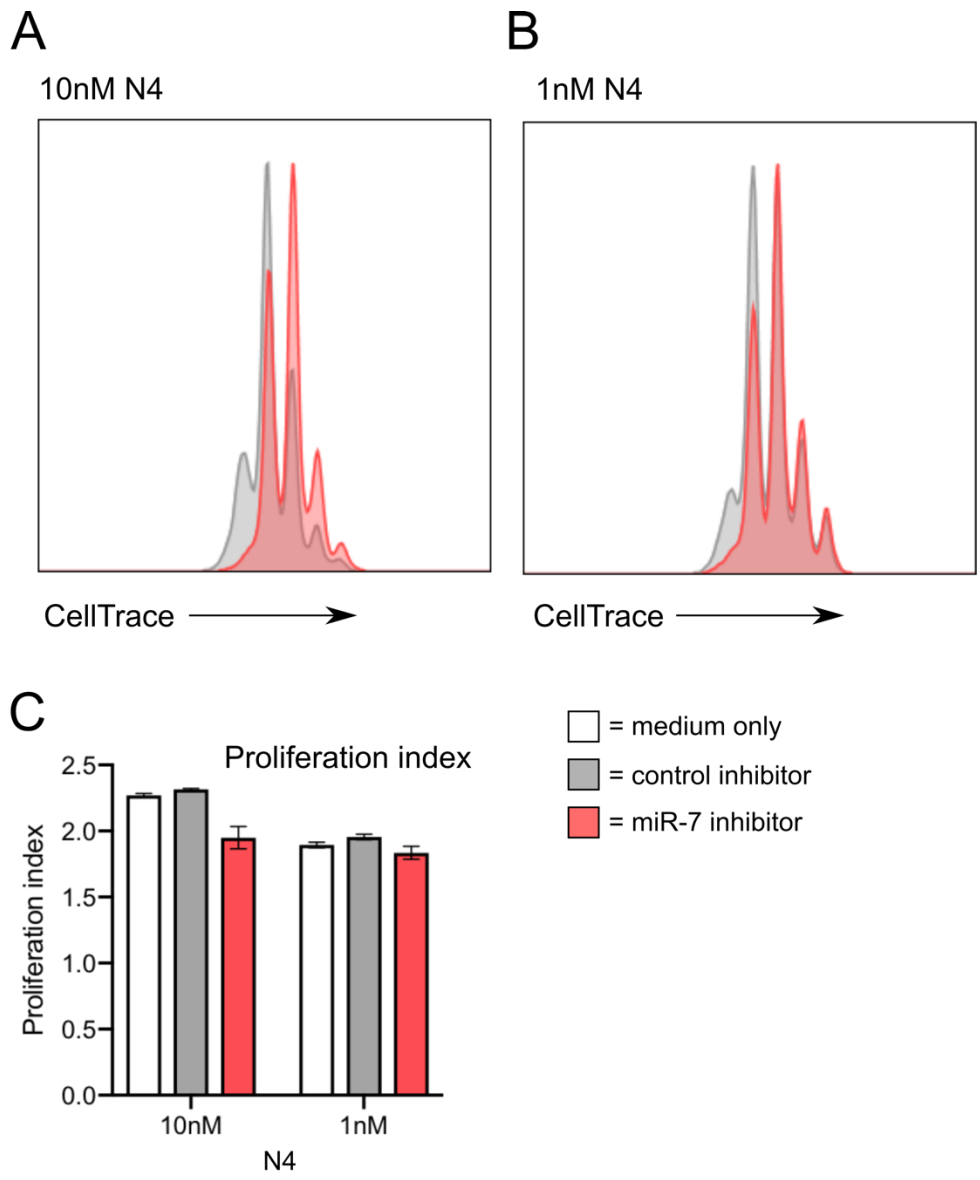

Figure 5.14 Cells receiving the miR-7a inhibitor proliferate less
A-C Cells were activated with 10nM (A) or 1nM (B) N4 and cultured with no inhibitors, with a negative control inhibitor, or a miR-7a inhibitor for 2 days. Cells were stained with CellTrace proliferation dye prior to activation.
A-B Fluorescence intensity of CellTrace on d2 measured by flow cytometry.
C Quantification of the proliferation index measured from CellTrace staining. Proliferation index is the total number of divisions divided by the number of cells that went into division.
The figure shows the mean and standard deviation of two biological replicates within one experiment.

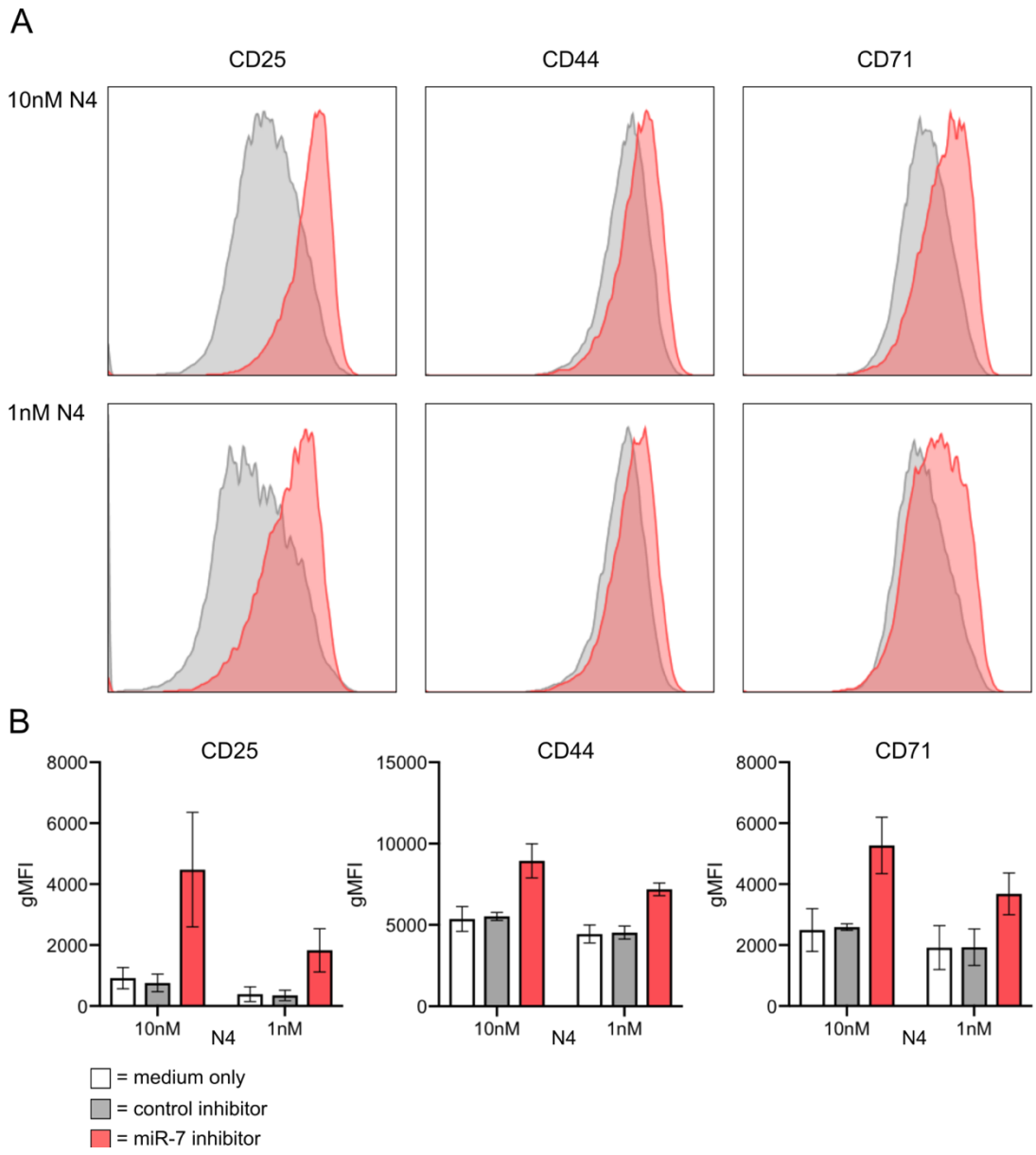

Figure 5.15 Cells receiving miR-7a inhibitor express higher levels of surface activation markers

A-B Cells were activated with 10 nM (A) or 1 nM (B) N4 and cultured with no inhibitors, with a negative control inhibitor, or a miR-7a inhibitor for 2 days.

A Expression of CD25, CD44 and CD71 measured by flow cytometry on d2. Figure is representative of two experiments.

B Geometric mean fluorescence intensity of CD25, CD44 and CD71.

The figure shows the mean and standard deviation of two biological replicates within one experiment. This is representative of two independent experiments.

5.3 Discussion

5.3.1 Summary of findings

miRNA expression was shown to change upon $CD8^+$ T cell activation, with differential expression of many miRNAs between naive and activated cells. In addition to changes in expression, miRNAs were also differentially distributed between HMW RISC and LMW RISC in activated T cells. The miRNA expression changes did not predict which RISC complex an individual miRNA was found in. Many miRNAs were found to be strongly downregulated, but what remained was predominantly found in HMW RISC. Similarly, many upregulated miRNAs were not enriched in HMW RISC but instead were found in both complexes, or in LMW RISC. Most miRNAs were found in both complexes to some extent.

5.3.2 miRNA expression and RISC organisation in naive T cells

miRNA association with HMW and LMW RISC has been previously studied in T cells (La Rocca *et al.*, 2015). The key finding from this study was that while the majority of miRNAs were downregulated upon T cell activation, they shifted to HMW RISC. The authors found that in naive cells most miRNAs were associated with LMW RISC, whereas in activated cells the miRNAs were mostly found in HMW RISC. We did not compare miRNA association between HMW and LMW RISC in naive cells, because we could not detect GW182 protein expression or HMW RISC prior to activation. If naive cells contain HMW RISC at very low levels (or undetectable in our study), this automatically suggests that HMW RISC association would increase upon activation.

miRNA expression is high in naive cells, but the cells may not express all of the factors required for efficient miRNA suppression of genes. LMW RISC does not contain GW182, which has been shown to be essential for miRNA suppressive function through the recruitment of proteins mediating mRNA degradation and translational repression (Behm-Ansmant *et al.*, 2006).

Despite downregulation upon activation, some miRNAs such as members of the let-7 and miR-15/16 families were shown to be better at suppressing a reporter construct in activated cells compared to naive (La Rocca *et al.*, 2015). miRNAs in naive T cells may therefore be stored in LMW RISC, ready to exert their action upon recruitment of GW182 and formation of HMW RISC. Since global transcription substantially increases upon T cell activation, some miRNA targets may only be expressed upon activation. These miRNAs may then play important roles in the early activation of cells. Consistent with this idea, Dicer deficient naive $CD8^+$ T cells that are deficient in miRNAs, appear normal with unchanged expression of the surface markers CD44 and CD62L (Zhang and Bevan, 2010). However upon activation these cells enter the cell cycle more rapidly and express higher levels of CD69, suggesting miRNAs are required at this stage to control level of activation (Zhang and Bevan, 2010).

5.3.3 HMW and LMW RISC in activated T cells

In activated T cells, both HMW and LMW RISC are present. Several possibilities could exist for the distribution of miRNAs between the two complexes, which were considered here: i) miRNAs may be evenly distributed in both complexes, ii) all miRNAs may be predominantly recruited to one complex upon activation or iii) distribution may vary for individual miRNAs. We clearly showed the third option to be true, with significant differential expression of miRNAs between the two complexes. This was also in agreement with the study by La Rocca *et al.*, where they noted that while most miRNAs were recruited to HMW RISC upon activation, there were differences for individual miRNAs. In other cell types, miRNA RISC-association has also been shown to change following a stimulus. In chondrocytes, IL-1β treatment was shown to dramatically change the profile of Ago-2 associated miRNAs, without a change in the expression of these miRNAs (Haseeb *et al.*, 2017). This suggested some specificity in RISC recruitment for these miRNAs, even though association with HMW or LMW RISC was not studied.

We studied the distribution of miRNAs between HMW and LMW RISC for upregulated and downregulated miRNAs. Upregulated miRNAs were on average more prevalent in HMW RISC compared to downregulated miRNAs (52% in HMW compared to 42%). Most miRNAs were found in both complexes to some extent. It might be expected, that at least a portion of an expressed miRNA needs to be found in HMW RISC for the miRNA to be functional. For highly expressed miRNAs, these may be found in both complexes because they have saturated HMW RISC. For example, miR-155 and miR-92 which were some of the most strongly upregulated miRNAs, were found in high levels in both complexes, and in fact enriched in LMW RISC. The proportion of miRNA in HMW RISC may be more important for less abundant miRNAs. If a miRNA is not very abundant or is downregulated upon activation, but most of this miRNA is found in HMW RISC, this could suggest that it is still functional. Conversely, if a lowly expressed miRNA is only found in LMW RISC, this may suggest that it is not actively suppressing its targets. Distribution between HMW and LMW RISC could therefore be another layer of regulation for the function of lowly expressed miRNAs. Specific recruitment to HMW RISC could allow even a small amount of miRNA to have a biological effect.

For the purpose of this study, we only considered HMW and LMW RISC as the two complexes that contain miRNAs, and not any intermediate complexes. Depending on the protein composition of these complexes, these could also be important in miRNA suppression. It is possible that some of the LMW RISC enriched miRNAs could be found in intermediate complexes and suppress their targets in these, depending on the protein co-factors. The intermediate complexes showed weak immunoprecipitation with GW182 which is usually needed for miRNA target suppression (Chapter 4). However non-GW182 containing RISC complexes may suppress miRNA target through alternative pathways, such as repression of translational elongation, as has been demonstrated in Drosophila (Wu, Isaji and Carthew, 2013).

5.3.4 Regulation of miRNA recruitment to HMW and LMW RISC

Since miRNAs were shown to be differentially distributed between HMW and LMW RISC, this suggests there could be some specificity to the recruitment to each complex. miRNA expression did not directly determine association with either complex, though the tendency was for low abundance downregulated miRNAs to be more enriched in LMW RISC. Instead, miRNA distribution in HMW and LMW RISC could hypothetically be influenced by factors such as target abundance, miRNA localisation, modifications in miRNA or Ago, and other RNA-binding proteins (RBPs), each of which is discussed below.

Availability of miRNA targets could influence RISC association of the miRNA. LMW RISC bound miRNAs were suggested not to be interacting with their targets (La Rocca *et al.*, 2015). High target abundance could therefore result in higher proportion of the miRNA in HMW RISC. It was previously shown that overexpression of mRNAs containing miRNA target sites increased the RISC-occupancy of these miRNAs (Flores *et al.*, 2014). miRNA target availability may change following T cell activation due to 3'UTR shortening of certain transcripts, thus potentially influencing RISC-association of these miRNAs (Sandberg *et al.*, 2008). Subcellular localisation of miRNAs has been suggested to be a big determinant of miRNA function. Recently, Ago-2 and GW182 were shown to form molecular condensates which concentrated miRNA targets with decay-mediating proteins, thus promoting miRNA function (Sheu-Gruttadauria and MacRae, 2018). miRNA localisation in the cell could determine its association with HMW or LMW RISC. Nuclear miRNAs were shown to be found in a LMW RISC and to be less effective at target suppression compared to cytoplasmic miRNAs in HMW RISC (Pitchiaya *et al.*, 2017). miRNA nuclear localisation and stability were affected by target and Ago abundance, with Ago loading and target binding competing with miRNA degradation (Pitchiaya *et al.*, 2017)

Modifications in the miRNA itself, or Ago and associated proteins could potentially influence recruitment to LMW or HMW RISC. miRNAs can be edited through a variety of methods, such as RNA editing or alternative cleavage of miRNA precursors, or non-templated nucleotide addition to mature miRNAs (Gebert and MacRae, 2019). 5' modification can affect the seed sequence and miRNA target pool, whereas 3' modifications generally affect the stability and turnover of the miRNA. 3' uridylation has been shown to play a role in targeting miRNAs for degradation following T cell activation (Gutiérrez-Vázquez *et al.*, 2017). miRNA function can also be regulated by phosphorylation in some cases. miR-34 was shown to be activated through 5' phosphorylation in response to DNA damage (Salzman *et al.*, 2016). An inactive pool of non-phosphorylated miR-34 was found non-associated with Ago-2, whereas phosphorylation led to loading onto Ago-2. Modifications of Ago proteins could also play a role in regulating miRNA loading. Ago phosphorylation on S387 has been previously shown to regulate association with GW182 and subcellular localisation to P-bodies (Zeng *et al.*, 2008; Horman *et al.*, 2013; Bridge *et al.*, 2017). Ago binding to miRNAs and mRNAs can also be affected by phosphorylation. Ago-2 phosphorylation cycle at S824-834 promoted target turnover (Golden *et al.*, 2017). Y529 phosphorylation was shown to reduce miRNA binding and was suggested to function as a molecular switch controlling miRNA loading on Ago (Rüdel *et al.*, 2011). Ago phosphorylation therefore regulates its miRNA, target and GW182 association.

Finally, other RBPs could influence miRNA recruitment to HMW and LMW RISC. Many Ago-interacting proteins have been described which can facilitate or counteract miRNA suppression of targets (Krol, Loedige and Filipowicz, 2010). For example, importin 8 was shown to stabilise Ago binding to target mRNAs, and heat shock protein 90 (HSP90) was shown to be a chaperone for miRNA loading (Weinmann *et al.*, 2009; Iwasaki *et al.*, 2010). Other mRNA interacting proteins that bind the target mRNA could also influence miRNA function. The RBP dead end 1 (DND1) was shown to bind mRNAs and prevent several miRNAs from binding to their target sites (Kedde *et al.*, 2007). The

RBP TDP-43 was shown to specifically disrupt the RISC association of miR-1 and miR-206, but not miR-133 family (King *et al.*, 2014). Some RBPs can promote or inhibit miRNA function depending on the context: HuR has been shown relieve miR-122 mediated suppression of Cat-1 in human hepatocarcinoma cells subject to stress conditions (Bhattacharyya *et al.*, 2006). Contrary to this, HuR was shown to promote let-7 mediated c-Myc suppression in cervical carcinoma cells by associating with c-Myc 3'UTR and recruiting let-7 loaded RISC to its target (Hyeon *et al.*, 2009). HuR has also been shown to play a role in T cells, promoting Th2 and Th17 differentiation by interacting with mRNAs coding for key cytokines and transcription factors (Stellato *et al.*, 2011; Chen *et al.*, 2013).

RBPs have been shown to interact with miRNAs in T cells as well. Roquin is an RBP known to be important for post-transcriptional regulation of mRNAs in T cells. It functions to maintain tolerance and guide T helper cell differentiation through suppression of its mRNA targets (Bertossi *et al.*, 2011; Vogel *et al.*, 2013). It was recently shown that Roquin interacts with miRNAs as well: it was shown to bind Ago-2, miR-146a and its target Icos in $CD4^+$ T cells to facilitate target decay (Srivastava *et al.*, 2015). Roquin also affected miR-146a stability, with increased 3' uridylation of this miRNA in the absence of Roquin. Furthermore, Roquin has been shown to interact with the miR-17~92 target Pten, preventing the binding of members of this cluster (Essig *et al.*, 2017). This led to increased mTOR signalling in the absence of Roquin, affecting differentiation of regulatory T cells and conventional $CD4^+$ T cells to Th17 and Tfh. Various RBPs have therefore been shown to influence function and target binding of specific miRNAs and could also play a role in miRNA recruitment or exclusion from HMW RISC.

5.3.5 HMW enriched miRNAs

We identified many miRNAs that were enriched in HMW RISC, summarised in Table 5.6. Some of these miRNAs, such as members of the let-7 family have been previously shown to be enriched in HMW RISC in activated T cells (La

Rocca *et al.*, 2015). However, our data differ from the study by La Rocca *et al.* in a few aspects. Firstly, instead of comparing miRNA association with HMW RISC between naive and activated cells, we focused on the distribution of miRNAs between HMW and LMW RISC in activated cells. Secondly, the previous study used a mix of $CD4^+$ and $CD8^+$ polyclonal T cells that were activated with anti-CD3 and anti-CD28 for 3 days in the presence of IL-2. Instead of a mixed polyclonal cell population, we used OT-I $CD8^+$ T cells that were activated with agonist peptide for 2 days. Even though many of the same miRNAs are expressed by $CD4^+$ and $CD8^+$ T cells, their functions may be quite different, particularly in respect to $CD4^+$ T cell differentiation to T helper subtypes, and $CD8^+$ T cell differentiation to CTLs (Rodríguez-galán, Fernández-messina and Sánchez-madrid, 2018). Activating cells through the TCR with cognate peptide is also different from non-specific activation with anti-CD3/28. Some miRNAs and their target genes were previously shown to be differentially regulated in T cells stimulated through different methods (Sun *et al.*, 2013).

5.3.6 Upregulated HMW enriched miRNAs

Well described regulators of T cell activation were among the most abundant miRNAs in HMW RISC: miR-155, miR-21 and miR-17~92 cluster have been widely studied in T cells. miR-155 and miR-17~92 cluster have already been broadly discussed in previous chapters and are well known for their roles in promoting $CD8^+$ T cell responses. miR-21 is another miRNA that is induced upon *in vitro* activation of T cells (Carissimi *et al.*, 2014). miR-21 inhibition was shown to increase apoptosis in T cells, and it has been suggested to target the pro-apoptotic protein Lats1 (Meisgen *et al.*, 2012; Teteloshvili *et al.*, 2017). miR-21 and miR-155 were not found enriched in HMW RISC, in fact miR-155 was found predominantly in LMW RISC. However, since these miRNAs are so abundant, the miRNAs were in fact found present at high levels in both complexes, and thus still appeared as some of the most abundant miRNAs in HMW RISC. Percentage of distribution between HMW and LMW RISC may

therefore be less informative for such highly expressed miRNAs. Other miRNAs that were not specifically enriched in HMW RISC but nevertheless abundant included miR-25, miR-16 and miR-191.

Upregulated				
miRNA	Expression FC	HMW/LMW FC	% HMW	CPM HMW
miR-210-3p	7.88	2.67	86	8805
miR-34a-5p	2.53	2.58	84	343
miR-7a-5p	1.85	2.44	84	24932
miR-18a-5p	5.17	2.27	80	566
miR-140-5p	0.71	2.23	81	331
miR-20b-5p	4.18	2.14	79	5658
miR-148b-3p	0.76	1.96	78	2078
miR-31-5p	6.51	1.88	77	2044
miR-106a-5p	4.75	1.84	76	2409
miR-17-5p	4.88	1.80	75	9124
Downregulated				
miRNA	Expression FC	HMW/LMW FC	% HMW	CPM HMW
miR-378c	-0.92	3.41	91	249
miR-28a-5p	-1.97	2.21	81	352
miR-378a-5p	-1.08	1.70	74	159
let-7f-5p	-0.57	1.46	72	92421
miR-1839-5p	-2.22	1.39	71	748
miR-15b-5p	-0.59	1.24	69	752
let-7a-5p	-1.14	1.22	68	37837
let-7e-5p	-1.03	1.09	66	312
miR-669p-5p	-1.40	1.03	66	840
let-7j	-1.77	0.87	62	210

Table 5.6 Summary of HMW RISC enriched miRNAs
The table shows the top 10 up - and downregulated miRNAs enriched in HMW RISC, based on FC difference between HMW and LMW RISC. Table shows Expression (log2 FC between naive and activated Ago-2 IP), HMW/LMW (log2 FC between HMW and LMW Ago-2 IP), % HMW (ratio in HMW as shown in Table 5.4) and average CPM in HMW RISC. Table includes miRNAs with AveExpr > 6 and FDR < 0.01 for 'Expression' and 'HMW/LMW' log2 FC.

miRNAs from the miR-17~92 cluster were consistently found upregulated and enriched in HMW RISC. The only miRNA of this cluster enriched in LMW RISC was miR-92-3p. Counterintuitively, this miRNA was however the most abundant miRNA in HMW RISC, similar to the other abundant miRNAs miR-155 and miR-21. The same trend for upregulation and HMW enrichment was true also for the related miRNA clusters miR-106b~25 and miR-106~363. Each of the three clusters is transcribed as a single pri-miRNA that is processed into multiple mature miRNAs. The clusters contain miRNAs from three families, each characterised by a shared seed sequence: miR-17, miR-18, miR-19 and miR-92 families (Mogilyansky and Rigoutsos, 2013). The miRNAs from the same cluster may however share targets, for example Pten was shown to contain seed sides for 5 of the 6 miRNAs of the miR-17~92 cluster (Wu *et al.*, 2012). The HMW RISC enrichment also appears to be regulated cooperatively for the miRNAs from the related clusters and families, with most found enriched in HMW RISC. Since the miRNAs are all expressed together, this could also lead to coordinated loading to RISC. Other properties such as the shared seed region and targets within a miRNA family could also influence enrichment in HMW RISC. Another miRNA family that was enriched in HMW RISC was miR-449/34. miR-34a has recently been shown to be an important T cell regulator. This miRNA was shown to be upregulated in both $CD4^+$ and $CD8^+$ T cells and targeted multiple components of the NF-κβ signalling pathway, causing downregulation of Nfkb1a and the TCR, detrimental to T cell function (Hart *et al.*, 2019). Interestingly, miR-34a shares a seed sequence with miR-449 family miRNAs miR-449a, 449b and 449c, which were also all upregulated and found in HMW RISC. miR-449 family was recently linked to $CD4^+$ T cell metabolism, specifically mitochondrial respiration. miR-449a was shown to be expressed in activated $CD4^+$ T cells, and reduction in expression decreased mitochondrial respiration (L. Huang *et al.*, 2018).

Other upregulated HMW RISC enriched miRNAs included mR-7a, miR-210-3p, miR-140, miR-31 and miR-148b. Some of these miRNAs have been described roles in T cells. For example, miR-31 has been implicated in $CD8^+$

T cell activation, and was suggested to promote IL-2 production in activated T cells (Xue *et al.*, 2013). In another setting, this miRNA was implicated in $CD8^+$ T cell exhaustion during viral infection and contributed to cell dysfunction particularly during exposure to type I interferons (Moffett *et al.*, 2017). miR-148 has been shown to be induced by T-bet in $CD4^+$ T cell and promoted cell survival (Maschmeyer *et al.*, 2018). miR-210-3p was shown to be enriched in HMW RISC, however interesting the 5p strand was enriched in LMW RISC. Originally it was assumed that one strand is selected as the guide strand whereas the other strand is rapidly destroyed (Schwarz *et al.*, 2003). However it is now understood that both strands can operate as guides, for example for miR-142, in which case the two strands have different seed sequences and could repress a different set of targets (Wu *et al.*, 2009). In the case of miR-210, miR-210-3p was the more abundant of the two strands in our study, and also one that has been previously described in T cells (Wang *et al.*, 2014). miR-210 was shown to be upregulated upon TCR stimulation, and expression further increased in hypoxic conditions, where miR-210 was upregulated by Hif1α. miR-210 was shown to target Hif1α in a negative feedback loop, causing inhibition of Th17 differentiation (Wang *et al.*, 2014).

5.3.7 Downregulated HMW enriched miRNAs

Downregulated HMW RISC enriched miRNAs included the let-7 family, miR-378 family and miR-28. Particularly, the let-7 family members were amongst the most abundant miRNAs in HMW RISC. Let-7 was also found to be enriched in HMW RISC in a separate study, and to more efficiently suppress a target reporter in activated cells compared to naive (La Rocca *et al.*, 2015). This family has been previously suggested to tone down $CD8^+$ T cell responses, particularly though targeting several T cell regulators such as Rictor, mTOR, Myc and Eomes. The miR-378 family was also downregulated but enriched in HMW RISC. miR-378 has no described role in T cells, but was shown to inhibit granzyme B in NK cells (Liu *et al.*, 2016). In other cell types it has been shown to regulate cell metabolism, to promote cell survival and reduce apoptosis

(Florczyk *et al.*, 2015). miR-28 has been shown to play a role in T cell exhaustion through targeting of PD-1 (Li *et al.*, 2016). High levels of these miRNAs in HMW RISC suggests that they may retain some functionality after downregulation, perhaps depending on the availability of their targets. These HMW enriched miRNAs and their proposed functions in T cells are summarised in Table 5.7.

miRNA	Expression change	RISC	Function
miR-17~92	Up	HMW	Regulation of T cell survival and proliferation
miR-7a	Up	HMW	Tumour suppressor, not described in T cells
miR-210	Up	HMW	Hypoxia inducible, inhibits Th17 response in $CD4^+$ T cells
miR-31	Up	HMW	May regulate IL-2 production, linked to exhaustion of $CD8^+$ T cells
miR-449/34	Up	HMW	miR-34a targets components of the NF-κβ pathway miR-449a regulates $CD4^+$ T cell mitochondrial respiration
miR-140	Up	HMW	Induced by T-bet in $CD4^+$ T cells, promotes cell survival
miR-21	Up	HMW/LMW	Anti-apoptotic in activated T cells
miR-155	Up	LMW	Key regulator of T cell survival and proliferation
let-7 family	Down	HMW	Negative regulation of CTLs, targets mTOR, Myc, Eomes
miR-378	Down	HMW	Inhibits granzyme B in NK cells
miR-28	Down	HMW	Plays a role in T cell exhaustion through targeting PD-1

Table 5.7 Function of HMW RISC enriched miRNAs in T cells

5.3.8 A role for miR-7a in T cell activation?

miR-7a was found to be consistently upregulated and enriched in HMW RISC in our study. Since this miRNA had not been previously described a role in T cells, we investigated its function by using an inhibitor. miR-7a is a known tumour suppressor, and targets components of the mTOR pathway in cancer, specifically Pik3c, p70s6k, eIF4E, Mknk1, Mknk2 and Mapkap1 (Fang *et al.*, 2011; Wang *et al.*, 2013). It has also been suggested to affect cell survival through targeting Bcl-2 (Xiong *et al.*, 2011). We found that inhibition of miR-7a resulted in decreased proliferation and higher expression of activation markers following $CD8^+$ T cell activation. All cells entered the cell cycle, but the cells went through fewer divisions, resulting in a lower total cell number. The cells also expressed higher levels of the IL-2 receptor CD25, transferrin receptor CD71 and the activation marker CD44. The cells may be more activated in the absence of miR-7a, or these surface markers may accumulate in the cell if proliferation is impaired. If miR-7a normally functions to suppress the mTOR pathway and/or cell survival through Bcl-2, miR-7a inhibition could promote cell activation. Further work is needed to understand the role of miR-7a and its targets in T cells.

Interestingly, miR-7 function in the brain has been shown to be regulated by a network of non-coding RNAs. miR-7 can be bound by a long-non coding RNA (lncRNA) Cyrano that promotes its degradation, or a circular RNA (circRNA) Cdr1as that has been suggested to stabilise miR-7 (Piwecka *et al.*, 2017; Kleaveland *et al.*, 2018). Furthermore, Cdr1as is regulated by another miRNA, miR-671 that causes its degradation. This complex interplay between the two miRNAs, lncRNA and circRNA is incompletely understood, but highlights how controlling the level and activity of this miRNA may be very important in some contexts. Interestingly, miR-671 was one of the most HMW RISC enriched miRNAs in activated OT-I T cells. Even though its expression was too low to pass most expression level filtering, 95% of the miRNA was found in HMW RISC (Table 5.4).

To understand miRNA function it is crucial to know their targets. Following identification of HMW RISC enriched miRNAs, we next aimed to identify the targets for these miRNAs.

CHAPTER 6:

Identification of miRNA targets using CLASH

6.1 Introduction

6.1.1 Current methods for miRNA target identification

In order to understand miRNA functions, their biological targets must be determined. Canonical miRNA targeting consists of the miRNA 5' seed region (nucleotides 2-7) binding to 3'UTR of the target mRNA through complementary base-pairing. This mode of recognition has been the basis for bioinformatic identification of targets, through scanning of target gene 3'UTRs for sites complementary to the miRNA seed. By this approach hundreds of potential target genes can be identified for each miRNA, due to likelihood of finding a match to the short length of the seed region. Many of these potential targets are false positives that may not be biologically relevant targets. Bioinformatically predicted targets require additional experimental validation, such as luciferase reporter assays, and over-expression or knock-down of miRNA followed by measurement of target gene expression by qPCR and/or western blotting (Kuhn *et al.*, 2008). However, this does not differentiate between direct and indirect targets. Furthermore, while many miRNA-target interactions are canonical, it has more recently become apparent that miRNA-mRNA interactions can involve positions in the miRNA beyond the seed, and can also target the mRNA at positions outside the 3'UTR (e.g. the coding regions). These non-canonical targets are not predicted bioinformatically.

More recently, the identification of miRNA targets has been facilitated by biochemical methods based on cross-linking immunoprecipitation (CLIP) of Ago proteins. UV-irradiation can be used to covalently cross-link RNA to RBPs which are then immunoprecipitated. This has been combined with high throughput sequencing of the RNA bound to the protein of interest in HITS-CLIP (high throughput sequencing of RNA isolated by CLIP) (Licatalosi *et al.*,

2008; Chi *et al.*, 2009). Ago HITS-CLIP has been used to isolate and sequence Ago-bound miRNAs and target mRNAs (Chi *et al.*, 2009). From the mRNA reads, Ago-binding sites named Ago-mRNA footprints, can be identified and were shown to be enriched for miRNA seed matches (Chi *et al.*, 2009). This complements bioinformatic identification of miRNA targets by restricting the sequence to be analysed for seed matches to the 45-60 nucleotide Ago-mRNA footprint. Many variations of the original protocol have been developed to study RNA-protein interactions, including photoactivatable-ribonucleoside-enhanced CLIP (PAR-CLIP, Hafner *et al.*, 2010), individual nucleotide resolution CLIP (iCLIP, König *et al.*, 2010; Huppertz *et al.*, 2014), infrared CLIP (irCLIP, Zarnegar *et al.*, 2016), enhanced CLIP (eCLIP, Van Nostrand *et al.*, 2016) and PABP-mediated mRNA 3' end retrieval by CLIP (PAPERCLIP, Hwang *et al.*, 2016).

While HITS-CLIP facilitates the identification of miRNA targets, these still need to be assigned computationally by searching for seed matches. Cross-linking, ligation and sequencing of hybrids (CLASH) and related methods include an additional RNA-RNA ligation step, physically linking miRNAs to their mRNA so targets can be identified directly (Kudla *et al.*, 2011; Helwak *et al.*, 2013; Helwak and Tollervey, 2014). Following Ago IP, the bound RNAs are sequenced and miRNA targets are identified from chimeric reads composed of both a miRNA and its target mRNA. This RNA-RNA ligation has been shown to naturally occur in the presence of endogenous ligases following RNA trimming, but adding an exogenous ligase increases the efficiency of chimera generation (Grosswendt *et al.*, 2014). Several other protocols involving RNA-RNA ligation have been described since, including modified in vivo PAR-CLIP (iPAR-CLIP, Grosswendt *et al.*, 2014), covalent ligation of endogenous Argonaute-bound RNAs CLIP (CLEAR-CLIP, Moore *et al.*, 2015), RNA hybrid and iCLIP (hiCLIP, Sugimoto *et al.*, 2017) and quick CLASH (qCLASH, Gay *et al.*, 2018). Generation of chimeras removes unambiguity in assigning miRNAs to their targets, which is particularly important for Ago-binding sites that may

contain complementarity to multiple miRNA seeds (Broughton and Pasquinelli, 2016). Furthermore, this allows the identification of non-canonical targets.

6.1.2 Non-canonical targeting

The chimeric reads identified from CLASH and related methods have been shown to be enriched in seed matches, however these canonical interactions only make up a proportion of chimeric reads. Canonical binding minimally requires a perfect match to the miRNA 6mer seed region (nucleotides 2-7 of miRNA), and binding can be enhanced by longer matches and an adenosine at position 1 of the target. Only 37% of miRNA-mRNA chimeras detected by CLASH in HEK cells, and ~30% by modified iPAR-CLIP in *C.elegans* and CLEAR-CLIP in mouse brain involved uninterrupted seed pairing (Helwak *et al.*, 2013; Grosswendt *et al.*, 2014). Other types of binding have been described, that can involve nucleotide mismatches or bulges in the seed region (Chi, Hannon and Darnell, 2012; Loeb, A. A. Khan, *et al.*, 2012). For the targets detected by iPAR-CLIP and CLEAR-CLIP, 80% of chimeras involved the seed region when 1-2 nucleotide mismatches were allowed. As well as binding through the seed region, the 3' end of the miRNA has also been suggested to contribute to binding, and may compensate for imperfect complementarity of the seed region (Moore *et al.*, 2015; Broughton *et al.*, 2016). The functionality of non-canonical sites that do not have perfect seed complementarity has been controversial. While many studies noted a slight but significant repression of these targets, a separate independent analysis found no effect (Helwak *et al.*, 2013; Agarwal *et al.*, 2015). While miRNAs canonically target the 3'UTR of mRNAs, many chimeric reads were shown to map to the coding sequence (CDS) of mRNAs (Helwak *et al.*, 2013; Moore *et al.*, 2015). While some studies found no significant suppression of miRNA binding sites in CDS, others have suggested a different mode of translational repression for these sites (Hsin *et al.*, 2018; K. Zhang *et al.*, 2018).

6.1.3 Summary of the CLASH protocol

We used a modified protocol of CLASH to identify miRNA targets in $CD8^+$ T cells. The key steps of the protocol are described below and in Figure 6.1. The first step in CLASH is the UV-crosslinking of RNA and RBPs. UV-irradiation is applied to a cell suspension after which the cells are lysed. Ago-2 is then immunoprecipitated from the lysate. Following the IP, the bound RNA is trimmed with RNase and the 5' end is phosphorylated to prepare the RNA for the ligation reaction. The ligase enzyme is incubated with the samples to produce chimeras of the miRNA and RNA target with which it interacts. Next, the ends of the RNA are dephosphorylated and a 3' adapter is added to the RNA, prior to running the samples on SDS-PAGE. We used an adaptor linked to IR800-dye to visualise RNA on the gel. The band corresponding to Ago-2 is cut from the gels and treated with proteinase K to release Ago-bound RNA. This RNA is then phenol-chloroform extracted and used for making sequencing libraries. From the sequencing reads, miRNA targets can be identified as chimeric miRNA-mRNA reads. With this method, we aimed to identify biologically relevant miRNA target pairs from activated $CD8^+$ T cells. We also attempted to enrich for chimeric reads by isolating GW182-bound Ago-2 or size separated HMW-RISC Ago-2.

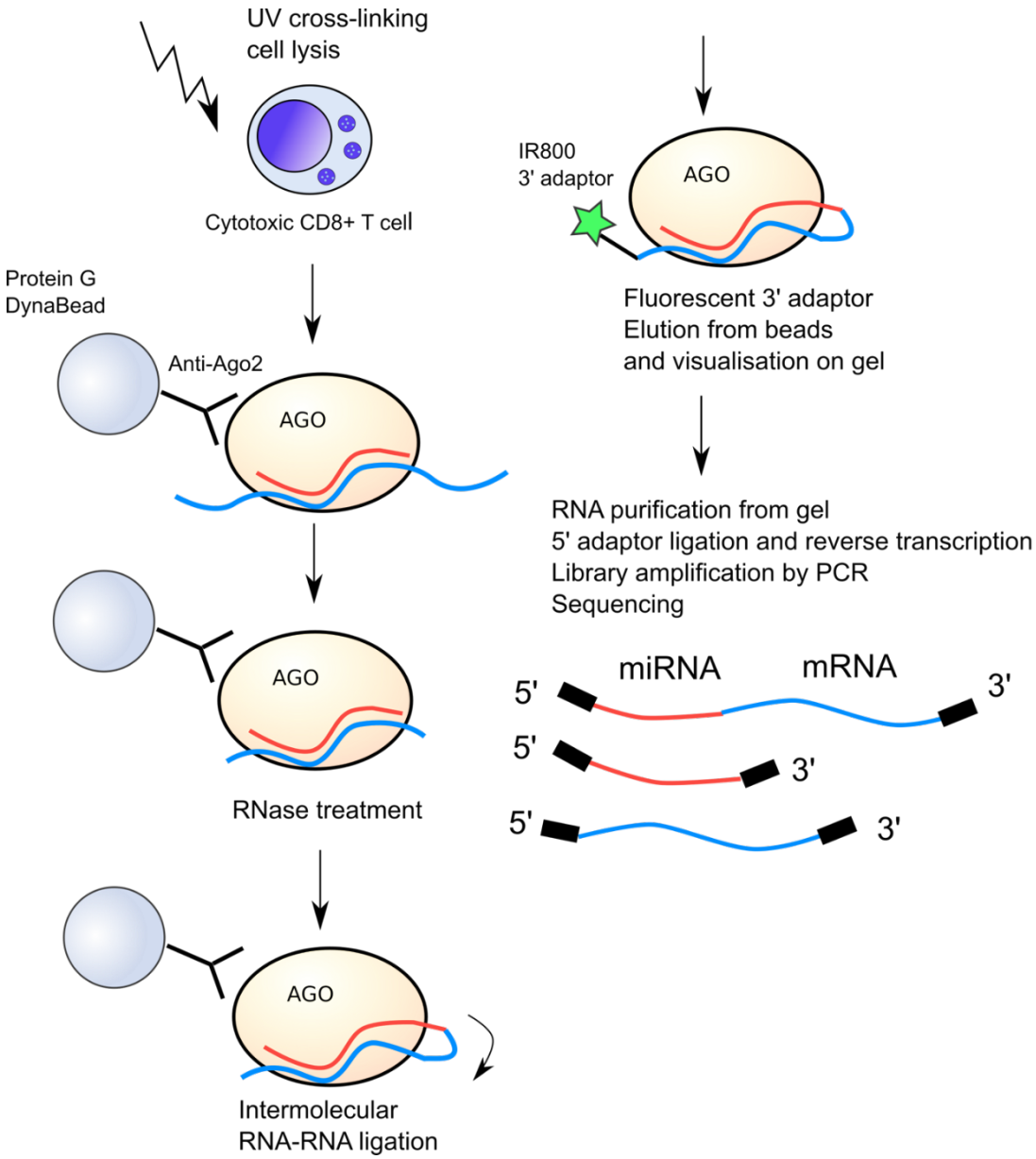

Figure 6.1 Summary of CLASH protocol
Overview of the CLASH protocol. Cells are UV-irradiated and lysed, followed by immunoprecipitation of Argonaute and interacting RNA. The miRNA-mRNA pairs are ligated together, purified, reverse transcribed, amplified and sequenced. Direct miRNA targets can be identified from miRNA-mRNA chimeric reads.

6.2 Results

6.2.1 Generation of CLASH libraries

To prepare CLASH libraries from OT-I $CD8^+$ T cells, the cells were activated with N4 for 2 days for the earlier time-point (d2), or cultured with IL-2 for a further 4 days for fully differentiated CTLs (d6). Proteins and bound RNAs were covalently cross-linked using a UV-crosslinker on ice, after which the cells were lysed. Ago-2 was immunoprecipitated from the lysates using magnetic beads. As a control, we used non-crosslinked samples. We hypothesised, that most of the miRNA-target interactions would be occurring in GW182-containing HMW RISC. We therefore immunoprecipitated GW182 and from the GW182 unbound fraction, Ago-2. Finally, we also immunoprecipitated Ago-2 from HMW and LMW RISC size-separated fractions (Table 6.1).

	Samples	Cross-link	IP
Experiment 1	Total Ago-2	Yes	Ago-2
D6 CTL	No cross-link control	No	Ago-2
Experiment 2	Total Ago-2	Yes	Ago-2
D6 CTL	GW182 bound Ago-2	Yes	GW182
	GW182 unbound Ago-2	Yes	Ago-2
	No cross-link control	No	Ago-2
Experiment 3	Total Ago-2 (1)	Yes	Ago-2
D2 T cells	Total Ago-2 (2)	Yes	Ago-2
(1) & (2) =	HMW RISC Ago-2 (1)	Yes	Ago-2
biological	HMW RISC Ago-2 (2)	Yes	Ago-2
replicates	LMW RISC Ago-2 (1)	Yes	Ago-2
	LMW RISC Ago-2 (2)	Yes	Ago-2

Table 6.1 Summary of three CLASH experiments
First experiment contains total Ago-2 IP from cross-linked cells and a non-cross-linked control from d6 CTLs. Second experiment contains total Ago-2 IP and GW182 IP from cross-linked cells, Ago-2 IP from GW182 IP unbound fraction, and a non-cross-linked control from d6 CTLs. Third experiment contains two biological replicates of total Ago-2 IP and Ago-2 IP from size separated HMW and LMW RISC, using cross-linked d2 activated T cells. Ago-2-flag mice were used for Experiments 1 and 2.

After the immunoprecipitations, we carried out the CLASH protocol as described above. Ago-2-RNA complexes were eluted from the IP-beads and ran on SDS-PAGE. To visualise Ago-2, the proteins and bound RNA were transferred on a membrane for western blotting. Ago-2 could be seen overlaying with a band corresponding to the IR800-dye labelled Ago-2 bound RNA (Fig.6.2A). The amount of Ago-2 co-immunoprecipitating with GW182 was very low compared to the total Ago-2 IP sample (Fig.6.2A). Similarly, amount of Ago-2 from the size separated HMW and LMW complexes was very low compared to total Ago-2 IP (not shown). The amount of input Ago-2 was lower for the GW182 IP and for size fractionated samples, and furthermore the repeated washing steps throughout the CLASH protocol may have led to additional loss of material. For all samples, the band corresponding to Ago-2 and bound RNAs was cut, then treated with proteinase K prior to RNA extraction.

Small RNA libraries were then generated from the extracted RNA in a process involving reverse transcription, addition of 5' adaptor, PCR amplification and gel purification of the product. A band of approximately 145 bp could be seen when the PCR product was measured on a Bioanalyzer, corresponding to the length of the miRNAs containing 3' and 5' adaptors. Above this strong band, a smear could be seen, containing longer fragments of RNA, such as mRNAs and possibly chimeric reads. A strong signal could be detected from all the samples after the PCR. Despite a low amount of co-immunoprecipitating Ago-2 from the GW182 IP, this sample contained lots of RNA (Fig.6.2B). Similarly, despite a low input, RNA could be isolated from the HMW and LMW RISC Ago-2 IP samples (Fig.6.2C).

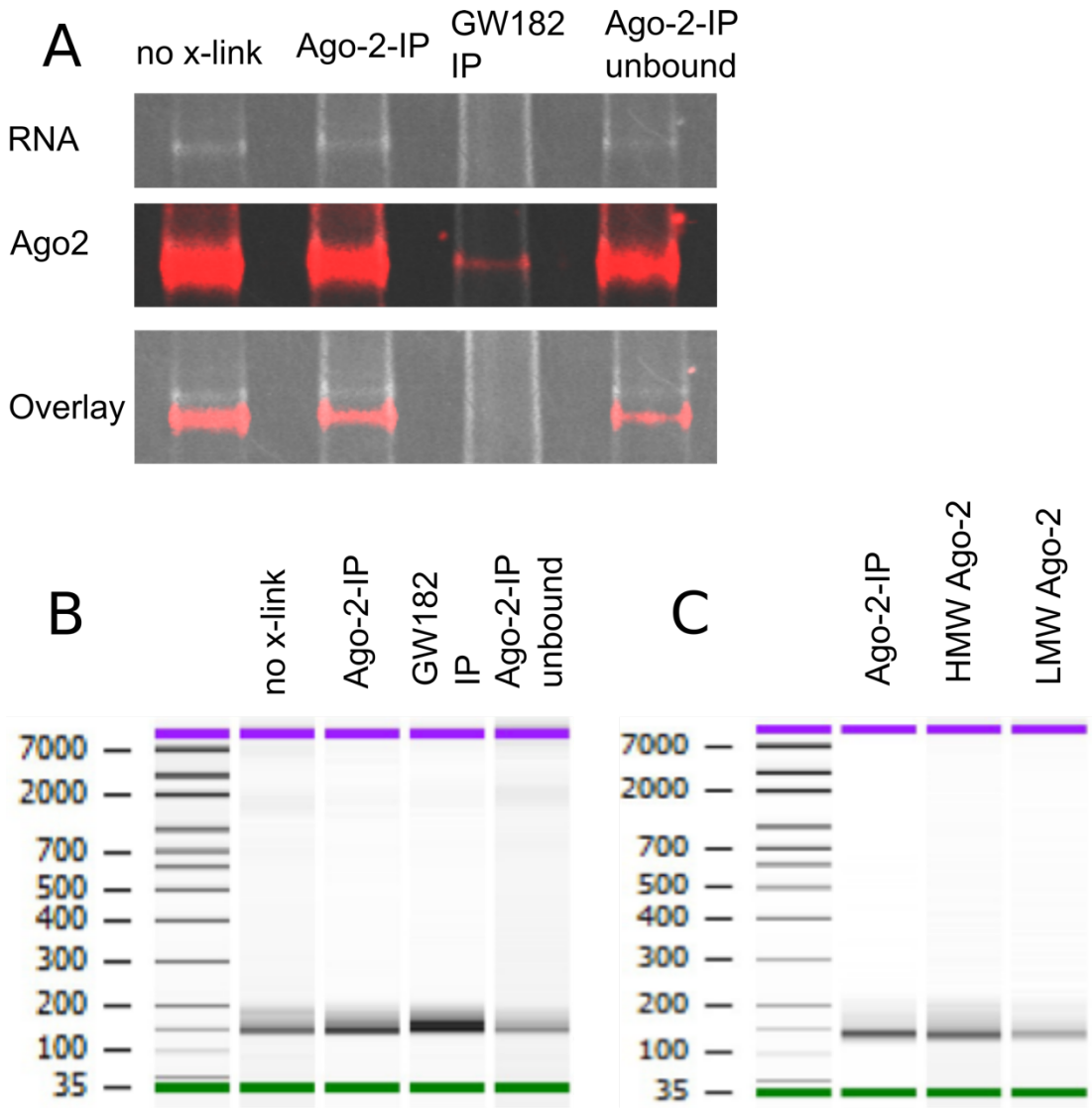

Fig 6.2 Preparation of CLASH libraries from CD8$^+$ T cells
A WB showing immunoprecipitated Ago-2 and GW182 with bound RNA containing the labelled 3'adapter (IR800-dye). Ago-2 and GW182 were immunoprecipitated from cross-linked d6 CTLs. In addition, Ago-2 was immunoprecipitated from the GW182 unbound fraction and from non-cross-linked cells. WB was probed with Ago-2 antibody. Overlay is shown with reduced intensity for Ago-2 to show overlay with RNA band.
B-C Bioanalyzer measurements showing CLASH libraries from the samples in A (B), and from total Ago-2 IP and Ago-2 IP from size separated HMW and LMW RISC, using cross-linked d2 activated T cells (C).

6.2.2 Identification of miRNA-mRNA chimeras and their binding properties

Following sequencing of the CLASH libraries, the reads were mapped to known mouse RNA families to identify miRNA, mRNA and chimeric reads from the three experiments. The total number of reads varied between experiments and between samples. All samples contained miRNA and protein coding (pc) reads, however in many cases rRNA also made up a large proportion of library. The total Ago-2 IP libraries contained 10-40% miRNA reads and around 10-20% pc reads (Fig.6.3A). rRNA reads were abundant in all libraries and made up more than 90% of the reads in some cases. Particularly the GW182 IP sample contained very few miRNAs reads, instead consisting 90% of rRNA. This experiment as a whole contained more ribosomal reads than the other two experiments. GW-unbound Ago-2 IP was similar to the total Ago-2 IP in its read composition (Fig.6.3A). The HMW and LMW RISC IPs contained fewer reads in total, as well as a smaller proportion of miRNA reads compared to the total Ago-2 IP (Fig.6.3A-B). The HMW RISC sample however had a similar proportion of pc reads than the total Ago-2 IP, whereas LMW RISC contained very few pc reads (Fig.6.3A). This is consistent with the idea that while HMW RISC and LMW RISC both contain miRNAs, these are mostly associated with their target mRNAs in HMW RISC. HMW RISC also contained a high proportion of ribosomal reads, which may be expected as HMW Ago complexes have previously been shown to co-fractionate with polysomes (Landthaler *et al.*, 2008)

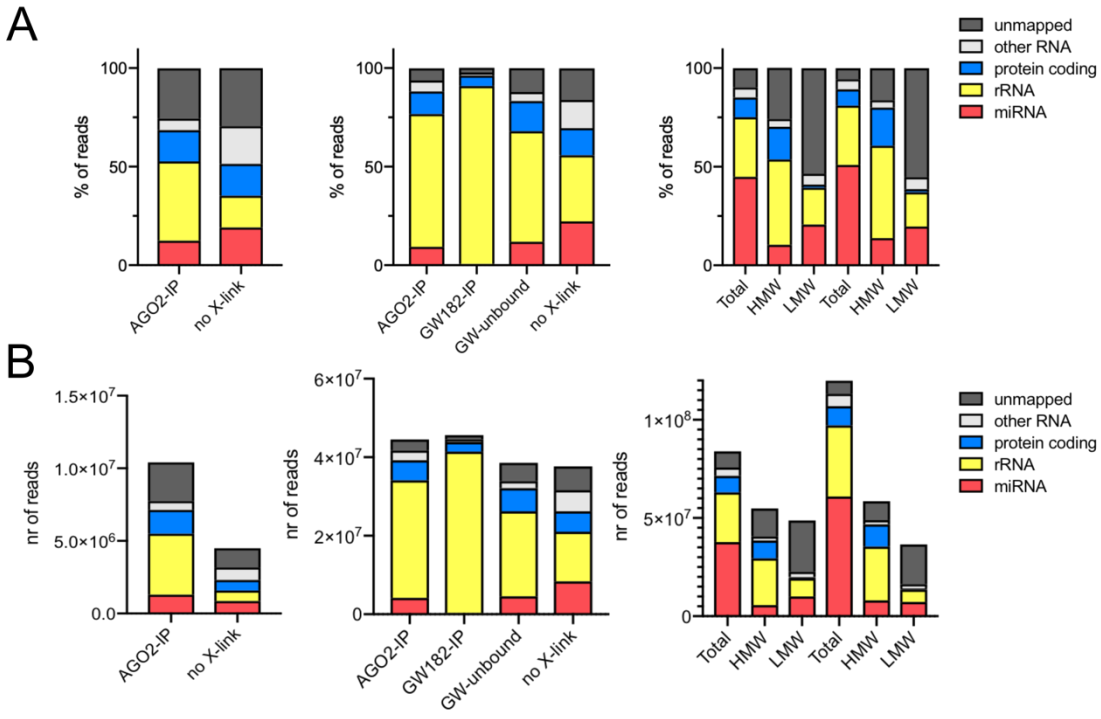

Figure 6.3 RNA composition of CLASH libraries
RNA biotypes in three separate CLASH experiments
A Proportion of RNA biotypes in three CLASH experiments, two from d6 CTLs (first and second graphs) and one from d2 activated cells (last graph). Proportion of reads corresponding to miRNAs, rRNAs, pc reads (mRNAs), other types of RNAs (including tRNA, lncRNA and uncategorised RNA) or unmapped reads is shown.
B Total number of reads for RNA biotypes.

Next, we calculated the number of chimeric reads for each sample. The chimeric reads were identified as mapping to both a miRNA and a protein coding region of the genome. The first experiment yielded 0.53% chimeric reads from the Ago-2 IP, as a proportion of total reads. However, in subsequent experiments this proportion was much lower, with approximately 0.01% chimeric reads of total reads. We filtered out low quality reads, and calculated the number of unique chimeric reads. We measured unique reads instead of total reads, since multiples of each unique reads may arise from PCR amplification which could be biased towards certain reads, and thus may not represent the true abundance of the reads. In the first experiment, the total Ago-2 IP contained 1769 unique chimeric reads whereas the other three total Ago-2 IPs had around 300-400 (Fig.6.4A). GW182 IP, GW-unbound-Ago-2 IP and HMW-Ago-2 IP yielded fewer chimeras than the total Ago-2 IPs, at around 100-250 unique chimeras, and the LMW-Ago-2 IP contained almost no chimeric reads (Fig.6.4A). Next, we analysed the type of binding in the chimeric reads by looking for perfect matches to the miRNA seed. For the total Ago-2 IPs, 7-23% of the chimeric reads contained a perfect seed match to the miRNA, depending on the experiment (Fig.6.4B). This was slightly less than expected based on previous CLASH experiments, in which approximately 30-40% of chimeric reads were reported to contain perfect seed matches (Helwak *et al.*, 2013; Grosswendt *et al.*, 2014; Moore *et al.*, 2015).

We had expected to enrich for bona fide chimeric reads by selecting GW182-bound Ago-2 or HMW RISC Ago-2, however, in fact this reduced the number of chimeras recovered. Both the GW182 IP and the HMW RISC IP contained much less Ago-2 as starting material compared to the total Ago-2 IP, which probably compromised efficient recovery of chimeric reads. Based on these results, we decided to consider only the total-Ago2 IP samples for further analysis, since these appeared to be the highest quality samples with the highest numbers of chimeras. For these samples, we determined the type of seed that was found, calculating the average proportion of seed matched chimeras with a 6mer (exact match to positions 2-7 of miRNA), offset 6mer

(positions 3-8), 7mer-A1 (positions 2-7 followed by an adenosine), 7mer m8 (positions 2-8) or 8mer (positions 2-8 followed by an adenosine) match. The predominant seed type was an offset 6mer (28.3%) followed by 6mer (26.2%), 7mer m8 (22%), 8mer (13%) and 7mer A1 (10.5%). Next, we looked whether the part of the chimera containing the mRNA mapped to the 3'UTR, CDS or 5'UTR of the gene. We found that for the reads with a canonical seed match, 41.6% matched 3'UTR and 54.5% CDS, with rest matching 5'UTR or regions in between. For the non-canonical targets, 50.6% matched 3'UTR and 44% CDS. Other CLASH experiments have similarly reported frequent binding to the CDS (Helwak *et al.*, 2013; Moore *et al.*, 2015).

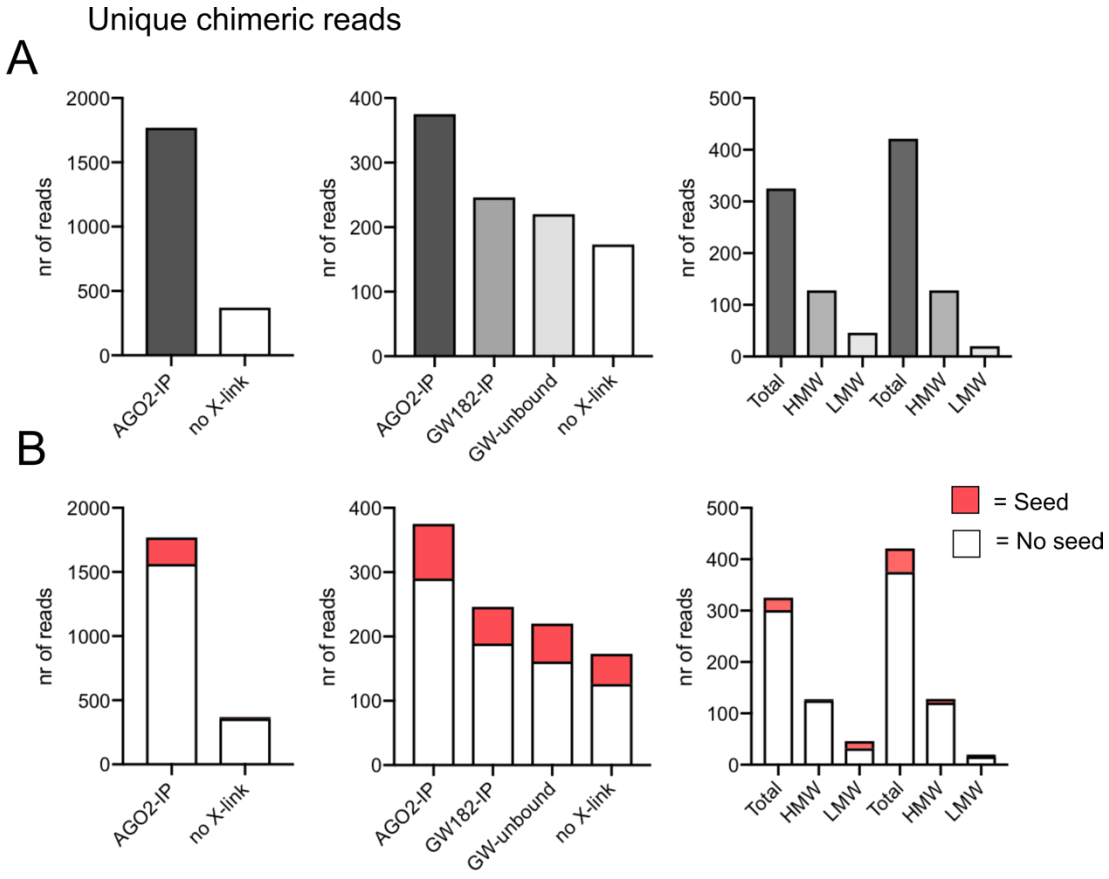

Figure 6.4 Number of unique chimeric reads from CLASH experiments
A Number of unique chimeric reads in three separate CLASH experiments as described in Table 6.1.
B Proportion of chimeric reads containing a perfect seed match.

6.2.3 Characterisation of miRNAs found in chimeric reads

We then identified which miRNAs were enriched in the chimeric reads. We calculated the number of unique chimeric reads per miRNA, and the number of unique targets per miRNA. These values differ since multiple unique reads could exist of a single miRNA-target interaction, that differ in the start position or length of the read. We considered chimeric reads containing a seed match separately from those that did not, combining data from all four total Ago-2 IPs. In all cases, miR-142a-3p had the most unique reads and unique targets, with a total of 35 unique targets containing a seed match and 339 that did not (Table 6.2). The number of potential targets identified was much higher for the chimeras not containing a seed match. These could be non-canonical interactions not involving a perfect seed match, or some could be non-specific background. Other miRNAs that had a high number of potential targets included other highly abundant miRNAs in T cells such as the 5p strand of miR-142a, miR-155, miR-21a and miRNAs from the 17~92 cluster. Of interest, many miRNAs identified as HMW enriched in the previous chapter, such as miR-210-3p, miR-7a, let-7 family and miR-378a were also abundant amongst the chimeric reads (Table 6.3). Finally, we measured how many miRNAs were targeting a single target mRNA, and found that all targets that were identified contained only a seed match for one, or maximum two miRNAs.

Seed match			No seed match		
miRNA	Unique reads	Unique targets	miRNA	Unique reads	Unique targets
miR-142a-3p	70	35	miR-142a-3p	757	339
miR-142a-5p	22	9	miR-21a-5p	275	115
miR-155-5p	21	3	miR-210-3p	86	37
miR-92a-3p	17	7	miR-16-5p	86	44
miR-27a-3p	11	9	miR-92a-3p	83	49
miR-27b-3p	9	6	miR-378a-3p	72	46
miR-16-5p	9	5	miR-155-5p	67	28
let-7i-5p	9	3	miR-147-3p	61	35
miR-22-3p	8	5	let-7i-5p	56	32
miR-23a-3p	8	6	miR-7a-5p	54	23
miR-29a-3p	6	5	miR-142a-5p	52	28
miR-210-3p	6	5	miR-103-3p	51	28
miR-324-5p	5	2	miR-26a-5p	43	16
miR-17-5p	5	4	let-7f-5p	43	24
let-7f-5p	5	1	miR-17-5p	42	23
miR-139-5p	4	1	miR-106a-5p	39	15
miR-296-5p	4	1	let-7d-5p	39	21
let-7g-5p	4	1	miR-27a-3p	38	25
let-7d-5p	4	3	miR-182-5p	38	18
miR-7a-5p	4	2	miR-19b-3p	32	14

Table 6.3 miRNAs with most chimeric reads
The top 20 miRNAs with the most chimeric reads. Chimeric reads from all four total Ago-2 IP experiments were pooled. Table is showing unique chimeric reads per miRNAs as well as number of unique targets, taken from chimeras containing a perfect seed match or no seed match.

6.2.4 Characterisation of miRNA targets found in chimeric reads

We then looked at how many miRNA targets were shared between the experiments. We compared the pc reads in chimeric reads between the two experiments using d2 activated T cells or d6 activated CTLs. We found poor overlap between the experiments, with 37 shared targets on d2 and 65 on d6 (Fig.6.5A-B). Most chimeric reads were therefore specific to one experiment. We also compared the overlap of targets recovered by GW182 IP or GW182-unbound Ago-2 IP, compared to the total Ago-2 IP. For these reads we again found little overlap between the three samples (Fig.6.5C). Due to the low number of chimeric reads that were found, these likely only provided a snap-shot of the true range of chimeric reads present in the cells.

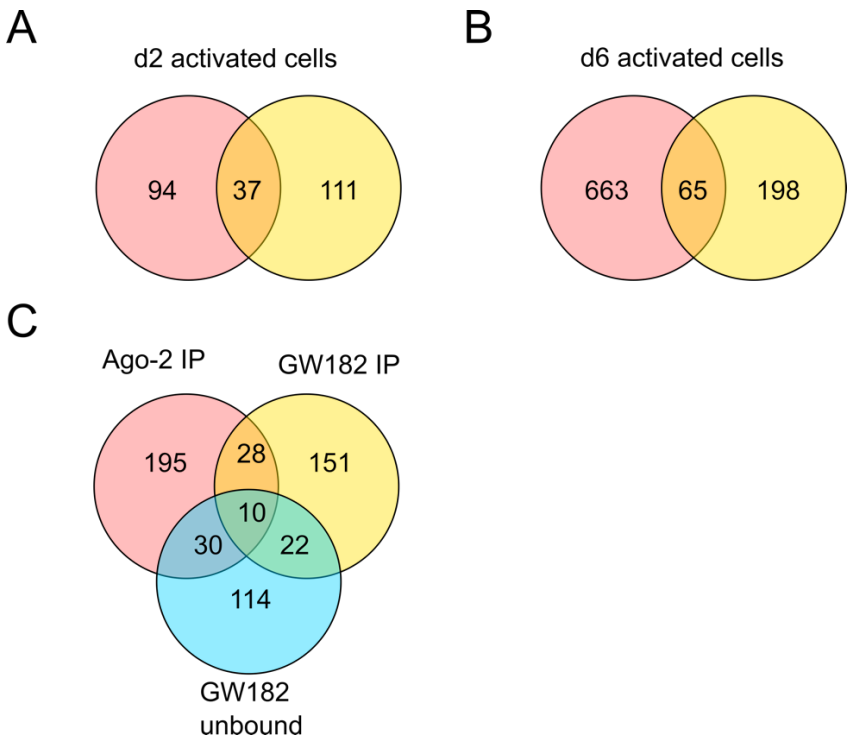

Figure 6.5 Shared miRNA targets between experiments
A-C Overlays of the number of unique miRNA targets from chimeric reads in different experiments.
A Targets in chimeras from total Ago-2 IP CLASH samples from d2 activated T cells.
B Targets in chimeras from total Ago-2 IP CLASH samples from d6 CTLs.
C Targets in chimeras from total Ago-2 IP, GW182 IP and GW182 unbound (Ago-2 IP) from d6 CTLs.

We also performed Gene Ontology (GO) enrichment analysis of the miRNA targets found in chimeric reads. For this analysis we combined data from all four Ago-2 IPs but only considered chimeras that contained a miRNA seed match. This showed the enrichment of several processes, related to T cell activation, cell migration and cell metabolism (Table 6.2). The TCR signalling pathway and lymphocyte activation and differentiation associated proteins included Ptpn22, Bcl-10, Id2, NF-κβ-inhibitor δ, Nfatc3, Roquin-1, and Cd28.

GO biological process	Nr of genes	Fold enrichment	P-value
Positive regulation of filopodium assembly	4	16.63	1.48E-04
Regulation of T cell receptor signaling pathway	5	15.72	2.71E-05
Dendritic spine development	4	14.32	2.50E-04
Adipose tissue development	4	13.93	2.75E-04
ATP synthesis coupled electron transport	5	11.72	9.90E-05
Regulation of antigen receptor-mediated signaling pathway	5	11.31	1.16E-04
Oxidative phosphorylation	5	10.07	1.93E-04
Aerobic respiration	5	9.91	2.06E-04
Cellular respiration	9	8.59	1.80E-06
Positive regulation of plasma membrane bounded cell projection assembly	6	7.3	2.33E-04
mRNA transport	6	7.3	2.33E-04
ATP metabolic process	8	6.06	7.37E-05
Negative regulation of lymphocyte activation	7	5.94	2.37E-04
Energy derivation by oxidation of organic compounds	9	5.92	3.13E-05
Aging	7	5.86	2.56E-04
Negative regulation of cellular catabolic process	9	4.94	1.20E-04
Homeostasis of number of cells	9	4.55	2.16E-04
Negative regulation of catabolic process	10	4.41	1.23E-04
Lymphocyte differentiation	9	4.33	3.08E-04

Table 6.2 GO term enrichment analysis of miRNA targets containing a canonical seed match
Targets from chimeric reads from all four total Ago-2 IP experiments were pooled and chimeras not containing a seed match were filtered out. The targets were analysed for GO term enrichment. Number of genes in each biological process (GO term) is shown, with fold enrichment and p-value. The top 20 significant hits are shown ranked by fold difference.

6.2.5 Bioinformatic validation of chimeric reads with TargetScan and Mirza

Since we found a large number of potential targets for several miRNAs, particularly ones that did not contain a perfect seed match, we further analysed these using available bioinformatic tools. We used TargetScan to identify predicted miRNA targets from the data and Mirza to calculate binding energies of potential novel targets. TargetScan is a target prediction program that combines information from the binding site and other features identified from experimental data to predict the most effectively targeted mRNAs (Agarwal *et al.*, 2015). TargetScan developers found no suppressive function to non-canonical sites and thus only consider types of canonical binding, which must include a perfect match to miRNA seed in the 3'UTR of the target mRNA. We additionally used the Mirza algorithm to predict miRNA targets (Khorshid *et al.*, 2013). This program combines energy parameters from CLIP data for a biophysical model to calculate the binding energy of the interaction and assigns a score based on this, with high scores indicating positive binding energy and increased likelihood that the binding is real. In contrast to TargetScan, Mirza also considers non-canonical targeting.

First, we separated the data into chimeric reads containing a perfect seed match, and those that did not, then calculated TargetScan and Mirza scores for these. The process for analysing chimeric reads is summarised in Figure 6.6. Most chimeric reads were found as a single unique read. However, as expected, the reads containing a seed match had high TargetScan and Mirza scores. Of the seed-containing targets in 3'UTR, 34% were predicted as targets by TargetScan. These are likely to be real interactions causing target suppression (Table 6.4). TargetScan has strict criteria for assigning predicted miRNA targets, whereas Mirza can be used to predict the binding energy for any pattern of complementarity in the interaction (beyond the seed site). Several interactions were found that were not TargetScan predicted targets for the miRNA but had high Mirza scores (Table 6.5). Many of these were interactions with the CDS of the target gene since these are not considered by

TargetScan (Table 6.6). These are also likely to be real interactions, but may not result in efficient target suppression. For the chimeras with a perfect seed match, gene annotation of the identified miRNA targets showed proteins involved in various processes such as regulation of gene transcription, cell metabolism, protein transport and signalling pathways, with very few T cell specific targets.

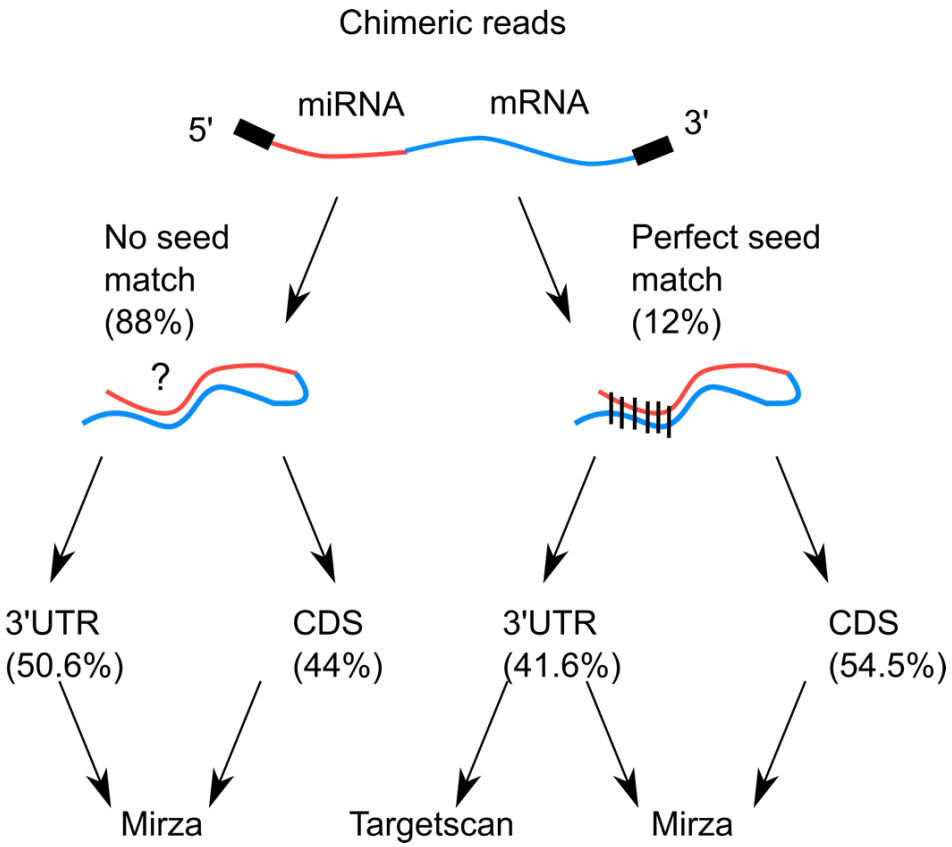

Figure 6.6 Bioinformatic analysis of chimeric reads
Chimeric reads from all four total Ago-2 IP experiments were pooled The reads were separated into those containing a perfect seed match to the miRNA and those not containing a seed match. Each group was divided into chimeric reads where the read maps to 3'UTR or CDS of the mRNA. Reads containing a perfect seed match in the 3'UTR were analysed by TargetScan and Mirza, whereas reads not containing a perfect seed match, or mapping to the CDS, were analysed by Mirza.

miRNA	Target	Unique reads	Mirza	TS	Gene Annotation
miR-147-3p	Ndufa4	1	2091.3	99	Transport, mitochondrion, oxidative phosphorylation
miR-27a-3p	Lpar6	1	306.2	99	Signal transduction, G-protein coupled receptor signaling pathway
miR-296-3p	Mt2	3	203.6	99	Cellular zinc ion homeostasis, nitric oxide mediated signal transduction
miR-142a-5p	Slc39a1	3	17.8	99	Metal ion transport
miR-92a-3p	Sertad3	1	3174.5	98	Regulation of transcription, negative regulation of cell growth
miR-17-5p	Nabp1	1	473.5	98	DNA repair
miR-25-3p	Sertad3	1	188.7	98	Regulation of transcription, negative regulation of cell growth
miR-23b-3p	Sbno1	1	136.1	97	Regulation of transcription
miR-32-5p	Srpr	3	101.6	97	Intracellular protein transport

Table 6.4 Chimeric reads containing a perfect seed match in 3'UTR
The top 10 chimeric reads ranked by TargetScan (TS) score out of 100.

miRNA	Target	Unique reads	Mirza	Gene Annotation
miR-26b-5p	Capn10	1	1150.9	Mitophagy, proteolysis
miR-20a-5p	Nabp1	1	457.6	DNA repair
miR-17-5p	Mtf1	2	316.2	Regulation of transcription, response to oxidative stress
let-7f-1-3p	Mkln1	1	210.6	Cell matrix adhesion, actin cytoskeleton reorganization
let-7g-5p	Hps1	4	168.6	Organelle organization, blood coagulation, positive regulation of natural killer cell activation
miR-210-3p	Aebp2	2	142.4	Regulation of transcription
miR-27b-3p	Fam46a	1	127.6	Regulation of gene expression
miR-23a-3p	Vrk3	1	120.2	Protein phosphorylation, negative regulation of ERK1 and ERK2 cascasde
miR-23b-3p	Fmr1	1	50.1	Regulation of alternative mRNA splicing
miR-24-3p	Rnf138	2	47.3	Protein ubiquitination, DNA repair
miR-142a-5p	Trps1	1	46.7	Regulation of transcription, cell development

Table 6.5 Chimeric reads containing a perfect seed match in 3'UTR
The top 10 chimeric reads that do not have a TargetScan score, ranked by Mirza score.

miRNA	Target	Unique reads	Mirza	Gene Annotation
miR-27a-3p	Jmjd1c	2	971.6	Epithelial cell morphogenesis, transcription
miR-210-3p	Fnbp1	1	515.9	Endocytosis, vesicle mediated transport
miR-106a-5p	Plekhm1	1	497.4	Protein transport, autophagy
miR-29a-3p	Fh1	1	484.3	Citric cycle (TCA cycle)
miR-27b-3p	Fam69a	1	392.6	Endoplastic reticulum membrane
miR-320-3p	Oaz1	1	291.8	Polyamine metabolic process
miR-324-5p	Anxa2	4	269.2	Angiogenesis, membrane raft assembly
miR-22-3p	Mertk	1	256.4	Natural killer cell differentiation, negative regulation of cytokine production
miR-378a-5p	Exo1	1	233.6	Immune system process, somatic hypermutation of immunoglobulin genes
miR-155-5p	mt-Nd1	18	232.1	Oxidative phosphorylation

Table 6.6 Chimeric reads containing a perfect seed match in CDS
Top 10 chimeric reads with a perfect seed match in CDS ranked by Mirza score.

Next, we inspected the chimeric reads that did not contain a perfect seed match, which was the vast majority of chimeras (88%). We calculated Mirza scores for these reads and found several chimeric reads with relatively high scores (Tables 6.7 and 6.8). These usually involved some binding in the seed region but contained a mismatch, a gap or bulge in the sequence. These interactions with relatively high Mirza scores are again likely to be real but may not cause target suppression, in particular for those found in the CDS. The non-canonical targets included the transcription factor Nfat5 as well as other transcription regulators and proteins linked to protein transport, oxidative phosphorylation, autophagy, hypoxic response and cell migration. Many chimeric reads also had very low Mirza scores (<1) with only short matches to the seed region or in some cases no clear pattern of binding which we concluded were likely to be non-specific interactions.

miRNA	Target	Unique reads	Mirza	Gene Annotation
miR-29b-3p	Nfat5	1	55.8	Cytokine production, regulation of transcription
miR-182-5p	Fam107b	3	36.4	Sensory perception of sound
miR-26a-5p	Wipi2	1	34.2	Autophagosome assembly
miR-23a-3p	Mlxip	1	32.2	Regulation of transcription
miR-17-5p	Cmtm3	1	31.5	Chemotaxis, positive regulation of BCR signaling pathway
miR-15b-5p	Pdap1	5	26.2	Platelet derived growth factor binding
miR-142a-3p	Ms4a4b	3	21.0	Integral component of plasma membrane
miR-27a-3p	Atp5f1	2	12.8	ATP synthesis coupled proton transport, oxidative phosphorylation
miR-21a-3p	Vmp1	2	12.6	Exocytosis, autophagy
miR-142a-3p	Efcab11	1	10.3	Calcium ion binding

Table 6.7 Chimeric reads with no seed match, mapping to 3'UTR
The top 10 chimeric reads without a perfect seed match, mapping to 3'UTR, ranked by Mirza score.

miRNA	Target	Unique reads	Mirza	Gene Annotation
miR-142a-3p	Smchd1	2	47.3	Inactivation of X chromosome by DNA methylation
miR-342-3p	Hsp90b1	3	25.2	Response to hypoxia, protein folding
miR-30e-5p	Ppib	1	21.3	Protein peptidyl-prolyl isomerization, protein folding
miR-142a-3p	Atp6v1e1	3	20.1	ATP hydrolysis coupled proton transport, oxidative phosphorylation
miR-145a-5p	Necap2	1	18.0	Protein transport, endocytosis
miR-21a-5p	Ssr1	1	17.6	Protein processing in endoplastic reticulum
miR-744-5p	Akna	2	17.4	Regulation of transcription
miR-21a-5p	Dhx36	1	13.7	Regulation of transcription
miR-378a-3p	Cpne3	1	13.2	Positive regulation of cell migration, cellular response to calcium ion
miR-361-5p	Acadm	1	12.8	Fatty acid degradation, oxidoreductase activity

Table 6.8 Chimeric reads with no seed match, mapping to CDS
The top 10 chimeric reads without a perfect seed match, mapping to CDS, ranked by Mirza score.

6.2.6 Identification of potential targets for specific miRNAs

Next, we examined the targets for specific miRNAs known to be important for T cell activation. We decided to look at targets for miR-142a-3p, since this miRNA had the most chimeric reads, and is also a known regulator of T cell proliferation. We also identified potential targets for miR-17 and miR-92 which are well known for their role in supporting effector T cell proliferation. Finally, we looked at the potential targets for the HMW RISC enriched miRNAs miR-7a and miR-210-3p.

miR-142a-3p had the most chimeric reads out of all miRNAs in all four experiments. This miRNA has previously been described to be abundant in T cells and to regulate T cell proliferation. A number of cell cycle regulatory genes have been shown to be dysregulated in miR-142 KO cells (Sun *et al.*, 2015; Mildner *et al.*, 2017). The atypical transcription factors E2f7 and E2f8 and the cell cycle regulator Cdkn1b were suggested to be direct targets of miR-142 (Sun *et al.*, 2015; Mildner *et al.*, 2017). We ranked the top 20 chimeric targets for miR-142-3p from our data by the Mirza scores (Table 6.9). These include targets that have a perfect seed match to miR-142 as well as some that do not. Many of the targets were found in the CDS whereas some were canonical targets in the 3'UTR. We identified a few genes that are linked to regulation of the cell cycle, notably Mki67 and Mcm6. Both of these however contain a seed match in the CDS of the gene, making it unclear whether these are functional targets. Potential canonical targets that were identified included Rc3h1 (Roquin-1) which is an mRNA binding protein that has a key role in suppressing spontaneous T cell activation and differentiation (Chang *et al.*, 2012; Vogel *et al.*, 2013). Another canonical target was Coro1c (coronin), which is a protein involved in regulation of cell adhesion and cytoskeleton, and has been shown to be enriched in F-actin rich membrane protrusions in activated T cells (Nal *et al.*, 2004).

Target	Site	Unique reads	Mirza	Seed match?	Gene Annotation
Rpl24	CDS	8	74.9	yes	Ribosomal large subunit assembly
Mki67	CDS	3	72.5	yes	Regulation of mitotic cell division
Smchd1	CDS	2	47.3	no	Inactivation of chromosome X by methylation
Ash1l	CDS	1	46.5	yes	Negative regulation of acute inflammatory response
Tm9sf2	CDS	1	45.7	yes	Endosome membrane
Gm13248	UTR5	1	42.4	yes	
Gtf3c2	UTR3	2	30.8	yes	Transcription
Zfp120	UTR3	1	28.3	yes	Regulation of transcription
Coro1c	CDS-UTR3	1	24.3	yes	Actin cytoskeleton organization, regulation of focal adhesion assembly
3110057O12Rik	UTR3	3	22.0	yes	
Ms4a4b	UTR3	3	21.0	no	Integral component of plasma membrane
Atp6v1e1	CDS	3	20.1	no	ATP hydrolysis coupled proton transport
Rc3h1	UTR3	1	19.4	yes	mRNA binding, regulation of T cell proliferation
Txnip	UTR3	2	19.3	yes	Regulation of transcription, response to oxidative stress
Srrm2	CDS-UTR3	1	18.4	yes	mRNA processing, RNA splicing
Tceb3	UTR3	1	13.4	yes	Regulation of transcription
Gng5	UTR3	1	13.1	yes	G-protein coupled signalling pathway
Ogt	CDS	7	13.0	yes	Regulation of protein phosphorylation, protein O-linked glycosylation
Mcm6	CDS	3	12.1	yes	DNA replication, cell cycle
Prss16	UTR3	1	11.9	yes	Proteolysis, serine-type peptidase activity

Table 6.9 Potential miR-142a-3p targets
The top 20 chimeric reads for miR-142a-3p, ranked by Mirza score.

Several potential targets were identified for miR-17 and miR-92. These miRNAs are encoded by the same miRNA cluster but have different seed sequences. The miRNAs from this cluster have however been suggested to regulate partly overlapping targets: for example, Pten was shown to be bound by five of the six miRNAs of the miR-17-92 cluster (Wu *et al.*, 2012). However, we could not find this target in our data, nor any other shared targets. We found one TargetScan-predicted target for each miRNA (Nabp1 and Sertad3) and potential novel targets involved in a variety of broad biological processes, such as regulation of transcription, DNA repair, proteolysis, cell metabolism and ribosome formation (Tables 6.10 and 6.11).

Target	Site	Unique reads	Mirza	Seed match?	Gene Annotation
Nabp1	UTR3	1	473.5	yes	DNA repair
Mtf1	UTR3	2	316.2	yes	Regulation of transcription, response to oxidative stress
Oas2	CDS	1	14.8	yes	Immune system process, purine nucleotide biosynthetic process
Ctsa	CDS	1	9.8	yes	Proteolysis involved in cellular catabolic process
Paip1	UTR3	1	2.3	no	Regulation of translation
Mipep	CDS	5	2.3	no	Proteolysis, peptide metabolic process
Tmem30a	UTR3	1	1.6	no	Transmembrane transport

Table 6.10 Potential miR-17-5p targets
Chimeric reads for miR-17-5p, ranked by Mirza score (excluding reads with Mirza score < 1).

Target	Site	Unique reads	Mirza	Seed match?	Gene Annotation
Sertad3	UTR3	1	3174	yes	Regulation of transcription
Mdh1	CDS	1	172.4	yes	Malate dehydrogenase activity, regulation of defense response to virus, citrate cycle (TCA)
Atp5j	UTR5	2	63.4	yes	ATP synthesis coupled proton transport
Atp10a	CDS	2	40.5	yes	Phospholipid transporting ATPase activity
Opa1	CDS	2	11.0	yes	Mitochondrial genome maintenance
Hmgcr	UTR3	3	10.2	yes	Lipid metabolic process, NADPH activity
Baz1b	UTR3	3	6.9	no	Chromatin remodeling, double-strand break repair
Cnot6l	CDS	3	4.5	no	mRNA deadenylation dependent decay
Ptpn22	CDS	6	2.8	yes	Phosphoprotein phosphatase activity, negative regulation of TCR signaling pathway
Gm10036	CDS	1	2.3	no	Ribosomal large subunit assembly
Rpl11	CDS	1	2.3	no	Ribosomal large subunit assembly

Table 6.11 Potential miR-92a-3p targets
Chimeric reads for miR-92a-3p, ranked by Mirza score (excluding reads with Mirza score < 1).

Finally, we looked at the potential targets for the HMW RISC enriched miRNAs miR-210-3p and miR-7a. miR-7a has been shown to target the mTOR signalling pathway in other cells types but has not been studied in T cells (Wang *et al.*, 2013). We only found two potential targets for miR-7a, both of which contained a perfect seed match (Table 6.12). One of these was an uncharacterised gene, whereas the other regulates tRNA synthesis. miR-210-3p has been shown to regulate $CD4^+$ T cell activation and responses to hypoxia by targeting Hif1α in a negative feedback loop. In our data, the only canonical target with a seed site in the 3'UTR was Aebp1 which has no reported role in T cells (Table 6.13). Potential non-canonical targets include the sodium ion transporter Slc9a3r1 (NHERF-1), which has been shown to play an inhibitory role in the formation of the immune synapse upon T cell activation, through linking the cytoskeleton and lipid rafts (Itoh *et al.*, 2014).

Target	Site	Unique reads	Mirza	Seed match?	Gene Annotation
AA474408	UTR3	2	2.4	yes	
Lars2	UTR3	2	1.7	yes	Aminoacyl tRNA biosynthesis

Table 6.12 Potential miR-7a-5p targets
Chimeric reads for miR-7a-5p, ranked by Mirza score (excluding reads with Mirza score < 1).

Target	Site	Unique reads	Mirza	Seed match?	Gene Annotation
Fnbp1	CDS	1	515.9	yes	Endocytosis, vesicle-mediated transport
Wdr12	UTR5	1	263.6	yes	Maturation of 5.8S rRNA
Aebp2	UTR3	2	142.4	yes	Regulation of transcription
Gatad2b	CDS	1	37.7	yes	Regulation of transcription, DNA methylation
Polh	CDS	4	10.2	no	DNA replication, DNA repair
Slc9a3r1	UTR3	6	9.5	no	Sodium ion transport, regulation of signaling pathways
Chtop	UTR3	4	5.1	no	mRNA export from nucleus
Chfr	UTR3	1	4.1	no	Protein polyubiquitionation, mitotic cell cycle
Kif21b	UTR3	2	1.9	no	Microtubule based movement
Prrc2a	CDS	1	1.5	no	Poly(A) protein binding, cell differentiation

Table 6.13 Potential miR-210-3p targets
Chimeric reads for miR-210-3p, ranked by Mirza score (excluding reads with Mirza score < 1)

6.3 Discussion

6.3.1 Generation of CLASH libraries – issues and future considerations

6.3.1.1 Target abundance and reproducibility

We generated CLASH libraries from activated $CD8^+$ T cells with the aim of identifying miRNA targets from chimeric reads. While we successfully isolated Ago-2 bound miRNAs and mRNAs, the main issue faced was a low recovery of chimeric reads. While one experiment yielded around 1,800 unique chimeric reads, the three other experiments only had a few hundred chimeras. This is not unprecedented, with most CLASH experiments producing a low proportion of chimeric reads, at 0.24% for modified iPAR-CLIP, 0.3-1% for qCLASH and ~2% for CLASH and CLEAR-CLIP (Helwak *et al.*, 2013; Grosswendt *et al.*, 2014; Moore *et al.*, 2015; Gay *et al.*, 2018). Since the number of chimeric reads was very low, many interactions were only supported by a single unique chimeric read. Similarly in the modified iPAR-CLIP only 18% of the chimeras were supported by more than a single read (Grosswendt *et al.*, 2014). The low number of chimeras is unlikely to represent a comprehensive view of the interactions that actually occur in the cell. Recovery of only a small proportion of miRNA-target interactions may also account for the poor reproducibility between experiments.

6.3.1.2 HMW RISC chimeric reads

We attempted to enrich for chimeric reads by isolating GW182-bound Ago-2 or size separated HMW RISC associated Ago-2. However, these additional steps resulted in reduced recovery of immunoprecipitated Ago-2, which significantly decreased the amount of starting material for the CLASH protocol. As a result, we ended up with fewer reads obtained from these samples compared to total Ago-2 IPs. From the GW182 IP, we recovered mostly rRNA and very few miRNAs and chimeric reads compared to other samples. This may have been RNA that was associated with GW182, or background noise

from the polyclonal GW182 antibody used for immunoprecipitation, despite attempts to reduce the background by gel purifying the band at the molecular weight of Ago-2. For HMW and LMW RISC Ago-2 IP, again we recovered fewer chimeric reads from these samples compared to total Ago-2 IP. While HMW and LMW RISC Ago-2 IPs had a similar proportion of miRNA reads, HMW Ago-2 IP contained more protein coding reads. Indeed, the number of protein coding reads was comparable between HMW RISC Ago-2 IP and the total Ago-2 IP, with essentially no reads from the LMW RISC IP, indicating that most of the pc mRNAs were contained in the HMW fraction. The number of chimeric reads was also much lower in LMW RISC compared to HMW RISC (~30 unique chimeras compared to ~130 in HMW RISC and ~350 in total Ago-2 IP). This supports the hypothesis that while LMW RISC contains miRNAs, these are predominantly not target-bound.

6.3.1.3 CLASH protocol modifications

While we started with the original CLASH protocol published by Helwak *et al.,* many modifications were made to the protocol to optimise it for our experiments. A key difference was the purification of endogenous Ago-2, instead of a tagged overexpressed protein to favour the recovery of biologically relevant targets. To make the protocol quicker and easier, instead of radioactive labelling of RNA, we used a 3' adaptor conjugated to IR800-dye, similar to one described in ir-CLIP (Zarnegar *et al.*, 2016). This allowed convenient visualisation using an Odyssey CLx scanner. We also used a kit by TriLink for making RNA libraries to speed up this step, enable more reproducibility between samples and reduce the amount of adaptor dimers in our datasets.

In the past few years, many new publications have reported modified protocols with improved HITS-CLIP and CLASH datasets. The following the steps could potentially be modified and significantly affect the outcome of the protocol:

- The first key step is cross-linking RNA to proteins. Cross-linking increased the number of chimeras that were recovered, even though some were found without cross-linking as well (Fig.6.4). Some protocols use chemical cross-linking instead of UV irradiation (Grosswendt *et al.*, 2014). Optimisation of cross-linking conditions may increase the amount of recovered RNA.
- Following the cross-linking, the cells are lysed and Ago-2 is immunoprecipitated on magnetic beads. The beads are washed several times in high-salt and low-salt washes throughout the protocol. The washing steps are crucial since these reduce amount of non-specific RNA that could co-purify. However very stringent washing conditions could lead to a loss of real signal. The washing conditions could therefore potentially be further optimised for maximal recovery of Ago-2 bound RNA.
- The amount of RNase and length of digestion could be adjusted for optimal RNA end trimming to allow ligation of the two ends.
- The yield of chimeric reads was increased in CLEAR-CLIP by optimising the ligation step, thus this may be crucial for recovering more chimeric reads (Moore *et al.*, 2015).
- The next key step after elution from the IP beads, is cutting the Ago-RNA complex from the gel. In HITS-CLIP, Ago bound to mRNAs was suggested to be found further up in the gel compared to miRNA-bound Ago (Chi *et al.*, 2009). We cut the gel around the molecular weight of Ago, as well as a section above it. The WB showed a clear RNA band at the molecular weight of Ago-2, suggesting that by cutting this band we enriched for Ago-bound RNAs. However, these may have been predominantly miRNAs which could saturate the sequencing reads, thus cutting a different section on the gel higher up might be better for enriching for chimeric reads (the same holding true when purifying the PCR products of the libraries prior to sequencing).
- Many of the reads that were recovered following sequencing were ribosomal reads. This may be because some of the targets that are

being bound by Ago were also be bound to ribosomes. HMW RISC has been shown to co-fractionate with ribosomal proteins (Landthaler *et al.*, 2008). Therefore, depletion of ribosomal RNA with commercially available kits may help to reduce unwanted reads focusing on the chimeric reads.

6.3.2 Non-canonical targets

6.3.2.1 Binding without miRNA seed

We evaluated the quality of the chimeric reads by searching for seed matches in the mRNA sequence. 12% of the reads contained a perfect seed match, showing that canonical miRNA targets could be identified with our CLASH protocol. 88% of the reads therefore did not contain a perfect seed match. This could be due to non-canonical binding not involving a perfect seed match, background from miRNA:mRNA pairs formed *ex vivo*, or issues with the bioinformatic analysis. For example, the seed matching site of the mRNA may be lost during the trimming and ligation of the chimeras, though we extended short pc sequences to 55 bp when looking for seed matches.

The chimeric reads that did not contain a perfect seed match may have instead involved imperfect pairing through the seed region and/or binding through the 3' end of the miRNA. This type of non-canonical binding has been widely reported in CLASH experiments. 37% of CLASH chimeric reads from HEK cells had uninterrupted seed pairing, whereas for chimeric reads in *C.elegans* detected by iPAR-CLIP and CLEAR-CLIP chimeras from mouse brain, this proportion was approximately 30% (Helwak *et al.*, 2013; Grosswendt *et al.*, 2014; Moore *et al.*, 2015). Most chimeras however involved some level of binding in the seed region. Both iPAR-CLIP and CLEAR-CLIP reported that 80% interactions involved the seed region when allowing for 1-2 mismatches or bulges (Grosswendt *et al.*, 2014; Moore *et al.*, 2015). In contrast, 46% of qCLASH identified chimeric reads had no recognisable seed-pairing even

when allowing for 2 mismatches (Gay *et al.*, 2018). Non-canonical interactions involving imperfect seed pairing were shown to be functional, however to a lesser extent compared to targets containing perfect seed matches (Helwak *et al.*, 2013; Grosswendt *et al.*, 2014; Moore *et al.*, 2015). Seed interactions were frequently complemented by pairing through the 3' end of the miRNA, both in our data and data published by others. This was shown to stabilise interactions, in particular those involving imperfect seed pairing (Moore *et al.*, 2015; Broughton *et al.*, 2016). Furthermore, this has been suggested to add specificity to miRNA targeting, meaning that members of the same miRNA family containing the same seed could in some cases target a different set of mRNAs based on 3' end pairing. Entirely seedless interactions have been identified for certain miRNAs as well, CLASH chimeras for miR-92a revealed 'seedless binding' involving a 3' motif, which was shown to result in weak target repression (Helwak *et al.*, 2013).

In $CD4^+$ T cells, HITS-CLIP found many non-canonical sites for mi-R-155 (Loeb, A. a. Khan, *et al.*, 2012). 40% of the identified Ago-binding sites did not contain a perfect seed match for miR-155, but were instead enriched for non-canonical sites containing a mismatch in the seed. Again these sites were shown to be functional, though the suppression was not as strong as for canonical sites. Another study examined miR-155 targets in four different immune cell types, including $CD4^+$ T cells, and found cell-type specificity for target suppression (Hsin *et al.*, 2018). Sites with 8mer seed complementarity were more likely to be suppressed in all cells, whereas those with only 6mer complementarity were more repressed in cells with high miR-155 expression. This however did not explain all the cell specific targeting. Approximately 25-45% of miR-155 dependent sites did not have a perfect seed match, and these were more cell type specific. The regulation of these targets was shown to be weaker than canonical targets, but significant repression was shown for several.

6.3.2.2 Binding to the coding region of mRNA

Frequent pairing to the CDS has been detected in both HITS-CLIP and CLASH datasets, with approximately half of the chimeric reads for miRNA:mRNA interactions mapping to the CDS (Loeb, A. a. Khan, *et al.*, 2012; Helwak *et al.*, 2013; Moore *et al.*, 2015; Gay *et al.*, 2018). Similar to this, in our data nearly half of the chimeric reads contained an mRNA CDS. Both seed-matched and non-seed containing chimeric reads involved CDS binding in similar proportions (55% and 45%, respectively). It was previously shown that pairing patterns were similar across different transcript regions such as 3'UTR and CDS (Moore *et al.*, 2015). In many cases binding to CDS has not been shown to lead to efficient target suppression (Loeb, A. A. Khan, *et al.*, 2012; Hsin *et al.*, 2018). It has been suggested that mRNAs with miRNA binding sites in both 3'UTR and CDS were more regulated than those with a site in 3'UTR only (Fang and Rajewsky, 2011). miRNA binding to CDS may therefore work cooperatively with sites in 3'UTRs. CLASH data showed some suppressive function for sites in CDS, though these were weaker than sites in 3'UTR (Helwak *et al.*, 2013). One study suggested that targeting the 3'UTR might be more efficient at causing mRNA degradation, whereas sites in CDS might lead to translational repression (Hausser *et al.*, 2013). This was supported by a recent study that showed 'ribosome stalling' for transcripts containing miRNA binding sites in CDS (K. Zhang *et al.*, 2018). Interestingly, this mode of repression was shown to require only minimal pairing through the miRNA seed region, and instead relied on 3' end pairing (K. Zhang *et al.*, 2018).

Most HITS-CLIP and CLASH experiments therefore support weak but significant suppression for at least a proportion of targets not containing a perfect seed match, and a potential effect for targets in CDS. This has however been challenged by an independent analysis where no significant effect on target mRNAs containing non-canonical sites was found in a thorough analysis of HITS-CLIP and CLASH data (Agarwal *et al.*, 2015). It was confirmed that real interactions can be formed through non-canonical binding, but it was

concluded that this did not cause significant repression of the target. The function of these non-canonical sites therefore remains to be confirmed.

6.3.3 Identification of potential novel miRNA targets

We identified several potential novel targets for miRNAs expressed in $CD8^+$ T cells. We first looked at the miRNA with the most chimeric reads across all experiments: miR-142a-3p. Both strands of miR-142 were expressed, however the majority of chimeric reads were for the more abundant miR-142a-3p. This miRNA has been described to regulate T cell proliferation through targeting of the atypical transcription factors E2f7 and E2f8, and the cell cycle inhibitor Cdkn1b (Sun *et al.*, 2015; Mildner *et al.*, 2017). Furthermore, miR-142 KO in T cells shows dysregulation of several cell cycle associated genes (Sun *et al.*, 2015; Mildner *et al.*, 2017). We also analysed potential targets for miR-17 and miR-92. These miRNAs are well known to target Pten 3'UTR in T cells (Wu *et al.*, 2012). We did not find these previously validated targets for miR-142, miR-17 or miR-92 from our data. This could be due to several reasons: i) a rapidly degraded target mRNA may not be captured ii) the time-point of targeting may be different, for example early in the activation instead of in CTLs iii) the low number of chimeric reads may not give a comprehensive overview of targets. For miR-142, we found some cell cycle associated targets from our data, notably Mki67 and Mcm6. A seed match for these miRNAs was found in the CDS, thus making it more uncertain whether binding leads to suppression of these genes. Other potentially interesting novel targets for miR-142a-3p included Coronin and Roquin-1, both of which could be validated experimentally (Table 6.9).

Finally, we also attempted to identify potential targets for the HMW RISC enriched miRNAs miR-7a an miR-210. Both these miRNAs were amongst those with most chimeric reads (Table 6.3). Other HMW enriched miRNAs, such as the let-7 family members and miR-378a miRNAs also appeared amongst these miRNAs, despite downregulated expression in activated T

cells. This supports our hypothesis that less abundant miRNAs could be actively suppressing their targets when in HMW RISC. Unfortunately, most of the targets identified for miR-7a and miR-210 had low predicted binding energy, making it unlikely that these are real interactions, or that the binding would cause target suppression. We did however identify some potential canonical and non-canonical targets that could be further validated (Tables 6.12 and 6.13).

The bioinformatic tools used in our study aid in short-listing miRNA:mRNA target pairs that are already predicted TargetScan targets or are likely to be true targets due to a perfect seed match or a high binding energy predicted by Mirza. This gives an overview of potential novel miRNA targets. However, true confirmation of an interaction would require experimental validation, such as overexpression or knock-down of a specific miRNA, and measurements of target suppression through reporter assays, qPCR and western blotting. Of interest, it has recently been suggested that miRNA targeting may be even more subtle than previously thought, based on the observation that individual variation between mice was shown to be stronger than the repressive effect of a miRNA on a target gene (Pinzón et al., 2017). It was concluded that this level of regulation would not be robust enough to affect gene function, and that miRNA effects may consequently be due to repression of a few dose-sensitive genes rather than global downregulation of all its potential targets (Pinzón et al., 2017; Seitz, 2017). Therefore, in addition to confirming miRNA binding to the target, it is important to investigate the biological effects of disrupting this interaction. It was however also noted that since many genes contain multiple miRNA binding sites, the collective effect of these may have a more notable effect, with such cooperativity previously described for many miRNAs (Grimson et al., 2007). Accurate detection of biologically important miRNA targets therefore remains a challenge, but CLASH-based methods have the potential to improve our understanding of this.

7.1 The role of miRNAs and HMW RISC in T cell activation

We set out to study the role of miRNAs in $CD8^+$ T cell activation. To get a global understanding of miRNA function, we measured miRNA expression in naive and activated cells T cells, studied the formation of RISC upon T cell activation, analysed differential association of miRNAs with HMW and LMW RISC and finally attempted to identify miRNA targets using CLASH.

T cell activation induces dramatic changes in the expression of miRNAs and RISC-associated proteins. Our results showed that miRNA expression changes dynamically during cell activation, in response to the strength of the activating signal and the cytokines influencing cell differentiation. In addition to this, the expression of the Ago-interacting protein GW182 increased upon activation leading to the formation of HMW RISC. We showed that just under half of Ago-2 was found in a complex with GW182, whereas the rest remained unbound. The GW182 associated Ago-2 in the HMW RISC could be separated from Ago-2 in LMW RISC following size exclusion chromatography.

When we sequenced HMW and LMW RISC associated miRNAs, we found many that were differentially distributed between the two complexes. Abundant miRNAs were mostly found in both complexes to some extent, though some were very strongly enriched in the HMW RISC. While many downregulated miRNAs were found enriched in LMW RISC, some miRNA families, such as the let-7 family and miR-378 family, were enriched in HMW RISC. We examined further the function of one specific miRNA that was enriched in HMW RISC, miR-7a. This miRNA was shown to be upregulated upon T cell activation and its inhibition caused changes in the T cell activation phenotype, with reduced cell proliferation and increased expression of activation markers. miR-7 has been shown to target components of the mTOR pathway in cancer cells, thus it is interesting to speculate that it may also target this pathway in T cells. We attempted to identify miRNA targets using CLASH. Efforts to enrich for

chimeric reads by isolating GW182 bound or HMW RISC associated Ago-2 were not successful compared to immunoprecipitating total Ago-2. Despite technical challenges, we identified several potential novel miRNA targets which could be experimentally validated in the future.

miRNA expression levels are commonly thought to reflect the functional capacity of a miRNA in a given cell context. However, despite high expression levels of miRNAs in naive T cells, the lack of GW182 may limit the formation of HMW RISC and efficient target suppression. Genetic studies of T cells deficient in Dicer or Ago-2 have shown that while naive cells display no abnormalities, activation of the cells results in aberrant differentiation and proliferation (Zhang and Bevan, 2010; Bronevetsky *et al.*, 2013). This suggests that miRNAs may play a key role at the early stages of activation when GW182 is first expressed. T cell activation requires rapid remodelling of the miRNA repertoire to support cellular changes guiding effector cell differentiation. In $CD4^+$ T cells global downregulation of miRNAs and Ago proteins was suggested to allow fast turnover of RISC upon activation (Bronevetsky and Ansel, 2013; Bronevetsky *et al.*, 2013). While we saw only slight downregulation of Ago upon activation, changes in RISC formation occurred due to increased expression of GW182. Recruitment of miRNAs to HMW RISC would allow activation-promoting miRNAs to be rapidly employed, while other miRNAs (whose targets are required for activation) may be sequestered in LMW RISC. We can speculate that distribution of miRNAs between these two complexes alongside expression changes could be an additional layer of regulation, particularly for less abundant miRNAs. miRNA expression did not directly correlate with association in HMW versus LMW RISC, though the tendency was for low abundance miRNAs that are downregulated upon activation to be present in LMW RISC. The enrichment of specific miRNAs and miRNA families in HMW RISC opens up the question of whether specificity exists in miRNA recruitment to this complex. It is not currently understood whether competition exists between miRNAs for binding HMW RISC, or how this would be regulated. While we and others (La Rocca *et al.*, 2015) noted

clear significant differences in miRNA association with the two complexes, it remains to be proven how important these differences are for miRNA biological function.

7.2 Future work

Several open questions remain in regards to the function, composition and recruitment of miRNAs to HMW RISC. We identified a range of intermediate MW RISC complexes from activated T cells, and it would be interesting to determine the exact protein composition of these complexes and whether they represent precursors of HMW RISC or separate entities. It is possible that these may promote miRNA target suppression through mechanisms that do not involve GW182, such as repression of translational elongation, which have been described in other cell types (Wu, Isaji and Carthew, 2013; K. Zhang *et al.*, 2018). The observation that miRNAs are differentially associated with HMW and LMW RISC opens up the possibility that miRNA recruitment to these is somehow regulated and not the same for each miRNA. More work is needed to understand the potential mechanisms that could underpin this. Active recruitment could involve miRNA modifications affecting their localisation or Ago-binding, whereas target availability may passively influence HMW RISC formation.

We identified miR-7a as a miRNA that is enriched in HMW RISC and showed preliminary results suggesting it may regulate T cell activation. In particular, T cell proliferation and expression of activation markers were affected by a miR-7a inhibitor. Further experiments are needed to understand the function of miR-7a in T cells in regard to its effect on the expression of transcription factors, cell cycle genes and effector molecules. In cancer cells, miR-7a has been shown to target components of the mTOR pathway, making this an interesting possibility to explore in T cells. Apart from miR-7a, we identified several other HMW RISC enriched miRNAs that have not been well characterised in $CD8^+$ T cells. For example, miR-210-3p plays a role in hypoxia and Th17 differentiation in $CD4^+$ T cells but has not been studied in detail in

$CD8^+$ T cells (Wang *et al.*, 2014). Furthermore, we identified several miRNAs that were downregulated but enriched in HMW RISC, such as the let-7 family and miR-378 family. It is interesting to speculate that these miRNAs may therefore be functional in activated T cells. La Rocca *et al.* also showed that the let-7 miRNA family is downregulated but enriched in HMW RISC in activated T cells, and additionally showed that this led to more efficient suppression of a target reporter in activated cells (La Rocca *et al.*, 2015). The miR-378 family has not been reported to play a role in T cells and it would be interesting to understand its function in naive and activated cells.

miR-7a, mR-210-3p, let-7 and miR-378 were also amongst the miRNAs with the most chimeric reads in CLASH data, supporting the idea that presence in HMW RISC translates to high rate of target association. However, for many of these we did not enrich for seed-matched targets and probably did not capture the real range of targets for these miRNAs. A poor recovery of chimeric reads was the main issue with the CLASH experiments and the protocol therefore requires further optimisation to increase the proportion of these, as discussed in Chapter 6. We attempted to bioinformatically validate the identified CLASH targets by searching for miRNA seed sites and TargetScan predicted targets, and by calculating binding energies for non-canonical targets with Mirza. While this allowed us to short-list high-confidence targets, this does not confirm the repression of these targets or prove the biological importance of the interactions. In particular the repression of non-canonical sites has been controversial and requires experimental validation. Target validation could be done globally by mRNA sequencing and/or proteomics to compare the levels of miRNA-targeted and non-targeted genes. For targets of individual miRNAs, inhibition or knock-down of the miRNA can be used to assess effects on mRNA and protein levels of potential targets.

7.3 Therapeutic implications

Understanding miRNA function and targets in $CD8^+$ T cells could have wide-ranging implications for health and disease. miRNAs are important players in various human pathologies: their dysregulation is frequent in cancer and in immunological, cardiovascular and infectious diseases. Increased understanding of miRNA function in these disorders has led to a surge in interest in the development of miRNA-based therapeutics, including miRNA inhibitors and miRNA mimic replacements. miRNAs are appealing therapeutic targets in many aspects due to their ability to target many components of a pathway with subtle effects on the individual proteins. However, the mode of function of miRNAs also poses additional challenges for therapeutic implication. The potential to target many different genes may cause unwanted or unexpected effects and redundancy between different miRNAs may allow for members of the same miRNA family to compensate for the loss of each other (Li and Rana, 2014). Technically, ensuring the stability, targeted delivery and efficient uptake of miRNAs into different tissues is not straight-forward (Kaczmarek, Kowalski and Anderson, 2017). Despite these challenges, the miR-122 inhibitor miravirsen, the first miRNA-based drug currently in clinical trials, has shown great promise for the treatment of HCV infection in Phase II trials (Janssen *et al.*, 2013). Since miRNAs are known to play key roles in the development and pathology of immune-based diseases including multiple sclerosis, type I diabetes and allergic diseases, these could be potential targets of future treatments (Luck, Muljo and Collins, 2015; Garo and Murugaiyan, 2016). However no approaches to target immune cells have yet advanced to clinical trials, with most drugs currently in pre-clinical trials aimed towards treating cancer or cardiovascular disease (Chakraborty *et al.*, 2017).

When developing miRNA-based drugs, it is crucial to know the exact targets of these miRNAs to prevent unwanted side-effects. miRNAs are frequently expressed by multiple cell types and may have cell-specific targets in these (Hsin *et al.*, 2018). Many miRNAs are expressed by both cells of the immune system and by cancer cells and could have opposing roles in each. For

example, miR-362 has been found elevated in multiple sclerosis and type I diabetes patients, with expression correlating with disease severity (Du *et al.*, 2009; Sebastiani *et al.*, 2011). Inhibition of miR-362 was shown to reduce Th17 mediated pathology in the mouse model EAE, whereas overexpression exacerbated disease by increased targeting of Ets-1. However, miR-362 was also shown to play a tumour suppressive role in malignant glioma by targeting Nob1 (Zhou *et al.*, 2013). Therefore, when considering targeting miR-362 for treating autoimmune diseases, the risk for potentially increased oncogenesis must be taken into account. In addition to the application of miRNA-targeting therapies for treating autoimmune diseases, miRNAs may have the potential to enhance T-cell based cancer immunotherapy. TCR engineered or chimeric antigen receptor (CAR) T cells hold a lot of promise for future cancer treatment. CD19 CAR T cell therapy has been successfully used to treat patients with B cell lymphoma or leukaemia. T cell therapy has however not yet been effectively applied for solid tumours. Key miRNAs could be targeted to enhance TCR sensitivity, and to improve T cell persistence and effector function against cancer cells (Ji, Hocker and Gattinoni, 2016; Z. Zhang *et al.*, 2018). Strikingly, co-transfection of CAR T cells with miR-17~92 was shown to improve anti-tumour responses against glioblastoma in mice with human xenographs (Ohno *et al.*, 2013). Furthermore, miRNA-based therapeutics may be used in combination with existing strategies. Overexpression of miR-153 in colon cancer cells was shown to improve CAR T cell mediated killing, in support of combining treatments (Q. Huang *et al.*, 2018). To start applying these novel therapeutic approaches to treating human disease, a deep understanding of the precise roles and targets of miRNAs in T cells is vital.

VII. Bibliography

Acuto, O., Bartolo, V. Di and Michel, F. (2008) 'Tailoring T-cell receptor signals by proximal negative feedback mechanisms', *Nature Reviews Immunology*, 8(9), pp. 699–712.

Agarwal, V. *et al.* (2015) 'Predicting effective microRNA target sites in mammalian mRNAs', *eLife*, 4, pp. 1–38.

Almanza, G. *et al.* (2010) 'Selected microRNAs define cell fate determination of murine central memory CD8 T cells', *PLoS ONE*, 5(6), pp. 1–10.

Ameres, S. L. and Zamore, P. D. (2013) 'Diversifying microRNA sequence and function', *Nature Reviews Molecular Cell Biology*. Nature Publishing Group, 14(8), pp. 475–488.

Araki, K. *et al.* (2009) 'mTOR regulates memory CD8 T cell differentiation', *Nature*, 460(7251), pp. 108–112.

Arvey, A. *et al.* (2010) 'Target mRNA abundance dilutes microRNA and siRNA activity', *Molecular Systems Biology*. Nature Publishing Group, 6(363), pp. 1–7.

Azzam, H. S. *et al.* (1998) 'CD5 Expression Is Developmentally Regulated By T Cell Receptor (TCR) Signals and TCR Avidity', *The Journal of Experimental Medicine*, 188(12), pp. 2301–2311.

Balagopalan, L., Coussens, N. P. and Sherman, E. (2010) 'The LAT Story : A Tale of Cooperativity ', *Cold Spring Harbor Perspectives in Biology*.

Ban, Y. H. *et al.* (2017) 'miR-150-Mediated Foxo1 Regulation Programs CD8 + T Cell Differentiation', *CellReports*, 20(11), pp. 2598–2611.

Banerjee, A. *et al.* (2010) ' Cutting Edge: The Transcription Factor Eomesodermin Enables CD8 + T Cells To Compete for the Memory Cell Niche ', *The Journal of Immunology*, 185(9), pp. 4988–4992.

Basu, R. and Huse, M. (2015) 'Mechanical communication at the immunological synapse', *Trends in Cell Biology*, 27(4), pp. 241-254.

Behm-Ansmant, I. *et al.* (2006) 'mRNA degradation by miRNAs and GW182 requires both CCR4 : NOT deadenylase and DCP1 : DCP2 decapping complexes', *Genes & Development*, 20, pp. 1885-1898.

Bernstein, E. *et al.* (2003) 'Dicer is essential for mouse development', *Nature Genetics*, 35(3), pp. 215–217.

Bertossi, A. *et al.* (2011) 'Loss of Roquin induces early death and immune deregulation but not autoimmunity.', *The Journal of experimental medicine*, 208(9), pp. 1749–56.

Bhattacharyya, S. N. *et al.* (2006) 'Relief of microRNA-Mediated Translational Repression in Human Cells Subjected to Stress', *Cell*, 125(6), pp. 1111–1124.

Boldin, M. P. and Baltimore, D. (2012) 'MicroRNAs, new effectors and regulators of NF-κB', *Immunological Reviews*, 246(1), pp. 205–220.

Boomer, J. S. and Green, J. M. (2010) 'An enigmatic tail of CD28 signaling.', *Cold Spring Harbor perspectives in biology*, 2(8).

Bridge, K. S. *et al.* (2017) 'Argonaute Utilization for miRNA Silencing Is Determined by

Phosphorylation-Dependent Recruitment of LIM-Domain-Containing Proteins', *Cell Reports*, 20(1), pp. 173–187.

Bronevetsky, Y. *et al.* (2013) 'T cell activation induces proteasomal degradation of Argonaute and rapid remodeling of the microRNA repertoire.', *The Journal of experimental medicine*, 210(2), pp. 417–32.

Bronevetsky, Y. and Ansel, K. M. (2013) 'Regulation of miRNA biogenesis and turnover in the immune system', *Immunological Reviews*, 253(1), pp. 304–316.

Broughton, J. P. *et al.* (2016) 'Pairing beyond the Seed Supports MicroRNA Targeting Specificity', *Molecular Cell*, 64(2), pp. 320–333.

Broughton, J. P. and Pasquinelli, A. E. (2016) 'A tale of two sequences: microRNA-target chimeric reads', *Genetics Selection Evolution*, 48:31.

Brownlie, R. J. and Zamoyska, R. (2013) 'T cell receptor signalling networks: branched, diversified and bounded.', *Nature reviews. Immunology*. Nature Publishing Group, 13(4), pp. 257–69.

Bushnell, B., Rood, J. and Singer, E. (2017) 'BBMerge – Accurate paired shotgun read merging via overlap', *PLoS ONE*, 12(10), pp. 1–15.

Carissimi, C. *et al.* (2014) 'MiR-21 is a negative modulator of T-cell activation', *Biochimie*, 107, pp. 319–326.

Castilla-Llorente, V. *et al.* (2012) 'Mammalian GW220/TNGW1 is essential for the formation of GW/P bodies containing miRISC', *Journal of Cell Biology*, 198(4), pp. 529–544.

Chakraborty, C. *et al.* (2017) 'Therapeutic miRNA and siRNA: Moving from Bench to Clinic as Next Generation Medicine', *Molecular Therapy - Nucleic Acids*, 8, pp. 132–143.

Chandran, P. A. *et al.* (2014) ' The TGF-β-inducible miR-23a cluster attenuates IFN-γ levels and antigen-specific cytotoxicity in human CD8 + T cells ', *Journal of Leukocyte Biology*, 96(4), pp. 633–645.

Chang, J. T. *et al.* (2007) 'Asymmetric T Lymphocyte Division in the Initiation of Adaptive Immune Responses', *Science*, 315(5819), pp. 1687–1691.

Chang, P.-P. *et al.* (2012) ' Breakdown in Repression of IFN-γ mRNA Leads to Accumulation of Self-Reactive Effector CD8 + T Cells ', *The Journal of Immunology*, 189(2), pp. 701–710.

Chang, T.-C. *et al.* (2008) 'Widespread microRNA repression by Myc contributes to tumorigenesis', *Nature Genetics* 40(1), pp. 43–50.

Chen, J. *et al.* (2013) 'Posttranscriptional Gene Regulation of IL-17 by the RNA-Binding Protein HuR Is Required for Initiation of Experimental Autoimmune Encephalomyelitis', *The Journal of Immunology*, 191(11), pp. 5441–5450.

Chen, Z. *et al.* (2017) 'miR-150 Regulates Memory CD8 T Cell Differentiation via c-Myb Article miR-150 Regulates Memory CD8 T Cell Differentiation via c-Myb', *Cell Reports* 20 pp. 2584–2597.

Chi, H. (2012) 'Regulation and function of mTOR signalling in T cell fate decisions', *Nature Reviews Immunology*. Nature Publishing Group, 12(5), pp. 325–338.

Chi, S. W. *et al.* (2009) 'Argonaute HITS-CLIP decodes microRNA-mRNA interaction maps.', *Nature*, 460(7254), pp. 479–486.

Chi, S. W., Hannon, G. J. and Darnell, R. B. (2012) 'An alternative mode of microRNA target recognition', *Nature Structural & Molecular Biology*, 19(3), pp. 321–327.

Cho, J. H. and Sprent, J. (2018) 'TCR tuning of T cell subsets', *Immunological Reviews*, 283(1), pp. 129–137.

Cobb, B. S. *et al.* (2006) 'A role for Dicer in immune regulation.', *The Journal of experimental medicine*, 203(11), pp. 2519–2527.

Courtney, A. H., Lo, W. L. and Weiss, A. (2018) 'TCR Signaling: Mechanisms of Initiation and Propagation', *Trends in Biochemical Sciences*, 43(2), pp. 108–123.

Couture, C. *et al.* (1996) 'Regulation of the Lck SH2 domain by tyrosine phosphorylation', *Journal of Biological Chemistry*, 271(40), pp. 24880–24884.

Curtsinger, J. M. *et al.* (1999) 'Inflammatory cytokines provide a third signal for activation of naive CD4+ and CD8+ T cells.', *Journal of immunology*, 162(6), pp. 3256–62.

Dario A. A. Vignali, L. W. C. and C. J. W. (2008) 'How regulatory T cells work', *Nat rev immunol*, 8(7), pp. 523–532.

Davey, B. G. M. *et al.* (1998) 'Preselection Thymocytes Are More Sensitive to T Cell Receptor Stimulation Than Mature T Cells', *Journal of Experimental Medicine*, 188(10), pp. 1867-74.

Davis, M. M. *et al.* (2002) 'Ligand Recognition By Aβ T Cell Receptors', *Annual Review of Immunology*, 16(1), pp. 523–544.

Davis, S. J. and van der Merwe, P. A. (2006) 'The kinetic-segregation model: TCR triggering and beyond', *Nature Immunology*, 7(8), pp. 803–809.

Dong, S. *et al.* (2006) 'T cell receptor for antigen induces linker for activation of T cell–dependent activation of a negative signaling complex involving Dok-2, SHIP-1, and Grb-2', *The Journal of Experimental Medicine*, 203(11), pp. 2509–2518.

Du, C. *et al.* (2009) 'MicroRNA miR-326 regulates T H -17 differentiation and is associated with the pathogenesis of multiple sclerosis', *Nature Immunology*, 10(12), pp. 1252–1259.

Dudda, J. C. *et al.* (2013) 'MicroRNA-155 is required for effector CD8+ t cell responses to virus infection and cancer', *Immunity*, 38(4), pp. 742–753.

Ebert, P. J. R. *et al.* (2009) 'An endogenous positively selecting peptide enhances mature T cell responses and becomes an autoantigen in the absence of microRNA miR-181a.', *Nature immunology*, 10(11), pp. 1162–1169.

Elkayam, E. *et al.* (2017) 'Multivalent Recruitment of Human Argonaute by GW182', *Molecular Cell*, 67(4), pp. 646-658.

Essig, K. *et al.* (2017) 'Roquin Suppresses the PI3K-mTOR Signaling Pathway to Inhibit T Helper Cell Differentiation and Conversion of Treg to Tfr Cells', *Immunity*, 47(6), pp. 1067-1082.

Eulalio, A., Huntzinger, E. and Izaurralde, E. (2008) 'GW182 interaction with Argonaute is essential for miRNA-mediated translational repression and mRNA decay.', *Nature structural & molecular biology*, 15(4), pp. 346–353.

Fabian, M. R. and Sonenberg, N. (2012) 'The mechanics of miRNA-mediated gene silencing: A look under the hood of miRISC', *Nature Structural and Molecular Biology*, 19(6), pp. 586–593.

Fang, Y. *et al.* (2011) 'MicroRNA-7 Inhibits Tumor Growth and Metastasis by Targeting the Phosphoinositide 3-Kinase/Akt Pathway in Hepatocellular Carcinoma', (2010), pp. 1852–1862.

Fang, Z. and Rajewsky, N. (2011) 'The impact of miRNA target sites in coding sequences and in 3'UTRs', *PLoS ONE*, 6(3), pp. 1–6.

Finlay, D. and Cantrell, D. a (2011) 'Metabolism, migration and memory in cytotoxic T cells.', *Nature reviews. Immunology*, 11(2), pp. 109–117.

Florczyk, U. *et al.* (2015) 'The Role of miR-378a in Metabolism, Angiogenesis, and Muscle Biology', *International Journal of Endocrinology*, 2015, pp. 1–13.

Flores, O. *et al.* (2014) 'Differential RISC association of endogenous human microRNAs predicts their inhibitory potential', *Nucleic Acids Research*, 42(7), pp. 4629–4639.

Frankish, A. *et al.* (2019) 'GENCODE reference annotation for the human and mouse genomes', *Nucleic Acids Research*, 47(D1), pp. D766–D773.

Garo, L. P. and Murugaiyan, G. (2016) 'Contribution of MicroRNAs to autoimmune diseases', *Cellular and Molecular Life Sciences*, 73(10), pp. 2041–2051.

Gaud, G., Lesourne, R. and Love, P. E. (2018) 'Regulatory mechanisms in T cell receptor signalling', *Nature Reviews Immunology*, 18(8), pp. 485–497.

Gay, L. A. *et al.* (2018) 'Modified Cross-Linking, Ligation, and Sequencing of Hybrids (qCLASH) Identifies Kaposi's Sarcoma-Associated Herpesvirus MicroRNA Targets in Endothelial Cells', 92(8), pp. 1–21.

Gebert, L. F. R. and MacRae, I. J. (2019) 'Regulation of microRNA function in animals', *Nature Reviews Molecular Cell Biology*, 20(1), pp. 21–37.

Gerlach, C. *et al.* (2016) 'The Chemokine Receptor CX3CR1 Defines Three Antigen-Experienced CD8 T Cell Subsets with Distinct Roles in Immune Surveillance and Homeostasis', *Immunity*, 45(6), pp. 1270–1284.

Golden, R. J. *et al.* (2017) 'An Argonaute phosphorylation cycle promotes microRNA-mediated silencing', *Nature*, 542(7640), pp. 197–202.

Goodnow, C. C. (2007) 'Multistep Pathogenesis of Autoimmune Disease', *Cell*, 130(1), pp. 25–35.

Gracias, D. T. *et al.* (2013) 'The microRNA miR-155 controls CD8(+) T cell responses by regulating interferon signaling.', *Nature immunology*, 14(6), pp. 593–602.

Grimson, A. *et al.* (2007) 'MicroRNA Targeting Specificity in Mammals: Determinants beyond Seed Pairing', *Molecular Cell*, 27(1), pp. 91–105.

Grosswendt, S. *et al.* (2014) 'Unambiguous Identification of miRNA:target site Interactions by Different Types of Ligation Reactions', *Molecular Cell*, 54(6), pp. 1042–1054.

Guan, T. *et al.* (2018) 'ZEB1, ZEB2, and the miR-200 family form a counterregulatory network to regulate CD8+T cell fates.', *The Journal of experimental medicine*, 215(4), pp.1153-1168.

Gutiérrez-Vázquez, C. *et al.* (2017) '3′ Uridylation controls mature microRNA turnover during CD4 T-cell activation', *Rna*, 23(6), pp. 882–891.

Hafner, M. *et al.* (2010) 'Transcriptome-wide Identification of RNA-Binding Protein and

MicroRNA Target Sites by PAR-CLIP', *Cell*, 141(1), pp. 129–141.

Hart, M. *et al.* (2019) 'miR-34a: a new player in the regulation of T cell function by modulation of NF-κB signaling', *Cell Death and Disease*, 10(2), pp. 1–14.

Haseeb, A. *et al.* (2017) 'Deep sequencing and analyses of miRNAs, isomiRs and miRNA induced silencing complex (miRISC)-associated miRNome in primary human chondrocytes', *Scientific Reports*, 7(1), pp. 1–10.

Hausser, J. *et al.* (2013) 'Analysis of CDS-located miRNA target sites suggests that they can effectively inhibit translation', *Genome Research*, 23(4), pp. 604–615.

He, J. *et al.* (2013) 'Direct cytosolic delivery of polar cargo to cells by spontaneous membrane-translocating peptides', *Journal of Biological Chemistry*, 288(41), pp. 29974–29986.

He, W. *et al.* (2017) 'MiR-21 is required for anti-tumor immune response in mice: An implication for its bi-directional roles', *Oncogene*, 36(29), pp. 4212–4223.

Helwak, A. *et al.* (2013) 'Mapping the human miRNA interactome by CLASH reveals frequent noncanonical binding', *Cell*, 153(3), pp. 654–665.

Helwak, A. and Tollervey, D. (2014) 'Mapping the miRNA interactome by cross-linking ligation and sequencing of hybrids (CLASH)', *Nature Protocols*, 9(3), pp. 711–728.

Hermiston, M. L., Xu, Z. and Weiss, A. (2003) 'CD45: A Critical Regulator of Signaling Thresholds in Immune Cells', *Annual Review of Immunology*, 21(1), pp. 107–137.

Hirahara, K. and Nakayama, T. (2016) 'CD4+ T-cell subsets in inflammatory diseases: Beyond the Th1/Th2 paradigm', *International Immunology*, 28(4), pp. 163–171.

Höck, J. *et al.* (2007) 'Proteomic and functional analysis of Argonaute-containing mRNA-protein complexes in human cells.', *EMBO reports*, 8(11), pp. 1052–60.

Hogquist, K. A. *et al.* (1994) 'T Cell Receptor Antagonist Peptides Induce Positive Selection', *Cell* 76, pp. 17-27.

Horman, S. R. *et al.* (2013) 'Akt-mediated phosphorylation of argonaute 2 downregulates cleavage and upregulates translational repression of MicroRNA targets', *Molecular Cell*, 50(3), pp. 356–367.

Howden, A. et al. (2019) 'Quantitative analysis of T cell proteomes and environmental sensors during T cell differentiation', *Nature Immunology* 20, pp. 1542-1554.

Hsin, J.-P. *et al.* (2018) 'The effect of cellular context on miR-155-mediated gene regulation in four major immune cell types', *Nature Immunology*, 19, pp.1137-45.

Huang, D. W., Sherman, B. T. and Lempicki, R. A. (2009) 'Systematic and integrative analysis of large gene lists using DAVID bioinformatics resources', *Nature Protocols*, 4(1), pp. 44–57.

Huang, L. *et al.* (2018) 'Role of miR-449a in the Activation and Metabolism of CD4+ Tcells', *Transplantation Proceedings,* 50, pp. 1519–1524.

Huang, Q. *et al.* (2018) 'MiR-153 suppresses IDO1 expression and enhances CAR T cell immunotherapy', *Journal of Hematology and Oncology*, 11(58).

Huppertz, I. *et al.* (2014) 'iCLIP: Protein-RNA interactions at nucleotide resolution', *Methods*, 65(3), pp. 274–287.

Hwang, H. W. *et al.* (2016) 'PAPERCLIP Identifies MicroRNA Targets and a Role of CstF64/64tau in Promoting Non-canonical poly(A) Site Usage', *Cell Reports*, 15(2), pp. 423–435.

Hyeon, H. K. *et al.* (2009) 'HuR recruits let-7/RISC to repress c-Myc expression', *Genes and Development*, 23(15), pp. 1743–1748.

Itoh, K. *et al.* (2014) 'Cutting Edge: Negative Regulation of Immune Synapse Formation by Anchoring Lipid Raft to Cytoskeleton Through Cbp-EBP50-ERM Assembly', *The Journal of Immunology*, 168(2), pp. 541–544.

Iwasaki, S. *et al.* (2010) 'Hsc70/Hsp90 chaperone machinery mediates ATP-dependent RISC loading of small RNA duplexes', *Molecular Cell*, 39(2), pp. 292–299.

Jameson, S. C. and Masopust, D. (2018) 'Understanding Subset Diversity in T Cell Memory', *Immunity* 48, pp.214-226.

Janas, M.M. et al. (2012) 'Reduced Expression of Ribosomal Proteins Relieves MicroRNA-Mediated Repression', *Molecular Cell* 46, pp. 171-186.

'Janeway's Immunbiology', Murphy, K. *et al*. (2012). 8th Edition.

Janssen, H. L. A. *et al.* (2013) 'Treatment of HCV infection by targeting microRNA', *New England Journal of Medicine*, 368(18), pp. 1685–1694.

Jenkins, M. K. and Johnson, J. G. (1993) 'Molecules involved in T-cell costimulation', *Current Opinion in Immunology*, 5(3), pp. 361–367.

Ji, Y. *et al.* (2015) 'miR-155 augments CD8+ T-cell antitumour activity in lymphoreplete hosts by enhancing responsiveness to homeostatic γc cytokines', 112(2), pp.476-481.

Ji, Y. *et al.* (2019) 'miR-155 harnesses Phf19 to potentiate cancer immunotherapy through epigenetic reprogramming of CD8 + T cell fate', *Nature Communications*, 10(1), pp. 1–12.

Ji, Y., Hocker, J. D. and Gattinoni, L. (2016) 'Enhancing adoptive T cell immunotherapy with microRNA therapeutics', *Seminars in Immunology*, 28(1), pp. 45–53.

Jindra, P. T. *et al.* (2010) 'Costimulation-dependent expression of microRNA-214 increases the ability of T cells to proliferate by targeting Pten.', *Journal of immunology*, 185(2), pp. 990–7.

Joshi, N. S. *et al.* (2007) 'Inflammation Directs Memory Precursor and Short-Lived Effector CD8+ T Cell Fates via the Graded Expression of T-bet Transcription Factor', *Immunity*, 27(2), pp. 281–295.

Kaczmarek, J. C., Kowalski, P. S. and Anderson, D. G. (2017) 'Advances in the delivery of RNA therapeutics: From concept to clinical reality', *Genome Medicine*, 9(1), pp. 1–16.

Kaech, S. M. *et al.* (2003) 'Selective expression of the interleukin 7 receptor identifies effector CD8 T cells that give rise to long-lived memory cells', *Nature Immunology*, 4(12), pp. 1191–1198.

Kaech, S. M. and Cui, W. (2012) 'Transcriptional control of effector and memory CD8+ T cell differentiation', *Nature Reviews Immunology*, 12(11), pp. 749–761.

Kästle, M. *et al.* (2017) 'De novo phosphorylation and conformational opening of the tyrosine kinase Lck act in concert to initiate T cell receptor signaling', *Science Signaling*, 10(462).

Kedde, M. *et al.* (2007) 'RNA-Binding Protein Dnd1 Inhibits MicroRNA Access to Target mRNA', *Cell*, 131(7), pp. 1273–1286.

Khan, A. a. *et al.* (2013) 'MicroRNA-17~92 regulates effector and memory CD8 T-cell fates by modulating proliferation in response to infections.', *Blood*, 121(22), pp. 4473–4483.

Khorshid, M. *et al.* (2013) 'A biophysical miRNA-mRNA interaction model infers canonical and noncanonical targets', *Nature Methods*, 10(3), pp. 253–255.

Kim, T. D. *et al.* (2017) 'MicroRNA-150 modulates intracellular Ca 2+ levels in naïve CD8+ T cells by targeting TMEM20', *Scientific Reports*, 7(1), pp. 1–13.

King, I. N. *et al.* (2014) 'The RNA-binding protein TDP-43 selectively disrupts MicroRNA-1/206 incorporation into the RNA-induced silencing complex', *Journal of Biological Chemistry*, 289(20), pp. 14263–14271.

Kleaveland, B. *et al.* (2018) 'A Network of Noncoding Regulatory RNAs Acts in the Mammalian Brain', *Cell*, 174(2), pp. 350-362.

Klein, L. *et al.* (2014) 'Positive and negative selection of the T cell repertoire: what thymocytes see and don't see', *Nature Reviews Immunology*, 14,(6) pp. 377–391.

König, J. *et al.* (2010) 'ICLIP reveals the function of hnRNP particles in splicing at individual nucleotide resolution', *Nature Structural and Molecular Biology*, 17(7), pp. 909–915.

Kozomara, A., Birgaoanu, M. and Griffiths-Jones, S. (2019) 'MiRBase: From microRNA sequences to function', *Nucleic Acids Research*, 47(D1), pp. D155–D162.

Krol, J., Loedige, I. and Filipowicz, W. (2010) 'The widespread regulation of microRNA biogenesis, function and decay', *Nature Reviews Genetics*, 11(9), pp. 597–610.

Kudla, G. *et al.* (2011) 'Cross-linking, ligation, and sequencing of hybrids reveals RNA-RNA interactions in yeast.', *Proceedings of the National Academy of Sciences of the United States of America*, 108(24), pp. 10010–10015.

Kuhn, D. E. *et al.* (2008) 'Experimental validation of miRNA targets', *Methods*, 44(1), pp. 47–54.

La Rocca, G. *et al.* (2015) 'In vivo, Argonaute-bound microRNAs exist predominantly in a reservoir of low molecular weight complexes not associated with mRNA', *Proceedings of the National Academy of Sciences*, 112(3), pp.767-772.

Lai, M. and Xiao, C. (2015) 'International Immunopharmacology Functional interactions among members of the miR-17 – 92 cluster in lymphocyte development , differentiation and malignant transformation', *International Immunopharmacology*, 28(2), pp. 854–858.

Landthaler, M. *et al.* (2008) 'Molecular characterization of human Argonaute-containing ribonucleoprotein complexes and their bound target mRNAs.', *RNA*, 14(12), pp. 2580–96.

Langmead, B. and Salzberg, S. L. (2012) 'Fast gapped-read alignment with Bowtie 2', *Nature Methods*, 9(4), pp. 357–359.

Lazzaretti, D., Tournier, I. and Izaurralde, E. (2009) 'The C-terminal domains of human TNRC6A, TNRC6B, and TNRC6C silence bound transcripts independently of Argonaute proteins', *Rna*, 15(6), pp. 1059–1066.

Li, Q. *et al.* (2016) 'miR-28 modulates exhaustive differentiation of T cells through silencing programmed cell death-1 and regulating cytokine secretion', *Oncotarget*, 7(33), pp. 53735–

53750.

Li, Q. J. *et al.* (2007) 'miR-181a Is an Intrinsic Modulator of T Cell Sensitivity and Selection', *Cell*, 129(1), pp. 147–161.

Li, S. *et al.* (2008) 'Identification of GW182 and its novel isoform TNGW1 as translational repressors in Ago2-mediated silencing.', *Journal of cell science*, 121(24), pp. 4134–4144.

Li, Z. and Rana, T. M. (2014) 'Therapeutic targeting of microRNAs: Current status and future challenges', *Nature Reviews Drug Discovery*, 13(8), pp. 622–638.

Lian, S. L. *et al.* (2009) 'The C-terminal half of human Ago2 binds to multiple GW-rich regions of GW182 and requires GW182 to mediate silencing.', *RNA*, 15(5), pp. 804–13.

Licatalosi, D. D. *et al.* (2008) 'HITS-CLIP yields genome-wide insights into brain alternative RNA processing.', *Nature*, 456, pp. 464–469.

Lin, R. (2014) 'Tageting miR-23a in CD8+ cytotoxic T lymphocytes prevents tumor-dependent immunosuppression', *Journal of Clinical Investigation*, 124(12), pp.5352-5367.

Lin, S. and Gregory, R. I. (2015) 'MicroRNA biogenesis pathways in cancer', *Nature Reviews Cancer*, 15(6), pp. 321–333.

Lind, E. F., Elford, A. R. and Ohashi, P. S. (2013) 'Micro-RNA 155 Is Required for Optimal CD8+ T Cell Responses to Acute Viral and Intracellular Bacterial Challenges.', *Journal of Immunology*, 190(3), pp. 1210–1216.

Liu, S. *et al.* (2016) 'Suppressed expression of miR-378 targeting gzmb in NK cells is required to control dengue virus infection', *Cellular and Molecular Immunology*, 13(5), pp. 700–708.

Loeb, G. B., Khan, A. A., *et al.* (2012) 'Transcriptome-wide miR-155 Binding Map Reveals Widespread Noncanonical MicroRNA Targeting', *Molecular Cell*, 48(5), pp. 760–770.

Love, M. I., Huber, W. and Anders, S. (2014) 'Moderated estimation of fold change and dispersion for RNA-seq data with DESeq2', *Genome Biology*, 15(12), pp. 1–21.

Lu, L. F. *et al.* (2015) 'A Single Mirna-Mrna Interaction Affects The Immune Response In A Context- And Cell-Type-Specific Manner', *Immunity*, 43(1), pp. 52–64.

Luck, M. E., Muljo, S. a. and Collins, C. B. (2015) 'Prospects for Therapeutic Targeting of MicroRNAs in Human Immunological Diseases', *The Journal of Immunology*, 194(11), pp. 5047–5052.

Lykken, E. A. and Li, Q. J. (2016) 'The microRNA MIR-191 supports T cell survival following common γ chain signaling', *Journal of Biological Chemistry*, 291(45), pp. 23532–23544.

Ma, F. *et al.* (2011) 'The microRNA miR-29 controls innate and adaptive immune responses to intracellular bacterial infection by targeting interferon-gamma', *Nature immunology*, 12(9), pp. 861–869.

Mandl, J. N. *et al.* (2013) 'T Cell-Positive Selection Uses Self-Ligand Binding Strength to Optimize Repertoire Recognition of Foreign Antigens', *Immunity*, 38(2), pp. 263–274.

Marcais, A. *et al.* (2014) 'microRNA-mediated regulation of mTOR complex components facilitates discrimination between activation and anergy in CD4 T cells', *Journal of Experimental Medicine*, 211(11), pp. 2281–2295.

Martin, M. (2011) 'Cutadapt removes adapter sequences from high-throughput sequencing

reads', *EMBnet.journal*, 17, pp. 10–12.

Martinez-Usatorre, A. *et al.* (2019) 'MicroRNA-155 expression is enhanced by T-cell receptor stimulation strength and correlates with improved tumor control in Melanoma', *Cancer Immunology Research*, 7(6), pp. 1013–1024.

Maschmeyer, P. *et al.* (2018) 'Selective targeting of pro-inflammatory Th1 cells by microRNA-148a- specific antagomirs in vivo', *Journal of Autoimmunity*, 89, pp. 41–52.

Masopust, D. *et al.* (2001) 'Preferential Localization of Effector Memory Cells in Nonlymphoid Tissue', 291(5512), pp. 2413–2417.

Mckeithan, T. W. (1995) 'Kinetic proofreading in T-cell receptor signal transduction (protein-tyrosine kinase/major histocompatibility complex/mathematical model)', *Immunology*, 92(May), pp. 5042–5046.

Mehta, A. and Baltimore, D. (2016) 'MicroRNAs as regulatory elements in immune system logic', *Nature Reviews Immunology*, 16(5), pp. 279–294.

Meisgen, F. *et al.* (2012) 'miR-21 is up-regulated in psoriasis and suppresses T cell apoptosis', *Experimental Dermatology*, 21(4), pp. 312–314.

Mi, H. *et al.* (2013) 'Large-scale gene function analysis with the panther classification system', *Nature Protocols*, 8(8), pp. 1551–1566.

Mildner, A. *et al.* (2017) 'Leukocyte and lymphoid organ ontogeny MicroRNA-142 controls thymocyte proliferation', *European Journal of Immunology*, 47, pp. 1142–1152.

Miosge, L. and Zamoyska, R. (2007) 'Signalling in T-cell development: is it all location, location, location?', *Current Opinion in Immunology*, 19(2), pp. 194–199.

Moffett, H. F. *et al.* (2017) 'The microRNA miR-31 inhibits CD8 + T cell function in chronic viral infection', *Nature Immunology*, 18(7), pp.791-799.

Mogilyansky, E. and Rigoutsos, I. (2013) 'The miR-17/92 cluster: a comprehensive update on its genomics, genetics, functions and increasingly important and numerous roles in health and disease', *Cell Death and Differentiation*, 20(12), pp. 1603–1614.

Mombaerts, P. *et al.* (1992) 'RAG-1-deficient mice have no mature B and T lymphocytes', *Cell* 68(5), pp. 869-77.

Moore, M. J. *et al.* (2015) 'miRNA-target chimeras reveal miRNA 3'-end pairing as a major determinant of Argonaute target specificity.', *Nature communications*, 6:8864.

Morgulis, A. *et al.* (2006) 'A fast and symmetric DUST implementation to mask low-complexity DNA sequences', *Journal of Computational Biology*, 13(5), pp. 1028–1040.

Muljo, S. a *et al.* (2005) 'Aberrant T cell differentiation in the absence of Dicer.', *The Journal of experimental medicine*, 202(2), pp. 261–269.

Mullokandov, G. *et al.* (2012) 'High-throughput assessment of microRNA activity and function using microRNA sensor and decoy libraries', *Nature Methods*, 9, pp. 840–846.

Na, Y. J. and Kim, J. H. (2013) 'Understanding cooperativity of microRNAs via microRNA association networks.', *BMC genomics*, 14 (Suppl 5).

Nal, B. *et al.* (2004) 'Coronin-1 expression in T lymphocytes: Insights into protein function during T cell development and activation', *International Immunology*, 16(2), pp. 231–240.

Nika, K. *et al.* (2010) 'Constitutively active lck kinase in T cells drives antigen receptor signal transduction', *Immunity*, 32(6), pp. 766–777.

Van Nostrand, E. L. *et al.* (2016) 'Robust transcriptome-wide discovery of RNA-binding protein binding sites with enhanced CLIP (eCLIP).', *Nature methods*, 13, pp. 1–9.

O'Connell, R. M. *et al.* (2010) 'Physiological and pathological roles for microRNAs in the immune system.', *Nature reviews. Immunology*, 10(2), pp. 111–122.

Ohno, M. *et al.* (2013) 'Expression of miR-17-92 enhances anti-tumor activity of T-cells transduced with the anti-EGFRvIII chimeric antigen receptor in mice bearing human GBM xenografts', *Journal for ImmunoTherapy of Cancer*, 1, pp. 1–12.

Olejniczak, S. H. *et al.* (2013) 'Long-lived microRNA-Argonaute complexes in quiescent cells can be activated to regulate mitogenic responses.', *Proceedings of the National Academy of Sciences of the United States of America*, 110(1), pp. 157–62.

Pao, L. I. *et al.* (2007) 'Nonreceptor Protein-Tyrosine Phosphatases in Immune Cell Signaling', *Annual Review of Immunology*, 25(1), pp. 473–523.

Parker DC (1993) 'T cell-dependent B cell activation', *Annual Review of Immunology*, 11, pp. 331–360.

Pearce, E. L. *et al.* (2003) 'Control of Effector CD8 $^{+}$ T Cell Function by the Transcription Factor Eomesodermin', *Science*, 302(5647), pp. 1041–1043.

Pelosi, M. *et al.* (1999) 'Tyrosine 319 in the interdomain B of ZAP-70 is a binding site for the Src homology 2 domain of Lck', *Journal of Biological Chemistry*, 274(20), pp. 14229–14237.

Pinzón, N. *et al.* (2017) 'MicroRNA target prediction programs predict many false positives', *Genome Research*, 27(2), pp. 234–245.

Pitchiaya, S. *et al.* (2017) 'Resolving Subcellular miRNA Trafficking and Turnover at Single-Molecule Resolution', *Cell Reports*, 19(3), pp. 630–642.

Piwecka, M. *et al.* (2017) 'Loss of a mammalian circular RNA locus causes miRNA deregulation and affects brain function', *Science*, 357(6357), pp. 1–14.

Pollizzi, K. N. *et al.* (2015) 'mTORC1 and mTORC2 selectively regulate CD8+ T cell differentiation', *Journal of Clinical Investigation*, 125(5), pp. 2090–2108.

Rao, R. R. *et al.* (2010) 'The mTOR Kinase Determines Effector versus Memory CD8 + T Cell Fate by Regulating the Expression of Transcription Factors T-bet and Eomesodermin', *Immunity*, 32(1), pp. 67–78.

Raphael, I. *et al.* (2015) 'T cell subsets and their signature cytokines in autoimmune and inflammatory diseases', *Cytokine*, 74(1), pp. 5–17.

Rodríguez-galán, A., Fernández-messina, L. and Sánchez-madrid, F. (2018) 'Control of Immunoregulatory Molecules by miRNAs in T Cell Activation', *Frontiers in Immunology*, 9, pp. 1–10.

Rüdel, S. *et al.* (2011) 'Phosphorylation of human Argonaute proteins affects small RNA binding', *Nucleic Acids Research*, 39(6), pp. 2330–2343.

Rudolph, M. G., Stanfield, R. L. and Wilson, I. A. (2006) 'How Tcrs Bind Mhcs, Peptides, and Coreceptors', *Annual Review of Immunology*, 24(1), pp. 419–466.

Sallusto, F., Geginat, J. and Lanzavecchia, A. (2004) ' Central Memory and Effector Memory T Cell Subsets : Function, Generation, and Maintenance ', *Annual Review of Immunology*, 22(1), pp. 745–763.

Salmond, R. J. *et al.* (2009) 'T-cell receptor proximal signaling via the Src-family kinases, Lck and Fyn, influences T-cell activation, differentiation, and tolerance', *Immunological Reviews*, 228(1), pp. 9–22.

Salmond, R. J. *et al.* (2014) 'The tyrosine phosphatase PTPN22 discriminates weak self peptides from strong agonist TCR signals', *Nature Immunology*, 15, pp. 875-882.

Salzman, D. W. *et al.* (2016) 'MiR-34 activity is modulated through 5′-end phosphorylation in response to DNA damage', *Nature Communications*, 7, pp. 1–9.

Samelson, L. E. *et al.* (2015) 'The Linker for Activation of T Cells (LAT) Signaling Hub: From Signaling Complexes to Microclusters', *Journal of Biological Chemistry*, 290(44), pp. 26422–26429.

Sandberg, R. *et al.* (2008) 'Proliferating Cells Express mRNAs with Shortened 3' Untranslated Regions and Fewer MicroRNA Target Sites', *Science*, 320(5883), pp. 1643–1647.

Schatz, D. G. and Ji, Y. (2011) 'Recombination centres and the orchestration of V(D)J recombination', *Nature Reviews Immunology*, 11(4), pp. 251–263.

Schenkel, J. M. and Masopust, D. (2014) 'Tissue-resident memory T cells', *Immunity*, 41(6), pp. 886–897.

Schwartz, R. H. (2003) 'T Cell anergy', *Annual Review of Immunology*, 21(1), pp. 305–334.

Schwarz, D. S. *et al.* (2003) 'Asymmetry in the assembly of the RNAi enzyme complex', *Cell*, 115, pp. 199–208.

Sebastiani, G. *et al.* (2011) 'Increased expression of microRNA miR-326 in type 1 diabetic patients with ongoing islet autoimmunity', *Diabetes/Metabolism Research and Reviews*, 27, pp. 862–866.

Seddon, B. and Zamoyska, R. (2003) 'Regulation of peripheral T-cell homeostasis by receptor signalling', *Current Opinion in Immunology*, 15(3), pp. 321–324.

Seitz, H. (2017) 'Issues in current microRNA target identification methods', *RNA Biology*, 14(7), pp. 831–834.

Selbach, M. *et al.* (2008) 'Widespread changes in protein synthesis induced by microRNAs', *Nature*, 455, pp. 58–63.

Shaw, A. S. *et al.* (1990) 'Short related sequences in the cytoplasmic domains of CD4 and CD8 mediate binding to the amino-terminal domain of the p56lck tyrosine protein kinase.', *Molecular and Cellular Biology*, 10(5), pp. 1853–1862.

Sheu-Gruttadauria, J. and MacRae, I. J. (2018) 'Phase Transitions in the Assembly and Function of Human miRISC', *Cell*, 173, pp. 1–12.

Simpson, L. J. and Ansel, K. M. (2015) 'MicroRNA regulation of lymphocyte tolerance and autoimmunity', *Journal of Clinical Investigation*, 125(6), pp. 2242–2249.

Smith, N. L. *et al.* (2015) 'miR-150 Regulates Differentiation and Cytolytic Effector Function in CD8 + T cells', *Scientific Reports*, 5:16399, pp. 1–11.

Srivastava, M. *et al.* (2015) 'Roquin binds microRNA-146a and Argonaute2 to regulate microRNA homeostasis', *Nature Communications*, 6:6253.

Stellato, C. *et al.* (2011) ' Coordinate Regulation of GATA-3 and Th2 Cytokine Gene Expression by the RNA-Binding Protein HuR ', *The Journal of Immunology*, 187(1), pp. 441–449.

Stemberger, C. *et al.* (2007) 'A Single Naive CD8+ T Cell Precursor Can Develop into Diverse Effector and Memory Subsets', *Immunity*, 27(6), pp. 985–997.

Stepanek, O. *et al.* (2014) 'Coreceptor scanning by the T cell receptor provides a mechanism for T cell tolerance', *Cell*, 159(2), pp. 333–345.

Sugimoto, Y. *et al.* (2017) 'Using hiCLIP to identify RNA duplexes that interact with a specific RNA-binding protein', *Nature Protocols*, 12(3), pp. 611–637.

Sullivan, B. M. *et al.* (2003) 'Antigen-driven effector CD8 T cell function regulated by T-bet', *Proceedings of the National Academy of Sciences*, 100(26), pp. 15818–15823.

Sun, Y. *et al.* (2013) 'Allogeneic T cell responses are regulated by a specific miRNA-mRNA network', *Journal of Clinical Investigation*, 123(11), pp. 4739–4754.

Sun, Y. *et al.* (2015) 'Mature T cell responses are controlled by microRNA-142', *Journal of Clinical Investigation* 125(7), pp. 2825-2840.

Surh, C. D. and Sprent, J. (2008) 'Homeostasis of Naive and Memory T Cells', *Immunity*, 29(6), pp. 848–862.

Sweeney, B. A. *et al.* (2019) 'RNAcentral: A hub of information for non-coding RNA sequences', *Nucleic Acids Research*, 47(D1), pp. D221–D229.

Takemoto, N. *et al.* (2006) ' Cutting Edge: IL-12 Inversely Regulates T-bet and Eomesodermin Expression during Pathogen-Induced CD8 + T Cell Differentiation ', *The Journal of Immunology*, 177(11), pp. 7515–7519.

Tanchot, C., Lemonnier, F. A. and Perarnau, B. (1997) 'Differential Requirements for Survival and Proliferation of CD8 Naïve or Memory T Cells', *Science*, 276, pp. 2057–2062.

Teteloshvili, N. *et al.* (2017) 'Argonaute 2 immunoprecipitation revealed large tumor suppressor kinase 1 as a novel proapoptotic target of miR-21 in T cells', *FEBS Journal*, 284(4), pp. 555–567.

Thaventhiran, T. (2013) 'T Cell Co-inhibitory Receptors-Functions and Signalling Mechanisms', *Journal of Clinical & Cellular Immunology*, S12:004.

Trifari, S. *et al.* (2013) 'MicroRNA-directed program of cytotoxic CD8+ T-cell differentiation.', *Proceedings of the National Academy of Sciences of the United States of America*, 110(46), pp. 18608–13.

Tsai, C.-Y. *et al.* (2013) 'MicroRNA miR-155 affects antiviral effector and effector Memory CD8 T cell differentiation.', *Journal of virology*, 87(4), pp. 2348–51.

Turvey, S. E. and Broide, D. H. (2010) 'Chapter 2: Innate Immunity', *Journal of Allergy and Clinical Immunology*, 125(2 Suppl 2), pp. S24-32.

Tuschl, T. *et al.* (2004) 'Human Argonaute2 mediates RNA cleavage targeted by miRNAs and siRNAs', *Molecular Cell*, 15(2), pp. 185–197.

Valitutti, S. *et al.* (1995) 'Serial triggering of many T-cell receptors by a few peptide-MHC complexes', *Nature*, 375, pp. 148–151.

Valitutti, S. and Lanzavecchia, A. (1997) 'Serial triggering of TCRs: A basis for the sensitivity and specificity of antigen recognition', *Immunology Today*, 18(6), pp. 299–304.

Veillette, A. *et al.* (1988) 'The CD4 and CD8 T cell surface antigens are associated with the internal membrane tyrosine-protein kinase p56lck', *Cell*, 55(2), pp. 301–308.

Veillette, A., Latour, S. and Davidson, D. (2002) 'Negative regulation of immunoreceptor signalling', *Annual Review of Immunology*, 20(1), pp. 669–707.

Victora, G. D. and Nussenzweig, M. C. (2012) 'Germinal Centers', *Annual Review of Immunology*, 30(1), pp. 429–457.

Vogel, K. U. *et al.* (2013) 'Roquin paralogs 1 and 2 redundantly repress the icos and ox40 costimulator mRNAs and control follicular helper t cell differentiation', *Immunity*, 38(4), pp. 655–668.

Wang, C., Collins, M. and Kuchroo, V. K. (2015) 'Effector T cell differentiation: are master regulators of effector T cells still the masters?', *Current Opinion in Immunology*, 37, pp. 6–10.

Wang, H. *et al.* (2014) 'Negative regulation of Hif1a expression and TH17 differentiation by the hypoxia-regulated microRNA miR-210', 15(4), pp. 393–402.

Wang, Y. *et al.* (2013) 'MicroRNA-7 Regulates the mTOR Pathway and Proliferation in Adult Pancreatic b -Cells', *Diabetes,* 62, pp.887-895.

Weinmann, L. *et al.* (2009) 'Importin 8 Is a Gene Silencing Factor that Targets Argonaute Proteins to Distinct mRNAs', *Cell*, 136(3), pp. 496–507.

Wells, A. C. *et al.* (2017) 'Modulation of let-7 miRNAs controls the differentiation of effector CD8 T cells', *eLife*, 26398, pp. 1–22.

Wodarz, D. and Jansen, V. A. A. (2001) 'The role of T cell help for anti-viral CTL responses', *Journal of Theoretical Biology*, 211(4), pp. 419–432.

Wu, H. *et al.* (2007) 'miRNA profiling of naive, effector and memory CD8 T cells', *PLoS ONE*, 2(10).

Wu, H. *et al.* (2009) 'Alternative processing of primary microRNA transcripts by Drosha generates 5′ end variation of mature microRNA', *PLoS ONE*, 4(10).

Wu, P., Isaji, M. and Carthew, R. W. (2013) 'Functionally Diverse MicroRNA Effector Complexes Are Regulated by Extracellular Signaling', *Molecular Cell*, 52(1), pp.113–123.

Wu, T. *et al.* (2012) 'Temporal expression of microRNA cluster miR-17-92 regulates effector and memory CD8+ T-cell differentiation', *Proceedings of the National Academy of Sciences*, 109(25), pp. 9965–9970.

Xiong, S. *et al.* (2011) 'MicroRNA-7 Inhibits the Growth of Human Non-Small Cell Lung Cancer A549 Cells through Targeting BCL-2', *International Journal of Biological Sciences*, 7(6), pp.805-814.

Xue, F. *et al.* (2013) 'miR-31 regulates interleukin 2 and kinase suppressor of ras 2 during T cell activation.', *Genes and immunity*, 14, pp.127-131.

Yang, J. *et al.* (2017) 'MiR-15a/16 deficiency enhances anti-tumor immunity of glioma-

infiltrating CD8+ T cells through targeting mTOR', *International Journal of Cancer*, 141(10), pp. 2082–2092.

Yang, L. *et al.* (2012) 'miR-146a controls the resolution of T cell responses in mice', *Journal of Experimental Medicine*, 209(9), pp. 1655–1670.

Yao, B. *et al.* (2012) 'Defining a new role of GW182 in maintaining miRNA stability', *EMBO reports*, 13(12), pp. 1102–8.

Yu, T. *et al.* (2016) 'MicroRNA-491 regulates the proliferation and apoptosis of CD8 + T cells', *Scientific Reports*, 6, pp. 1–13.

Zarnegar, B. J. *et al.* (2016) 'irCLIP platform for efficient characterization of protein-RNA interactions.', *Nature methods*, 13(6), pp. 498-492.

Zeng, Y. *et al.* (2008) 'Phosphorylation of Argonaute 2 at serine-387 facilitates its localization to processing bodies', *Biochemical Journal*, 413(3), pp. 429–436.

Zhang, K. *et al.* (2018) 'A novel class of microRNA-recognition elements that function only within open reading frames', *Nature Structural and Molecular Biology*, 25(11), pp. 1019–1027.

Zhang, N. and Bevan, M. J. (2010) 'Dicer controls CD8+ T-cell activation, migration, and survival.', *Proceedings of the National Academy of Sciences of the United States of America*, 107(50), pp. 21629–21634.

Zhang, Z. *et al.* (2018) 'Regulation of memory CD8 + T cell differentiation by MicroRNAs', *Cellular Physiology and Biochemistry*, 47(6), pp. 2187–2198.

Zhao, S. *et al.* (2017) 'QuickMIRSeq: A pipeline for quick and accurate quantification of both known miRNAs and isomiRs by jointly processing multiple samples from microRNA sequencing', *BMC Bioinformatics*, 18(1), pp. 1–14.

Zhou, J. *et al.* (2013) 'MicroRNA-326 Functions as a Tumor Suppressor in Glioma by Targeting the Nin One Binding Protein (NOB1)', *PLoS ONE*, 8(7).